SEQUENCE STRATIGRAPHY, DEPOSITIONAL HISTORY, AND HYDROCARBON POTENTIAL OF THE MANCOS SHALE, UINTA BASIN, UTAH

by

Andrew Donald McCauley

A thesis submitted to the faculty of
The University of Utah
in partial fulfillment of the requirements for the degree of

Master of Science

in

Geology

Department of Geology and Geophysics

The University of Utah

December 2013

The University of Utah Graduate School

STATEMENT OF THESIS APPROVAL

The thesis of **Andrew Donald McCauley**

has been approved by the following supervisory committee members:

Lauren P. Birgenheier	, Chair	**8/28/13** Date Approved
Cari Johnson	, Member	**9/10/13** Date Approved
Robert Ressetar	, Member	**8/28/13** Date Approved

and by **John M. Bartley**, Chair/Dean of

the Department/College/School of **Geology and Geophysics**

and by David B. Kieda, Dean of The Graduate School.

ABSTRACT

The Mancos Shale, an organic-lean marine mudstone dominated by detrital quartz and clay, was deposited into the Upper Cretaceous Western Interior Seaway. It is a proven source rock with potential as a target for hydrocarbon production from horizontal drilling and hydraulic fracturing, but prospective reservoir target intervals from its 4,000 ft (1220 m) thickness must be identified and characterized. The distribution of lithofacies throughout the Mancos has not previously been studied in detail, so this formation remains undifferentiated and the relationship with paleodepositional up- and downdip strata undefined. Previous core-based analysis has provided a depositional and sequence stratigraphic framework for predicting the distribution of lithofacies in the Mancos. However, a unified, basin-wide facies and sequence stratigraphic correlation which tests existing outcrop and core-based models is lacking. 157 wireline logs were chronostratigraphically correlated across the basin to build a regional subsurface map and cross sections that highlight stacking patterns, regional facies relationships, stratal architecture, and sequence stratigraphy within a depositional framework. A sequence stratigraphic model is established for the Mancos Shale, which incorporates seminal outcrop-based models from strata of central Utah, Mancos core, and stacking patterns identified from wireline log data.

The Mancos thickens to the north and west, matching regional trends of tectonically driven subsidence, the most significant control on accommodation. The

Mancos Shale consists of 29 4th order T-R cycles, which can be stacked to form four 3rd order cycles and a single 2nd order cycle. Whereas the stacking patterns of 2nd and 3rd order cycles are consistent across the basin, suggesting allocyclic control, 4th order cycles are more variable, influenced by both allocyclic and autocyclic controls. Deposition of the Mancos evolved from a low gradient ramp, to a deeper water basin, which was then infilled by basin-floor fans. Two organic-rich facies associations, each corresponding to transgressive and early highstand sequence sets, heterolithic facies of the Juana Lopez and lowermost Blue Gate (FA1) and sediment starved shelf deposits of the Lower Blue Gate (FA2) offer the most prospective intervals for unconventional hydrocarbon production. Preliminary petrophysical analysis and basin modeling corroborate this analysis.

TABLE OF CONTENTS

LIST OF FIGURES

ACKNOWLEDGEMENTS

This project would not have been possible without the dedicated help from many people. I would first like to thank my advisor, Dr. Lauren Birgenheier, for her help introducing me to the Mancos, in the field, in the literature, in our discussions, and for guiding me from "squiggle matching" to a more detailed understanding of this formation. Her countless hours of editing my writing should not go unrecognized. The other members of my committee, Dr. Cari Johnson and Dr. Robert Ressetar, each provided great support during my time in Utah. Other faculty in the department and researchers involved in the project, Dr. John Bartley, Dr. Stephanie Carney, Dr. Bill Keach, Dr. John McLennan, and Dr. Lisa Stright, each exposed me to different questions and research tools to consider in my own work. In addition, several undergraduate researchers have done some really nice work with different aspects of Mancos petrophysics, Ryan Hillier, Laini Larsen, and Ziqiang Yuan. James Taylor provided invaluable logistical support. I also need to thank Brendan Horton for the detailed work he did to lay the groundwork for this study, and his efforts to bring me up to speed and help me get rolling on the project during my first year. This interdisciplinary project has exposed me to a number of intelligent and dedicated researchers across a variety of related fields.

My experience at the University of Utah has been overwhelmingly positive, thanks to the people here in the department and the natural beauty of this place. The

dedicated faculty and staff have made this a great environment to learn and work. My classmates have been a pleasure to work with, and their help with matters both technical and nontechnical have each been greatly appreciated. Finally, I would like to thank my wonderful family for their unwavering support of my efforts to work with rocks.

CHAPTER 1

TRANSGRESSIVE-REGRESSIVE CYCLES IN THE MANCOS SHALE, UINTA BASIN, UTAH

Abstract

The Upper Cretaceous Mancos Shale is an organic-lean, silty mudstone deposited across much of the Western Interior Seaway of North America during the Sevier Orogeny. This formation is dominated by fine-grained detrital quartz and clay with a few carbonate-rich intervals. Development of hydrocarbons from this 4,000 ft (1,220 m) thick mudstone requires a detailed understanding of lateral and vertical heterogeneity of lithofacies, geomechanical properties, and hydrocarbon potential. Correlation of gamma-ray logs, tied to detailed core descriptions, reveals that the Mancos Shale consists of twenty-nine 4th order transgressive-regressive (T-R) cycles, which can be mapped through marine mudstone deposits of the eastern Uinta Basin in Utah. T-R cycles include genetically related strata bounded by maximum regressive surfaces (MRS) and include a maximum flooding surface (MFS) that separates a lower transgressive phase from an upper regressive phase. The change in claystone and siltstone content from one T-R cycle relative to the underlying T-R cycle indicates the net change in the relative position of shoreline, either basinward (net regressive) or landward (net transgressive) during that period of deposition. Four 3rd order T-R cycles in the Mancos Shale are formed by the

cumulative changes in relative shoreline of stacked sets of 4th order T-R cycles, and one 2nd order T-R cycle is established by these component 3rd order cycles.

Analysis of basin-wide stacking patterns distinguishes regionally significant surfaces from local heterogeneities and aids in the interpretation of offshore sequence stratigraphy and in differentiating allocyclic versus autocyclic controls on deposition. Driving mechanisms for relative sea level change vary with hierarchical rank. Correlative 4th order T-R cycles display generally consistent stacking patterns, but lateral variations are commonly present, suggesting the influence of both autocyclic and allocyclic controls. In contrast, 3rd order T-R cycles are characterized by consistent trends in relative sea level changes throughout the study area, suggesting allocyclic controls dominate relative sea level changes of this rank. 3rd order relative sea level changes can be tied to the global eustatic record, whereas 2nd order temporal trends are common to other deposits of the Western Interior Seaway and appear to mainly reflect tectonic activity in the Sevier hinterland. Furthermore, regional thickening from south to north within the Mancos Shale suggests an increase in tectonic subsidence rates from south to north across the Uinta Basin. Two transgressive intervals, corresponding to 4th order cycles 5 and 12, offer the most promising targets for hydrocarbon production because they correspond to 2nd, 3rd, and 4th order transgressive strata. This study establishes a regionally significant sequence stratigraphic framework to identify and predict internal distribution of lithofacies, providing a first-pass tool for assessing the relative hydrocarbon potential of intervals within the Mancos Shale, from gamma ray logs.

Introduction

Development of horizontal drilling and hydraulic fracturing allows the production of natural gas and oil directly from organic-rich mudstone, strata previously considered too impermeable to serve as hydrocarbon reservoirs. The need to characterize these poorly-understood unconventional reservoirs has contributed to a rapid expansion of research and a growing recognition of the dynamic and varied depositional environment that typifies many mud-dominated systems (Schieber, 1999; Aplin and Macquaker, 2011). The stratigraphic evolution of mudstone-dominated successions and relationships between sedimentation and base-level change are still enigmatic, particularly as they relate to the lateral continuity of reservoir properties and corresponding variations in production characteristics. However, from an exploration perspective, this is precisely the challenge: to develop a meaningful genetic framework to guide development for the target mud-dominated portion of the stratigraphy, which is typically geographically removed from the paleodepositional updip equivalent succession.

The Mancos Shale was first described by Cross and Purington (1899) as "an almost homogenous body of soft, dark gray or nearly black, carbonaceous clay shale, varied only by the presence of a few thin bands or concretions of pure limestone … there are no practicable horizons for the subdivision of the complex in areal mapping" (p. 4). This perception that mudstones are homogenous bodies of uniform deposition has been significantly revised by new research. Research concerning mudstone depositional processes (e.g., Schieber et al., 2007; Macquaker et al., 2007, 2010; Bhattacharya and MacEachern, 2009), mudstone porosity and permeability (e.g., Loucks et al., 2009, 2012; Slatt and O'Brien, 2011; Chalmers et al., 2012; Modica and Lapierre, 2012), and

mudstone sequence stratigraphy (e.g., Abouelresh and Slatt, 2012; Angulo and Buatois, 2012; Slatt and Rodriguez, 2012) has begun to fill significant knowledge gaps. The transition between proximal marine facies and their downdip equivalents remains poorly understood, particularly in relatively shallow epicontinental settings, like those of the Cretaceous Western Interior Seaway. Defining a meaningful stratigraphic framework has been particularly problematic in an unusually thick package like the Mancos Shale, which is at least 4,000 ft (1,220 m) thick in the Uinta Basin. Understanding the relationships between important lithological properties such as permeability, total organic carbon (TOC), mineralogy, and depositional setting will allow better reservoir modeling of and production from these tight hydrocarbon plays.

Multidisciplinary study of the Mancos Shale provides the opportunity for exploring the relationship between rock properties, depositional environment, and sequence stratigraphy in offshore siliciclastic mudstone. Stacking pattern analysis has been used to demonstrate a relationship between organic richness and transgressive packages in a variety of shale formations (Slatt and Rodriguez, 2012). This relationship is further confirmed in high-resolution core analysis of the Mancos Shale (Kennedy, 2011; Horton, 2012). Horton (2012) identified eleven lithofacies from Mancos cores, which were placed in an offshore depositional framework, consisting of the prodelta, mudbelt, and sediment-starved shelf environments, in order from proximal to distal relative to shoreline siliciclastic input. Kennedy (2011) and Horton (2012) also developed preliminary sequence stratigraphic models from Mancos cores, suggesting that proximal to distal trends could be identified in core and given a sequence stratigraphic context. Lithofacies were tied to systems or sequence tracts, allowing reservoir facies to

be targeted based on their relationship with changes in relative sea level. However, the regional and stratigraphic extent of these sequence stratigraphic models has yet to be tested.

Previous workers in the Mancos Shale have either focused in detail on a relatively small region and/or stratigraphic interval (e.g., Molenaar and Wilson, 1990; Molenaar and Cobban, 1991; Hampson et al., 1999; Anderson and Harris, 2006) or a more extensive interval with few surfaces of correlation within the main body of the Mancos Shale (e.g., Johnson, 2003a; Hettinger and Kirschbaum, 2003; Kirschbaum, 2003; Rose et al., 2004; Anna, 2012), so there is a limited established framework for identifying lateral sequence stratigraphic and facies transitions. Analysis of stacking pattern variations between time-correlative packages of marine shale within the Mancos from wells around the basin establishes the degree of lateral depositional changes in these strata. This study seeks to define a chronostratigraphic and genetic framework to meaningfully divide the Mancos Shale in the depositionally distal, eastern portions of the Uinta Basin.

Transgressive-regressive (T-R) cycles provide insight into the sequence stratigraphy of distal depositional environments where stratal architecture and genetic surfaces, including correlative conformities, are often cryptic (Embry, 2002). Recent workers have predominantly applied a T-R sequence model to analysis of offshore shales, including identification of 2^{nd}, 3^{rd}, and 4^{th} order T-R cycles (e.g., Lash and Engelder, 2011; Sonnenberg, 2011; Hammes et al., 2011). This study uses a database of several hundred well logs to create a basin-wide subsurface genetic correlation of T-R sequences within the depositionally most distal expression of the Mancos Shale in the eastern Uinta

Basin. The Mancos Shale is an offshore system influenced by both fluvial deltaic and wave-dominated deposition from the western shoreline of the Cretaceous Western Interior Seaway. Fundamentally, grain size varied as a function of distance from this shoreline; changes in average grain size reflect relative sea level fluctuation, and can be correlated with this in mind. Stacking patterns of individual wells are compared to identify which changes in relative sea level are regionally correlative and hence reflect allocyclic controls, such as eustasy and tectonic subsidence, and which are only locally evident and hence reflect autocyclic delta lobe switching or local topographic variation. This ultimately allows for the identification of regionally significant sequence stratigraphic surfaces. By placing stacking patterns in a sequence stratigraphic model, lateral and vertical changes in facies can be identified and predicted in this distal marine shale, and a model established for variability within other fine-grained deposits of the Cretaceous Western Interior Seaway.

Geologic Background

During the Cretaceous, western North American geology was dominantly influenced by the Sevier and subsequent Laramide Orogenies. In central Utah, the Sevier Orogeny was characterized by north-south trending thrust faulting propagating from west to east (DeCelles, 1994). The loading of the overthickened Sevier orogenic belt created an adjacent foreland basin, or foredeep, to the east as flexural loading caused rapid subsidence adjacent to the thrust front (DeCelles and Giles, 1996) (Figure 1). This faulting contributed to crustal thickening and a high standing plateau along the orogenic foreland (Livaccari, 1991), which rapidly shed sediment into this adjacent basin (Johnson, 2003b). The forebulge migrated progressively eastward over the duration of

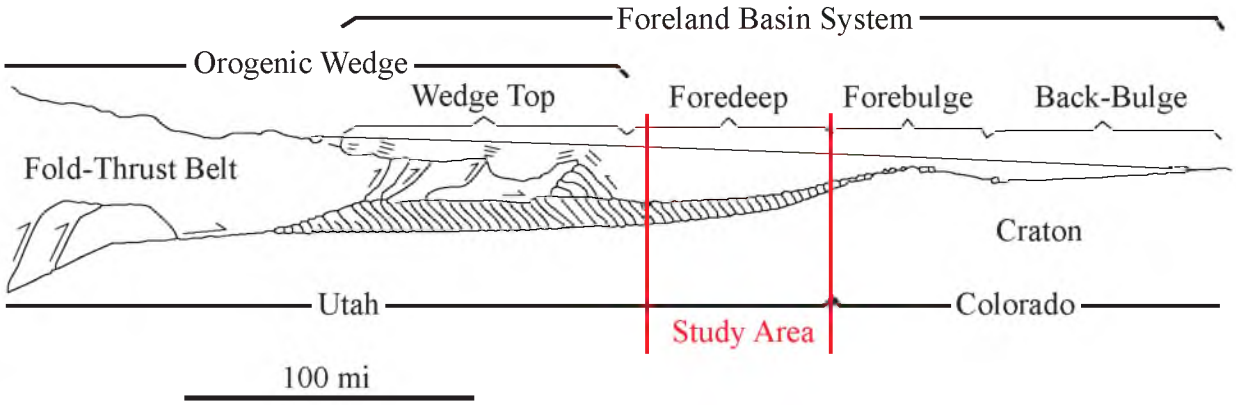

Figure 1: Foreland basin schematic and relative position of Mancos Shale deposition in the Uinta Basin (modified from DeCelles and Giles, 1996).

Sevier thrust propagation (DeCelles and Coogan, 2006), which contributed to an unconformity between the Dakota and Mancos Formations in the Uinta Basin during the Lower Turonian, but had moved east of the basin by the Middle Turonian (White et al., 2002; Kirschbaum and Mercier, 2013). This north-south trending foreland basin formed the Western Interior Seaway during Cretaceous sea-level highstand, an epicontinental seaway linking the paleo-Gulf of Mexico to the Arctic Ocean.

The Western Interior Seaway extended more than 3,000 mi (4,800 km) from north to south and up to 1,000 mi (1,600 km) in width, from the Sevier thrust front in Utah to present-day Ohio (Figure 2). This broad depression had fairly uniform structure, with active tectonic subsidence to the west and a ramped shallowing to the east (Kauffman, 1977) (Figure 3). The Mancos Shale and equivalent marine mudstone units were deposited across much of the seaway from the Cenomanian through the Early Campanian, approximately 96 to 80 Ma (Schwans, 1995). Marine deposition was dominated by siliciclastic, silt- and clay-sized detritus delivered from the western coastline, with local and regional variations in depositional style, such as wave- versus river-dominated delta systems, and during periods of variable rates of tectonically driven subsidence, with increasing calcareous deposits along the shallower, eastern margin (Kauffman, 1977) (Figure 3). The Mancos Shale in the Uinta Basin consists of five major lithostratigraphic members, the basal Tununk Shale Member, which is overlain by the Juana Lopez Member, the Blue Gate Shale Member, the Prairie Canyon or Mancos B Member, and the uppermost Buck Tongue. These offshore strata variously interfinger with proximal marine and coastal plain deposits to the west, including the Ferron and Emery Sandstones, and members of the Mesaverde Group, including the Star Point

Figure 2: Paleogeographic map of western North America and the Western Interior Seaway at ~85 Ma during the Santonian of the Late Cretaceous. Present day Utah outlined in black. Study area indicated on map, located along western margin of the interior seaway (modified from Blakey, 2013)

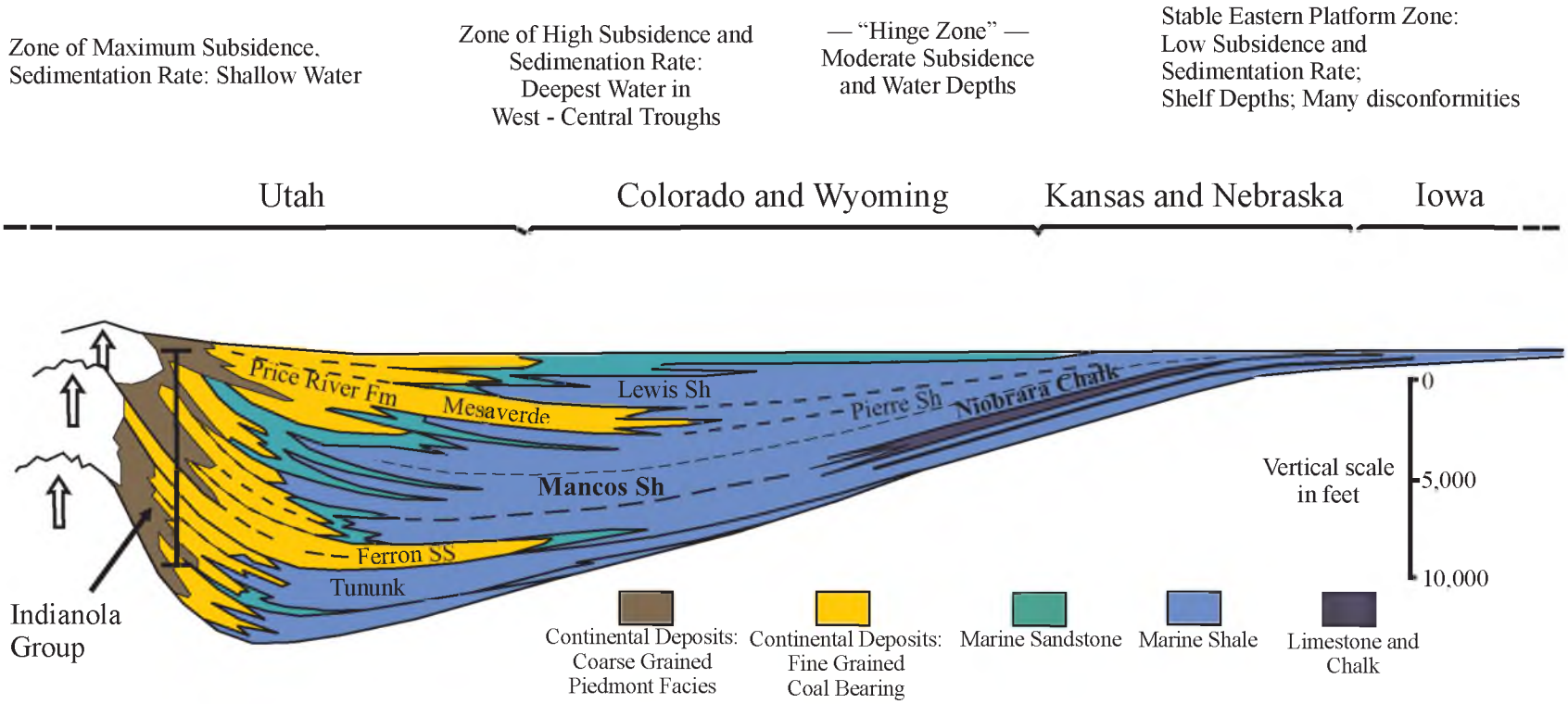

Figure 3: Generalized regional stratigraphy of the Upper Cretaceous Western Interior Basin between Utah and the mid-continent. Mancos shale deposited into offshore transition between various continental and marine sandstones to the west and carbonate rich shales, marls, and chalks to the east (adapted from Kauffman, 1977).

Sandstone, Blackhawk Formation, and Castlegate Sandstone (Fouch et al., 1983) (Figure 4). The chronostratigraphic relationships between the proximal marine and coastal plain deposits in the west and the more distal marine lithostratigraphic members that make up the Mancos Shale are not well defined.

The Late Cretaceous was a time of global greenhouse conditions and highstand sea level. High levels of atmospheric CO_2 produced during accelerated sea floor spreading and enhanced off-ridge volcanism contributed to hothouse conditions and stimulated organic carbon production (Arthur et al., 1985). Extensive mudstone deposits over continental shelves and in deeper water during the Cretaceous record thirteen major eustatic fluctuations in sea level (Cooper, 1977) and three major ocean anoxic events (Arthur and Schlanger, 1979; Jenkyns, 1980). Higher order cyclical changes in deep-water strata during the Cenomanian–Turonian (Sageman et al., 1997; Meyers et al., 2012) and Coniacian–Santonian (Locklair and Sageman, 2008) have been tied to orbital forcing and Milankovitch periodicities. The interplay between eustasy, global climate, and local Sevier foreland tectonics are recorded by changes in sedimentary structures and the lithology of strata deposited in the Western Interior Seaway.

Petroleum source rocks deposited during the Late Cretaceous highstand are abundant worldwide, and the Western Interior Seaway is no exception. Other organic-rich shales of the seaway, including the Niobrara and Mowry Formations, are proven source rocks in many petroleum systems of the Rocky Mountains and central United States (Kirschbaum, 2003; Sonnenberg, 2011). The Mancos Shale, which thermally matured during the subsidence and burial of the Uinta Basin by the Laramide Orogeny

Figure 4: Relative positions and chronology of Mancos Shale members and associated stratigraphy from west to east of Uinta Basin, UT. Members of the Mancos Shale and other Upper Cretaceous stratigraphy are labeled; members of the Blackhawk Formation are abbreviated (SC = Spring Canyon; A = Aberdeen; K = Kenilworth; S = Sunnyside; G = Grassy; D = Desert).

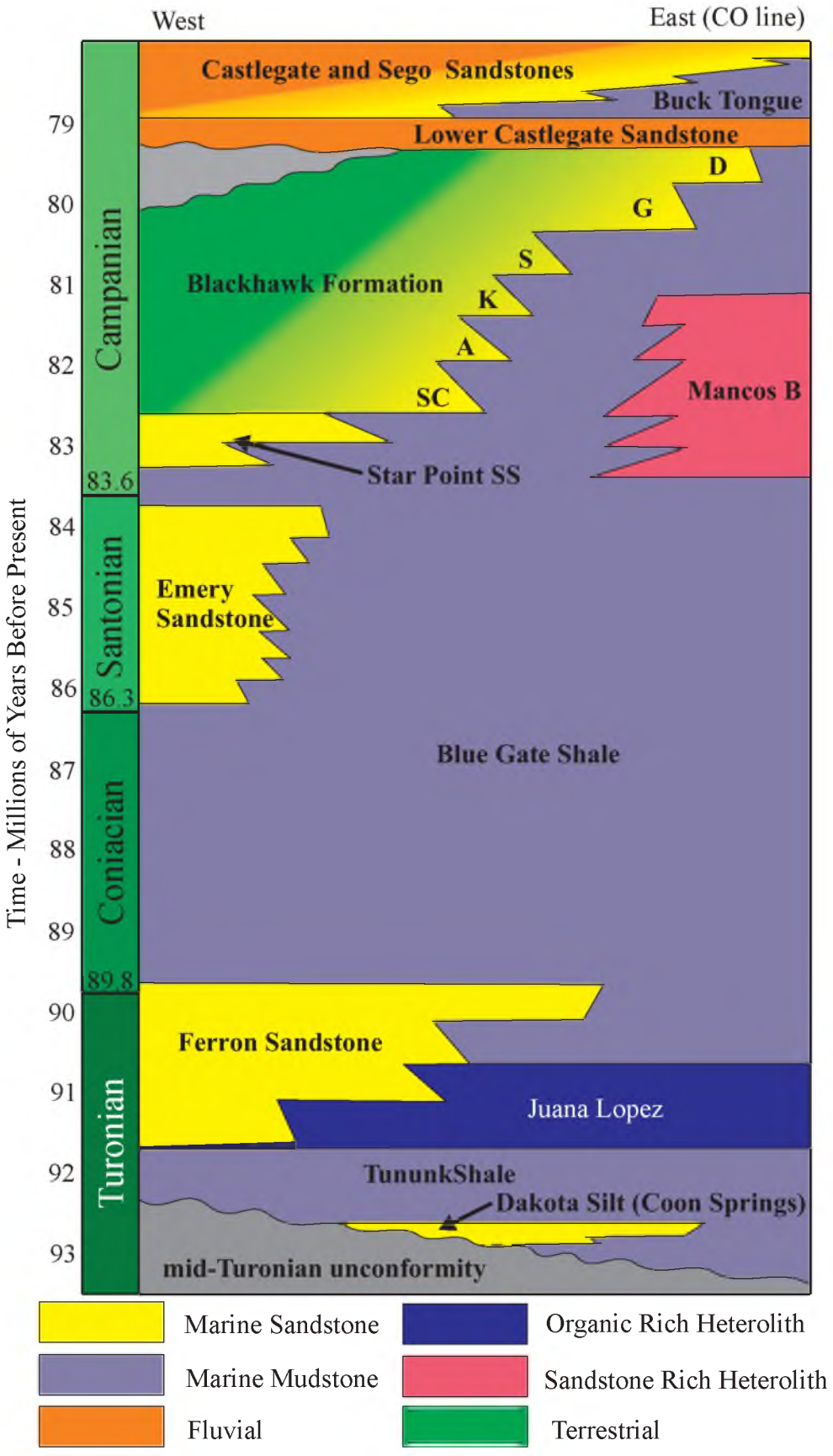
West
East (CO line)
Castlegate and Sego Sandstones
Buck Tongue
Lower Castlegate Sandstone
D
G
S
K
A
SC
Blackhawk Formation
Mancos B
Star Point SS
Emery Sandstone
Blue Gate Shale
Ferron Sandstone
Juana Lopez
TununkShale
Dakota Silt (Coon Springs)
mid-Turonian unconformity
Campanian
Santonian
Coniacian
Turonian
83.6
86.3
89.8
79
80
81
82
83
84
85
86
87
88
89
90
91
92
93
Time - Millions of Years Before Present
Marine Sandstone
Marine Mudstone
Fluvial
Organic Rich Heterolith
Sandstone Rich Heterolith
Terrestrial

(Nuccio and Roberts, 2003), is also a lean, but proven hydrocarbon source rock (Kirschbaum, 2003).

Dataset

Log data from 453 wells that penetrated the Mancos Shale across the Uinta Basin were compiled into a database. The sources of well data are varied: some data were downloaded from the Utah Department of Natural Resources' Division of Oil, Gas, and Mining database (DOGM, 2013), and a significant amount of data was donated by Anadarko Petroleum Corporation, Bill Barrett Corporation, Del Rio, Gasco, Pioneer Resources, Questar (now QEP Resources), Wind River Resources Corporation, and XTO Energy (now ExxonMobil Corporation). The types of data vary from well to well, but include gamma ray, resistivity, neutron porosity and density, sonic, borehole image, and mud logs. Of the 453 wells, 280 include wireline log data; 157 were used to construct regional cross sections and/or isopach maps (Figure 5; Appendix A). Well log data were collected independently by various well operators over the past half century, so differences in logging tools, borehole conditions, and operator procedures all contribute to variations in absolute values recorded from wells in the dataset. For that reason, well-to-well trends are reliable but absolute values are not.

Wireline log data are collected in newly drilled wells by lowering a tool on wireline into the borehole and recording rock properties from the drilled interval. Wireline tools can record a variety of rock properties, including natural occurring gamma radiation, electrical resistivity, sonic interval transit time, artificial neutron radiation response, and photo-electric response. These petrophysical data can be used to identify

Figure 5: Distribution of data throughout the Uinta Basin, concentrated primarily in southeast and northeast portions of the basin. Extent of preserved, post-Mancos strata outlined in black. 457 wells included in database (Appendix A) are marked as red (gas), green (oil), or black (dry) circles. Cross sections are marked as heavy blue (Figure 7), purple (Figure 8), or red (Figure 9) lines.

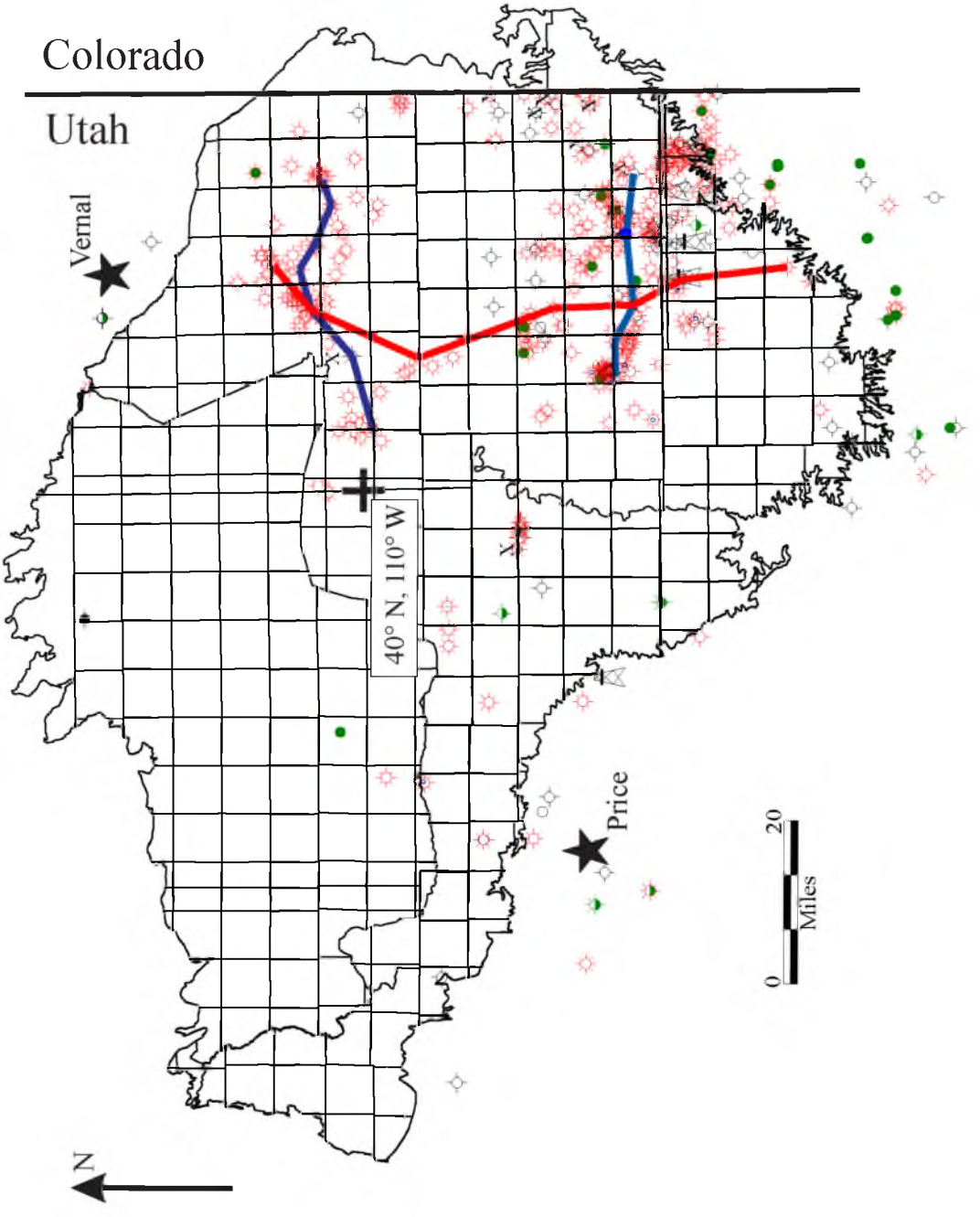
Colorado
Utah
Vernal
40° N, 110° W
Price
20
0
Miles
N

rock type and properties, including porosity, geomechanical properties, organic content, and water and hydrocarbon saturations (Fertl and Chilingar, 1988; Passey et al. 1990; Mullen et al., 2007; Passey et al., 2010; Vernik and Milovac, 2011). Log suites, the type of log data recorded from each borehole, varied from well to well.

Recent core-based investigations by Kennedy (2011) and Horton (2012) provided very useful detailed lithologic descriptions, high-resolution geochemical data, and geomechanical test results. These core data are from among the 280 wells with log data, and were consulted alongside the wireline logs to provide ground truth from unweathered strata in the subsurface. Kennedy (2011) described core from a 1,712 ft (520 m) interval of the River Gas of Utah #1 (RGU-1) well, from three miles SW of Price, UT, spanning the top of the Tununk Member through the Ferron Sandstone and Lower Blue Gate Shale to the lower Emery Sandstone. Horton (2012) evaluated core taken from four wells: 120 ft (36 m) intervals from three Questar wells roughly 25 miles south of Vernal, UT, the Glen Bench 1M-4-8-22R (abbreviated "Q1" in Horton, 2012), Red Wash 8ML-6-9-24 (Q8; Horton, 2012), and Glen Bench 16M-28-8-21 (Q16; Horton, 2012), and two 120' (36 m) intervals of the Pioneer Natural Resources Main Canyon Federal #23-7-15S-23E (P1 and P2; Horton, 2012), located roughly 40 mi (64 km) south of the Questar wells (Figure 5). These cores were taken from different intervals of the Lower Blue Gate Member, and demonstrate its vertical and lateral facies variability. The core descriptions considered details of subsurface lithology, sedimentology, and stratigraphy at the centimeter scale. Geochemical analysis included thin section, x-ray fluorescence, x-ray diffraction, QEMSCAN analysis, and TOC-RockEval pyrolysis (Horton, 2012). The RGU-1 cored interval was sampled at irregular intervals of tens of feet, designed to

systematically capture facies variability, for geomechanical properties from unconfined compression tests, triaxial compression tests, and indirect tensile strength tests (Kennedy, 2011). Complete descriptions of these core analyses and methods are available from Kennedy (2011) and Horton (2012).

Existing depositional and stratigraphic models developed primarily from outcrop and core by previous workers provided the primary lithologic background for the log-based stratigraphy in this study; this work described members of the Mancos Shale, including the Lower Blue Gate, Juana Lopez, and Tununk Members (Molenaar and Cobban, 1991; Anderson and Harris, 2006; Kennedy, 2011; Horton, 2012), Ferron Sandstone (Riemersma and Chan, 1991; Anderson and Ryer, 2004; Fielding, 2010), Emery Sandstone (Edwards et al., 2005), isolated sandstone bodies that are distal Blackhawk Formation equivalents, such as the Hatch Mesa Sandstone (Pattison, 2005; Pattison et al., 2007; Pattison et al., 2009), Mancos B (Cole et al., 1997; Hampson et al., 1999), and overlying strata of the Mesaverde Group (Yoshida, 2000; Miall and Arush, 2001; Kirschbaum and Hettinger, 2004). Key localities of previous studies were visited. These earlier stratigraphic relationships guided the correlations presented here. Three-dimensional seismic data that cover a portion of the study area were available and were valuable for confirming structural continuity between subsurface correlations.

Methods and Approach

PETRA was used for this study, in part because it contains correlation, geostatistical, and petrophysical modules that can be applied to formation mapping and evaluation. Well data were loaded as .LAS files, which allow scale manipulation during

correlation as well as quantitative petrophysical evaluation. Wells were selected for use in regional correlation based on the quality of available wireline log data, spacing relative to other available wells, penetration through the Mancos, and the availability of core or borehole image data. Regional correlations relied most extensively on gamma-ray logs, which serve as a proxy for lithology by indicating relative proportions of claystone and siltstone in the shale (Bhuyan and Passey, 1994); however, resistivity, density, and neutron porosity logs provided supplementary tools in some areas of the basin.

Stratigraphic correlation is based on a chronostratigraphic approach in which genetic surfaces and packages were identified in the logs and mapped across the study area. Parasequences (*sensu* Catuneanu et al., 2009) include genetically related strata bounded by flooding surfaces and provided initial chronostratigraphic surfaces for correlation. Mancos core descriptions demonstrate the existence of parasequences characterized by 1) an upwards shallowing or increase in grain size ranging from claystone to siltstone to very fine-grained sandstone overlain by 2) an abrupt increase in finer-grained (e.g., siltstone or claystone) content marking a flooding surface (Horton, 2012) (Figure 6). In gamma ray logs, this is often recorded as a gradual upward decreasing trend overlain by a sharp increase in gamma ray, marking a flooding surface. Lithofacies variations identified as parasequences in core are recorded in gamma ray fluctuations through those intervals, although the relative magnitude of these facies shifts between core and gamma logs are often inconsistent (Figure 6). Initial correlation efforts focused on correlating parasequences and their corresponding flooding surfaces. However, generally these surfaces could only be carried five to ten miles from a given well and were determined to represent localized depositional events.

Figure 6: Correlation between gamma ray log and core analysis with T-R cycle analysis (this paper) and sequence tract analysis (Horton, 2012), respectively. 4th order MFS, MRS, and stacking patterns labeled on well log (left). Core description includes facies description, parasequence stacking patterns, and interpreted systems tracts (lowstand system tract, LST; highstand system tract, HST; transgressive system tract, TST) of Horton (2012) (right). Parasequence bounding flooding surfaces (FS) identified in core (right) correspond to fluctuations in the gamma log and 4th order T-R cycles (left; 50–300 ft (15–90 m) scale) correspond generally with core based sequences (right; 5–30 ft (1.5–9 m) scale), although identified surfaces may vary by a few tens of feet. Modified from Horton (2012).

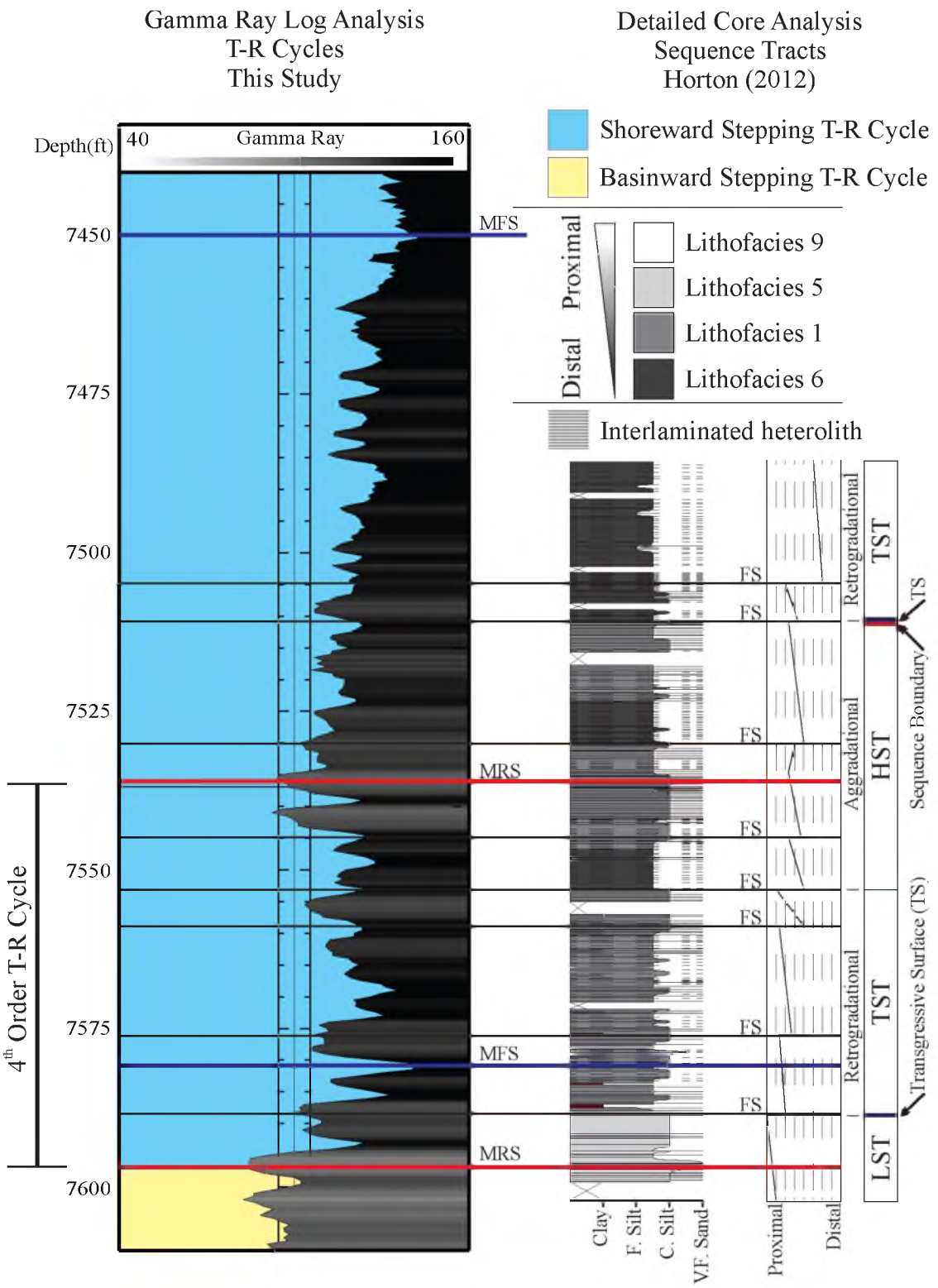
Gamma Ray Log Analysis
T-R Cycles
This Study
Detailed Core Analysis
Sequence Tracts
Horton (2012)
Depth(ft)
40
Gamma Ray
160
7450
7475
7500
7525
7550
7575
7600
MFS
MRS
MFS
MRS
4th Order T-R Cycle
Shoreward Stepping T-R Cycle
Basinward Stepping T-R Cycle
Proximal
Distal
Lithofacies 9
Lithofacies 5
Lithofacies 1
Lithofacies 6
Interlaminated heterolith
FS
Retrogradational
Aggradational
Retrogradational
TST
HST
TST
LST
TS
Sequence Boundary
Transgressive Surface (TS)
Clay
F. Silt
C. Silt
V.F. Sand
Proximal
Distal

Stacking patterns are affected by changes in relative shoreline (Catuneanu and Zecchin, 2013). In deep-water systems, relative sea level rise is commonly preserved as packages of gradually deepening facies (recorded as a gradual increase in gamma ray) overlying a maximum regressive surface (MRS) and below a maximum flooding surface (MFS). Regressive strata correspond to shallowing upwards or gradual upwards decreasing gamma-ray activity above an MFS and below an MRS. T-R cycles are bounded by the beginning of transgressive events (Johnson et al., 1985), and identified in the offshore realm by the maximum regressive surface (Embry and Johannessen, 1992). The combination of MRSs and MFSs was used to define stacked T-R cycles (Figure 6). Transgressive-regressive cycles bounded by MRSs preserve the genetic relationships between parasequences in environments without preserved sharp or abrupt flooding events (Embry, 1990; 2002). T-R cycle boundaries correspond to subaerial unconformities updip, significant time equivalent records of sea level fall, allowing regional chronostratigraphic correlation (Embry 2002). T-R cycles share many shortcomings of the genetic sequence model of Galloway (1989) (also called an R-T cycle), including the influence of sedimentation on sequence boundary formation, which become potentially diachronous. However, T-R cycles are less likely to include genetically unrelated material within the same sequence and are more effectively integrated with the subaerial unconformity sequence boundaries of depositional sequence models (Embry, 2002; Catuneanu et al., 2009).

T-R cycles were correlated from well to well across the eastern Uinta Basin based on stratigraphic position as well as well log morphology or logfacies and available core and nearby outcrop data. These regional correlations were used to identify the regionally

correlative genetic units within the Mancos Shale in order to develop an internal stratigraphic architecture and roughly chronostratigraphic framework of surfaces (MRSs) through the formation. Wherever possible, the top of the Lower Castlegate (Lawton, 1986) was used to datum stratigraphic cross sections because it is regionally extensive and easily identified by a blocky, clean log signature associated with fluvial channels overlain by the Buck Tongue transgression (Yoshida, 2000), is roughly time correlative (Fouch et al., 1983), and is the typical datum of Upper Cretaceous cross sections by other workers (e.g., Yoshida, 2000; Hampson et al., 2001; Kirschbaum, 2003; Johnson 2003b; Pattison, 2005). Most correlations were based on approximately 5 mi (8 km) well-to-well spacing. This frequency captures lateral changes in stratigraphy and fits the availability of well data.

Results

The regional extent and architecture of T-R cycles through the Mancos Shale is evaluated from three cross sections (Figures 7, 8, and 9) and the observed patterns and north-to-south variations are summarized (Figure 10). T-R cycles are mapped across the basin at three scales, the 4^{th}, 3^{rd}, and 2^{nd} order, each identified by their approximate depositional duration in geological time; 4^{th} order record several hundred thousand, 3^{rd} order a few million, and 2^{nd} order a couple tens of millions of years (Slatt and Rodriguez, 2012). 4^{th} order cycles are the fundamental unit of regional correlation because they are the smallest regionally correlative interval of genetically related strata in the Mancos, and demonstrate a number of fluctuations in sedimentation across the study area. In contrast, higher rank cycles, of the 3^{rd} and 2^{nd} order, demonstrate consistent stacking patterns

Figure 7: West to east stratigraphic cross section hung on top of the Lower Castlegate across 25 mi (40 km) of the southeastern Uinta Basin (Figure 4). Gamma ray logs plotted with scales of 0 to 170 API. 4th order T-R cycles (1–27) document variations in stacking patterns, shoreward stepping (blue), basinward stepping (yellow), and vertically stepping (green) throughout the Mancos Shale. Relative shoreline trajectory and hence relative sea level is described at the right (red = regression, blue = transgression, green = aggradation) and indicates the presence of four 3rd order cycles. Each 4th order cycle is bounded by an upper and lower MRS, and includes a marked MFS. Well # and associated details are listed in Appendix A.

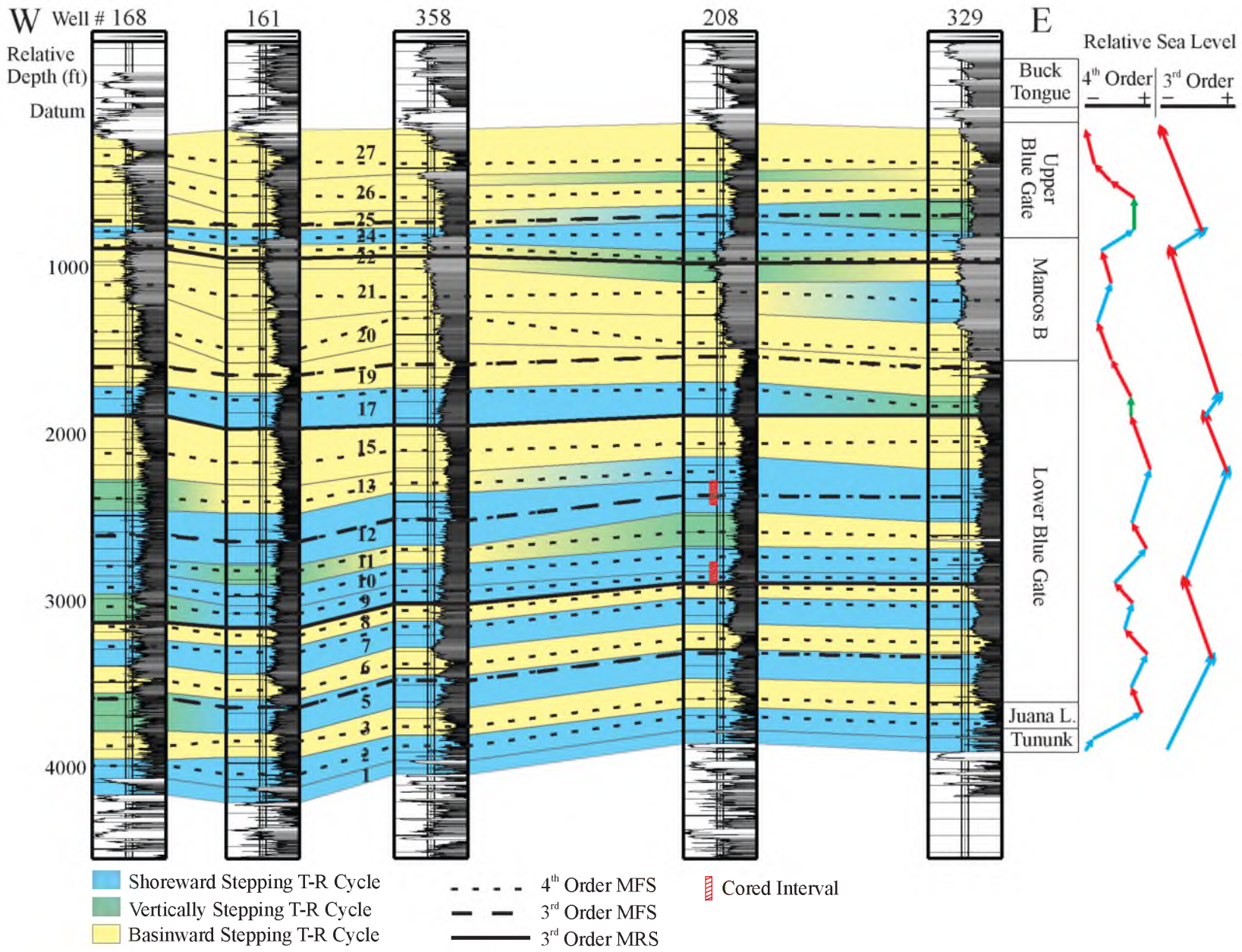
W
Well # 168
161
358
208
329
E
Relative Depth (ft)
Datum
1000
2000
3000
4000
27
26
25
24
22
21
20
19
17
15
13
12
11
10
9
8
7
6
5
3
2
1
Relative Sea Level
4th Order
3rd Order
Buck Tongue
Upper Blue Gate
Mancos B
Lower Blue Gate
Juana L.
Tununk
Shoreward Stepping T-R Cycle
Vertically Stepping T-R Cycle
Basinward Stepping T-R Cycle
4th Order MFS
3rd Order MFS
3rd Order MRS
Cored Interval

Figure 8: West to east stratigraphic cross section hung on the top of the Lower Castlegate across 30 mi of the northeastern Uinta Basin (Figure 4). Gamma ray logs plotted on 0 to 170 API scale. 4th order T-R cycles (1–29) are illustrated to document variations in stacking patterns throughout the Mancos Shale. MRS and MFS of four 3rd order T-R cycles are identified. Net changes of relative sea level are indicated (right), blue arrows indicate rising sea level, red arrows indicate falling sea level, and green indicates no net change. Well # and associated details listed in Appendix A.

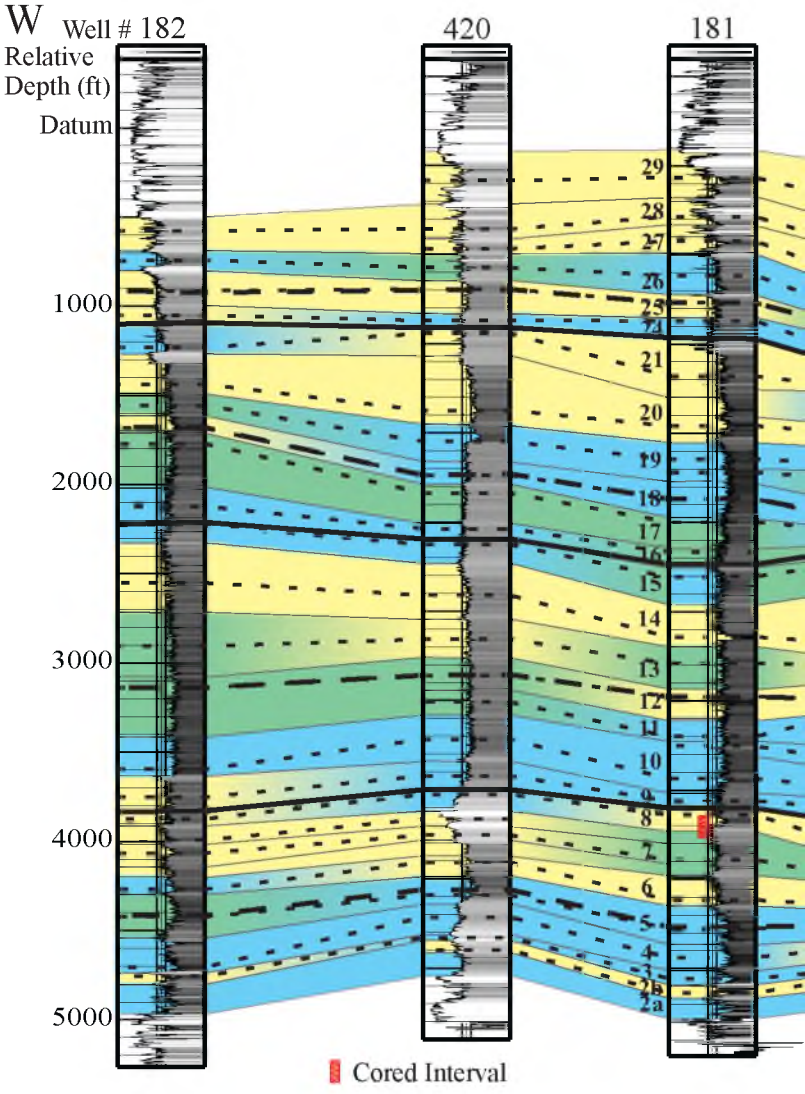
W
Well # 182
420
181
Relative
Depth (ft)
Datum
1000
2000
3000
4000
5000
29
28
27
26
25
24
21
20
19
18
17
16
15
14
13
12
11
10
9
8
7
6
5
4
3
2b
2a
Cored Interval

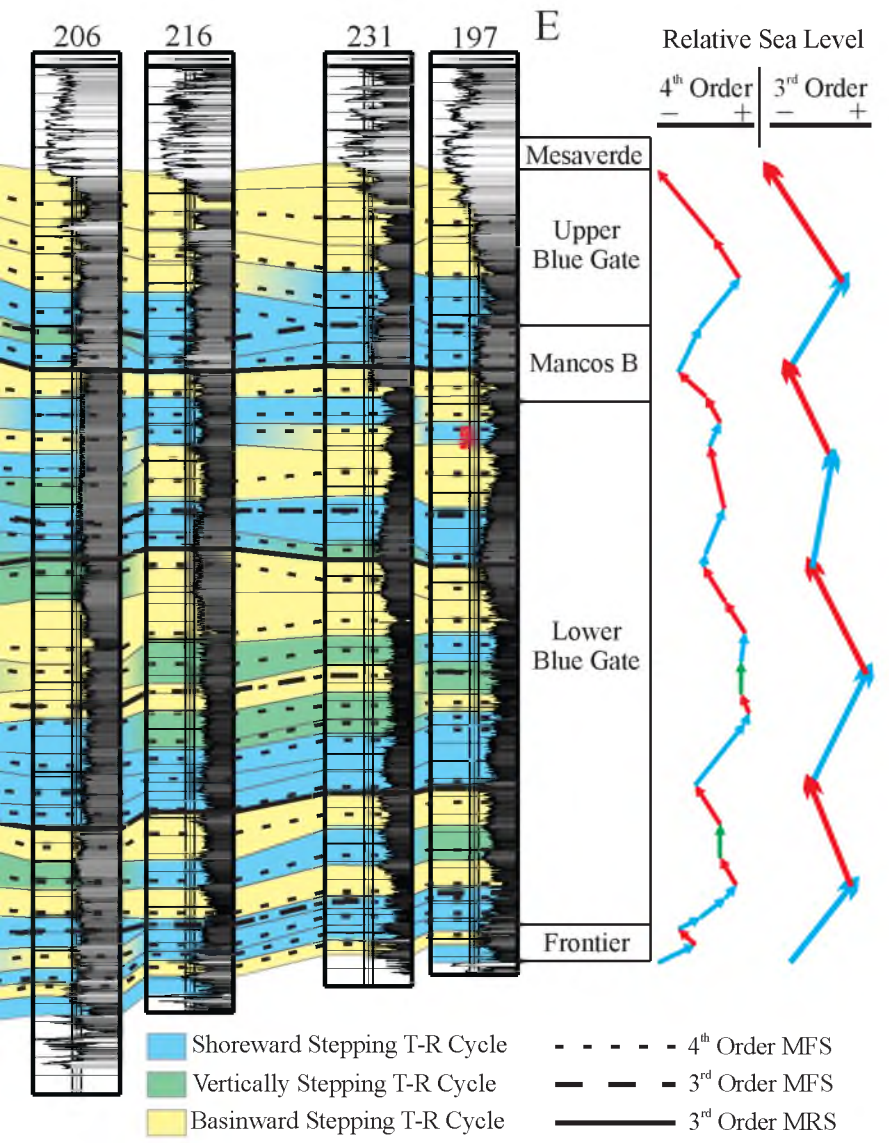
206
216
231
197
E
Relative Sea Level
4th Order
3rd Order
– +
– +
Mesaverde
Upper Blue Gate
Mancos B
Lower Blue Gate
Frontier
Shoreward Stepping T-R Cycle
Vertically Stepping T-R Cycle
Basinward Stepping T-R Cycle
4th Order MFS
3rd Order MFS
3rd Order MRS

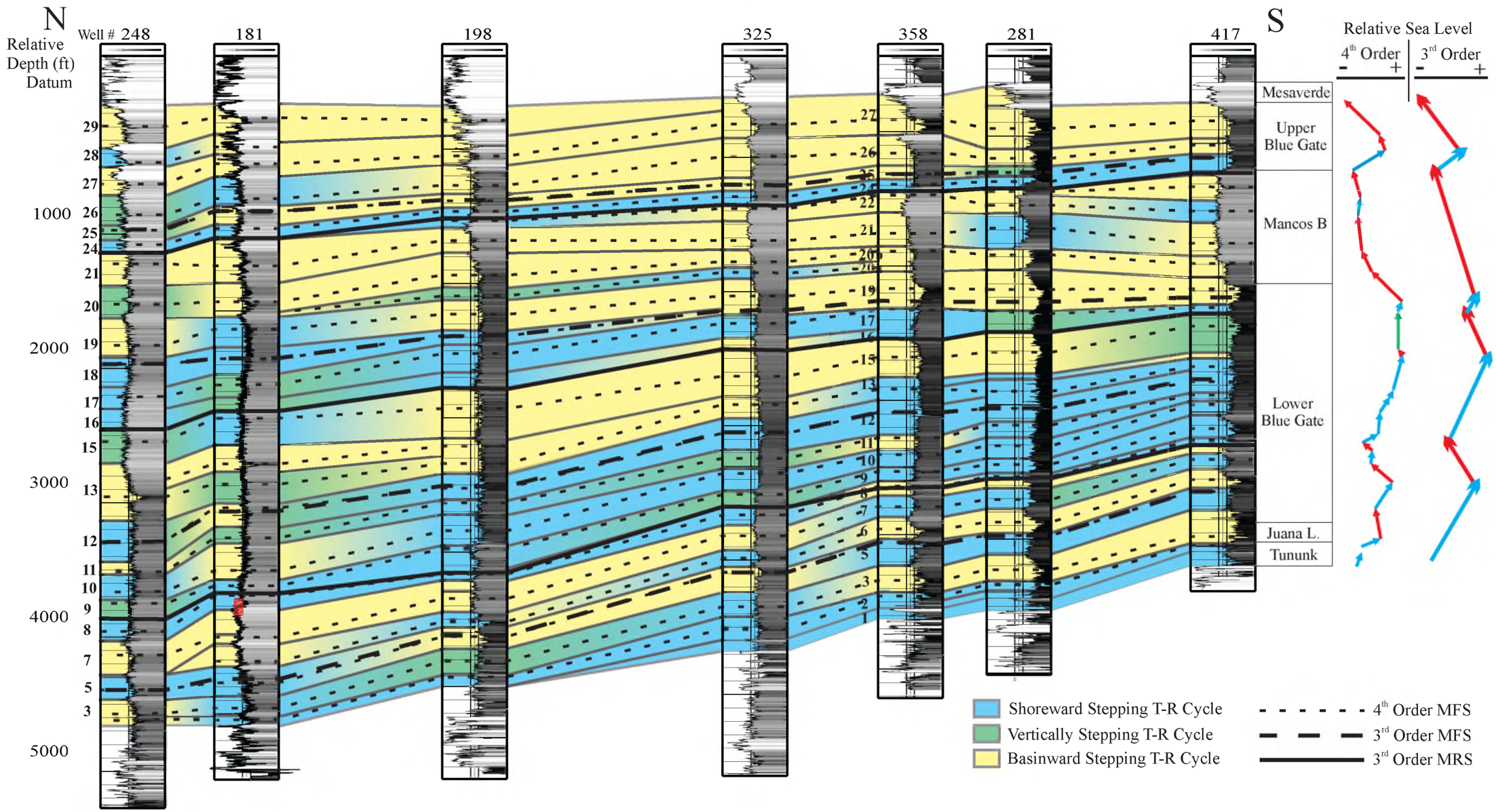

Figure 9: North to south stratigraphic cross section hung on top of the Lower Castlegate across 60 mi of the eastern Uinta basin. Gamma ray logs are plotted on a 0 to 170 API scale. 4th order cycles (1–29) document variations in stacking patterns, shoreward stepping (blue), basinward stepping (yellow), and vertically stepping (green) throughout the Mancos. Relative shoreline trajectory and hence relative sea level is described at the right (red = regression, blue = transgression, green = aggradation) and indicates the presence of four 3rd order cycles. Each 4th order cycle is bounded by an upper and lower MRS and includes a marked MFS. Well # and associated details listed in Appendix A.

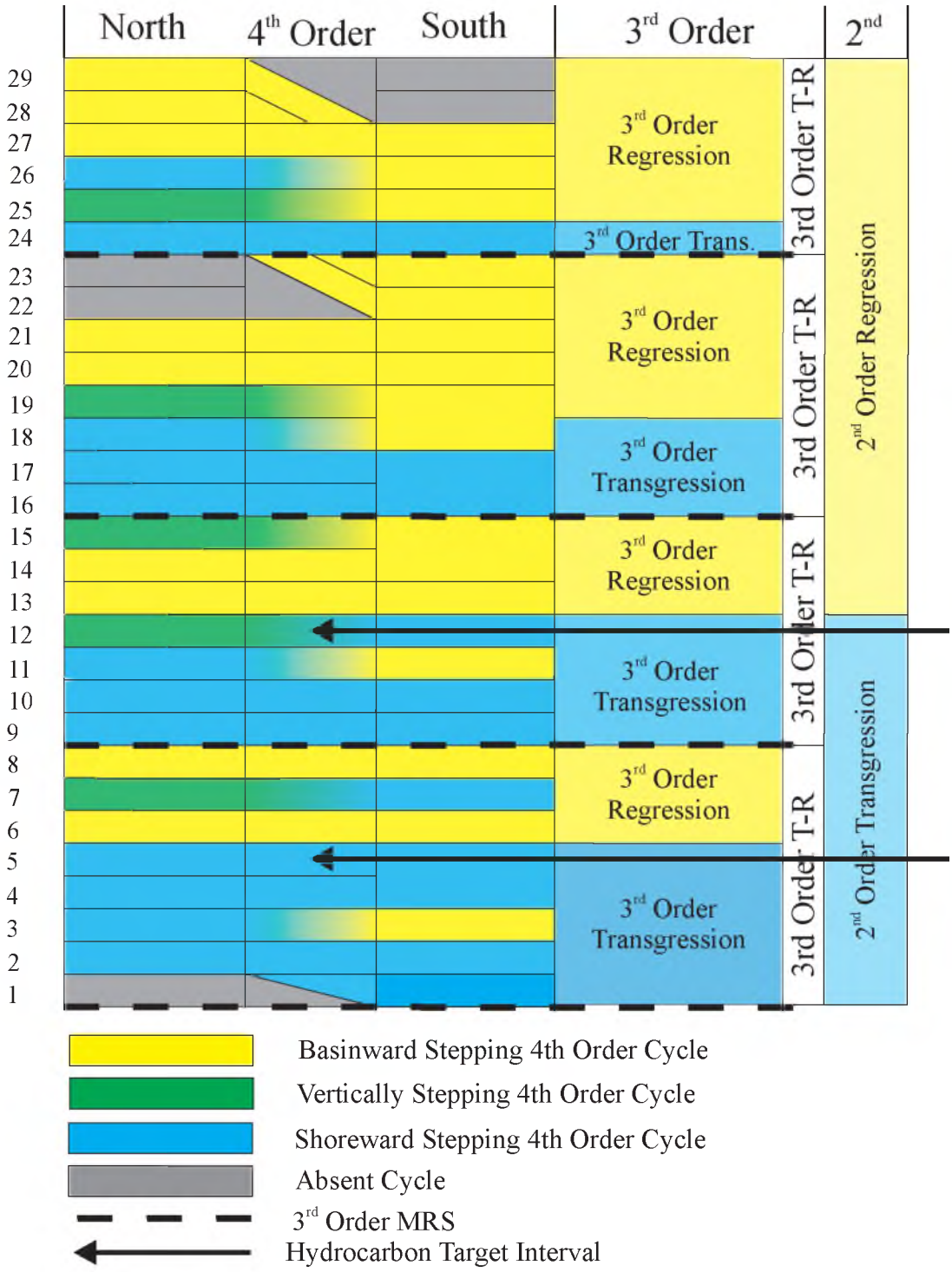

Figure 10: Summary of stacking patterns observed in 4th order T-R cycles from northern and southern portions of the Uinta Basin (Figures 7 and 8). 4th order cycles listed along left edge (1 to 29). 2nd and 3rd order cycles identified along right side of figure, broken into transgressive and regressive intervals.

across the study area, suggesting uniform dominant depositional controls across the basin.

The distal Mancos Shale in the eastern Uinta Basin contains twenty-nine 4th order T-R cycles between the underlying Dakota Formation and overlying Mesaverde Group. These T-R cycles are numbered 1 through 29 (oldest to youngest) and are correlated through the study area (Figures 7, 8, and 9). However, not all 4th order T-R cycles are found in all areas of the basin; some cycles are truncated by others. For instance, cycle 24 truncates 22 and 23 (Figure 9). Some cycles amalgamate with others laterally, such as 16 and 17 (Figures 9 and 10). The T-R cycles vary in vertical thickness from less than 100 ft (30 m) to more than 300 ft (90 m) and can be traced laterally across much of the study area, an area of about 1,000 mi^2 (2,600 km^2).

4th order T-R cycles are each assigned a dominant stacking pattern, either basinward stepping (i.e., progradational or net regressive) or shoreward stepping (i.e., retrogradational or net transgressive), based on the net change in relative sea level from the upper MRS of one cycle to the upper MRS of the underlying cycle. Some cycles, without a clear net change in relative sea level, are considered vertically stepping (aggradational). In general, most correlative 4th order T-R cycles share dominant stacking patterns, so genetically related strata will demonstrate consistent changes in the position of relative shoreline across the study area. However, there are time-equivalent changes in stacking patterns from well to well, demonstrating some local controls on this scale, such as cycle 7, which dominantly steps shoreward in the south and east, but basinward in the north and west (Figures 8 and 9).

East-west cross sections through the eastern Uinta Basin (Figures 7 and 8) illustrate internal Mancos stratigraphy as well as regionally significant trends in basinward stepping versus shoreward stepping stacking pattern distribution in 4th order T-R cycles. The well log gamma-ray morphology follows similar patterns laterally and vertically throughout the cross section, generally characterized by sharp changes in shoreline movement at MRSs, and more gradual changes during MFSs. These high gamma-ray bow trends are typical of mudstone-rich, clastic sedimentation in basinal settings unconstrained by base level (Milton and Emery, 1996). The high gamma-ray bow indicates a mud-dominated system, with sharp MRS inflections typical of rapid, coarse-grained depositional events.

Variations are also present in the 4th order T-R cycle record between the northern and southern portions of the basin (Figures 9 and 10). The northern portion of the Mancos Shale is roughly 40% thicker than the south, but this is not accommodated evenly though all of the T-R cycles. Thickening corresponds primarily with the middle (cycles 13–19) and upper (cycles 28 and 29) Mancos. Other intervals are of fairly uniform thickness across the study area, or are more dominant in the south. The lowermost Mancos (cycles 1 and 2) onlaps the underlying unconformity towards the north, where these cycles are not present. Some Mancos B equivalent intervals (cycles 22 and 23) are also missing from the north (Figures 9 and 10). The north is characterized by a greater abundance of vertically stepping 4th order T-R cycles. The addition of cycles 16 and 18 in the north causes the corresponding transgressive package, which is characterized only by cycle 17 in the south, to be significantly thicker in the north (Figure 9).

4th order T-R cycles are grouped by stacking patterns to establish alternating packages or sets of dominantly shoreward or basinward stepping strata. Cycles 1 through 5 indicate a consistently shoreward stepping interval, whereas the overlying cycles, 6 through 8, are dominantly basinward stepping (Figure 10). This pattern of alternating, regionally significant shoreward and subsequently basinward stepping 4th order T-R cycles is found throughout the Mancos in the eastern Uinta Basin. Four laterally continuous shoreward stepping packages, consisting of cycles 1 through 5, 9 through 12, 16 through 18, and 24 alternate with four basinward stepping packages, consisting of cycles 6 through 8, 13 through 15, 19 through 23, and 25 through 29 (Figure 10).

Combining a shoreward stepping package of 4th order T-R cycles with an overlying basinward stepping package of 4th order T-R cycles defines a 3rd order T-R cycle, including the net transgression and subsequent net regression of shoreline bounded by regionally extensive, 3rd order MRSs. The Mancos Shale contains four 3rd order T-R cycles, made up of 4th order cycles 1 through 7, 8 through 15, 16 through 23, and 24 through 29, respectively.

Dominant shoreline directional (basinward vs. shoreward) stacking patterns of these 3rd order T-R cycles are consistent throughout the entire study area (Figures 7, 8, and 9), though thicknesses of individual 3rd order T-R cycles vary, largely from north to south, more so than east to west. The basal 3rd order cycle thins to the north, onlapping the underlying mid-Turonian unconformity, whereas the upper three 3rd order cycles thicken to the north. The shoreward stepping cycles of the upper two 3rd order cycles are thicker to the north, but record a similar magnitude facies change as thinner packages to the south, suggesting the transgression in the south was more abrupt or more poorly

preserved (Figure 9). Based on the relative sea level indicated by MRSs between 3rd order T-R cycles, the lower two 3rd order cycles (4th order cycles 1 through 12) can be considered dominantly shoreward stepping, whereas the upper two cycles (4th order cycles 13 through 29) are dominantly basinward stepping. These 3rd order stacking patterns can be integrated into a single 2nd order T-R cycle over the full interval of the Mancos Shale, with an MFS corresponding to 4th order T-R cycle 12 (Figure 10). 3rd order transgressive intervals are much thicker, and represent more significant base level shifts during 2nd order transgression than during the upper Mancos 2nd order regression. Conversely, 3rd order regressions are thicker and correspond to greater base level shifts during 2nd order regression than during the 2nd order transgression of the lower Mancos (Figures 7, 8, and 9).

Discussion

Whereas 3rd order stacking patterns recorded in the Mancos Shale are very consistent across the basin, variable stacking patterns of time-correlative 4th order T-R cycles are present in some cases (e.g., cycles 3, 7, and 19; Figures 7, 8, and 9), emphasizing the increasingly important influence of local depositional control over shorter timescales of deposition. These local variations in stacking patterns are most evident along the northern margin of the basin (Figure 8), but are evident from different intervals across the study area. Local variations suggest autocyclic influences on deposition, such as deltaic lobe shifting, local faulting, or updip hinterland changes in weathering or fluvial drainage patterns, are influencing sediment supply. This variability in stacking patterns emphasizes the importance of identifying regionally significant

patterns with the correlation between different areas of the basin. This mud-dominated environment displays a high degree of variability, indicative of the dynamic nature and depositional heterogeneity of the prodelta, mudbelt, and sediment-starved shelf depositional environments (*sensu* Horton, 2012). The basin-wide continuity of 3rd order cycles suggests these are controlled by increasingly allocyclic processes, such as eustasy and regional tectonics, whereas the lateral variability of many 4th order stacking patterns suggests an increased influence from local depositional processes that are likely modifying basin-wide controls.

The epicontinental Cretaceous Western Interior Seaway was a relatively shallow but wide basin filled predominantly by mud-dominated deposits. In this basin, small vertical changes in sea level would have had a significant impact on the shoreline location, such that the shoreline migrated long horizontal distances along the shallow shelf, perpendicular to shoreline (Franczyk et al., 1992), and coarse-grained material from shore could be deposited well into the basin. Specifically, abrupt changes in grain size and interpreted depositional proximity to paleoshoreline are evident from core. For example, the coal-bearing, paralic Ferron Sandstone Member is sharply overlain by marine mudstone (Kennedy, 2011). Additionally, admixed marine sandstone deposited in the proximal mudbelt is sharply overlain by laminated and massive claystone, distal sediment-starved shelf facies (Horton, 2012). Based on outcrop description and well log characteristics, a number of other depositional environments have been documented in the Mancos Shale. These include the isolated offshore sandstone and heterolithic bodies of the Mancos B (Cole et al., 1997) and distal Blackhawk Formation (Pattison, 2005; Pattison et al., 2007), as well as claystone-rich fissile shale of the Juana Lopez Member

(Molenaar and Cobban, 1991). Despite these abrupt stratigraphic changes in depositional environment and lithology within the Mancos Shale, the 3rd order stacking patterns remain consistent across the basin, suggesting the consequences of an allocyclically driven relative sea level change can be identified from wireline logs despite changes in marine depositional environments and associated lithofacies. 3rd order stacking patterns provide a robust model for identifying sequence stratigraphic patterns between various depositional environments of the marine realm.

Geochronology of the Mancos Shale is based in large part on biostratigraphy of lithostratigraphic members reported by Fouch et al. (1983) and Molenaar and Cobban (1991), with some modifications (e.g., Schwans, 1995; Ryer, 2004). The lower 3rd order T-R cycle, including 4th order cycles 1 through 7, corresponds with the Middle and Late Turonian and Early Coniacian based on the biostratigraphy of the Tununk, Juana Lopez, and Ferron Sandstone members (Molenaar and Cobban, 1991), with which the cycle is largely correlative (Figure 11). The overlying three 3rd order T-R cycles are less well constrained by biostratigraphy, but correspond to the Upper Coniacian, Santonian, and Lower Campanian portions of the Blue Gate Shale (Fouch et al., 1983). Regression of the second 3rd order cycle, including 4th order cycles 8 through 15, corresponds to the Middle Santonian Emery Sandstone (Fouch et al., 1983). Regression of the third 3rd order cycle corresponds to earliest Campanian Mancos B deposition (Anna, 2012), and the fourth 3rd order cycle terminates at the base of the Middle Campanian Castlegate Formation (Fouch et al., 1983) (Figure 11). This chronology suggests the lower 3rd order T-R cycle records four million years of deposition, whereas the upper three cycles

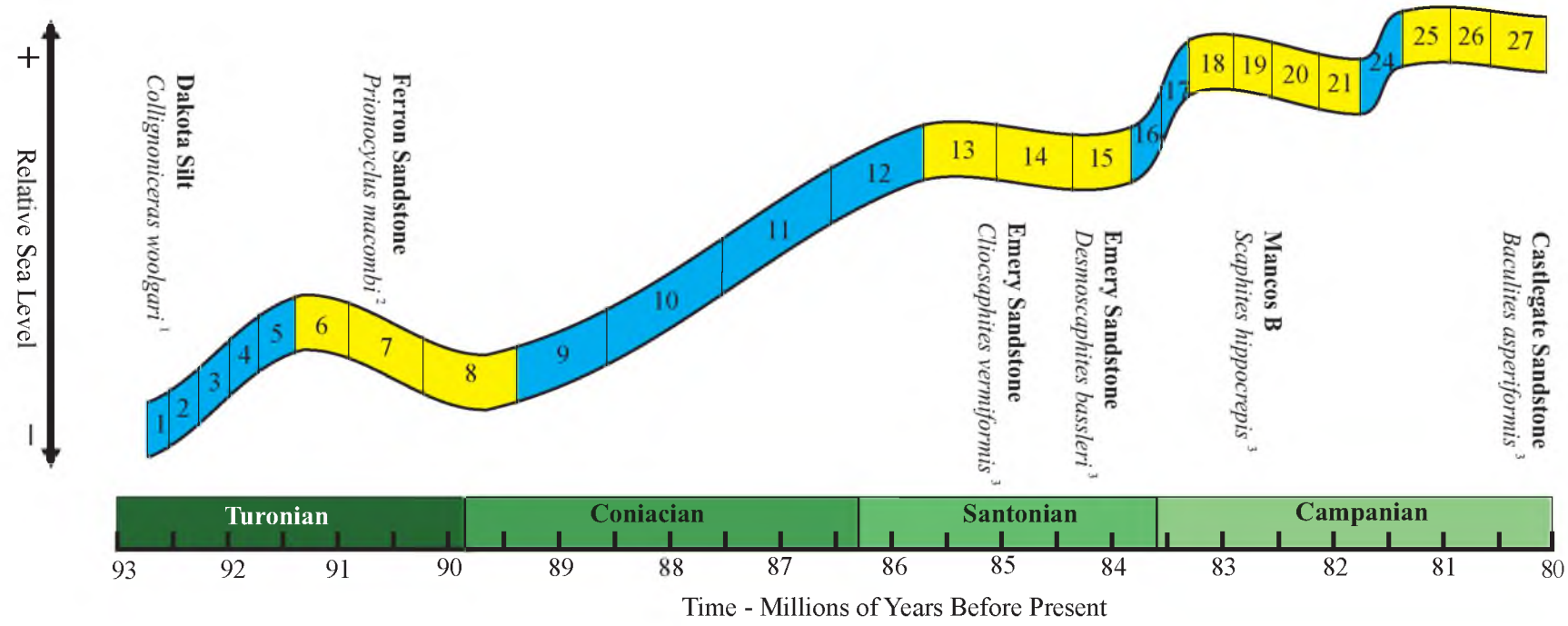

Figure 11: Relative sea level change over time during deposition of Mancos Shale, Uinta Basin based on variations in stacking patterns of 4th order T-R cycles (Figures 7, 8, and 9). Each 4th order T-R cycle is labeled (1-29) based on its relative stratigraphic position and is colored based on dominant stacking trends. Blue indicates transgression and yellow indicates regression. Biostratigraphic control points are indicated.

[1]Molenaar and Cobban (1991); [2] Gardner et al. (2004); [3] Fouch et al. (1983)

together record about twelve million years, each cycle corresponding to three to five million years.

The distribution of transgressions and regressions in the Mancos suggests a semi-periodicity to the 3rd order T-R cycle in the Western Interior Seaway (Figure 11). Similar trends exist in a number of eustasy-proxy curves from the Upper Cretaceous (Miller at al., 2003) (Figure 12). Although available geochronology lacks sufficient resolution to confirm these global relationships (Miall, 1992; 1994), regressions in the Mancos Shale may correlate with regressions in other geologic records (Figure 12), suggesting a common, eustatic trigger may contribute to periods of falling relative sea level. Previous work on the Western Interior Seaway has focused on a few, longer term cycles like the Greenhorn and Niobrara Cyclothems (Kauffman, 1969; Tibert et al., 2009), which appear to match the 2nd order trends observed in the Mancos Shale, suggesting a higher rank pattern may be controlled by the tectonics of the Sevier thrust belt and corresponding foreland basin. 3rd order transgressions in the Mancos stratigraphic scheme presented here appear thin and of low magnitude when they occur during periods of 2nd order regression. For example, cycle 24 alone constitutes the entire transgressive interval of the uppermost 3rd order cycle.

During the greenhouse conditions of the Late Cretaceous, glacioeustasy was suppressed (Arthur et al., 1985). Instead, eustasy was driven by global tectonic and oceanic thermal histories. Although the relative influence of tectonics and eustasy remains complicated at many orders of sedimentary cyclicity (Gardner, 1995a), it appears likely that tectonically driven controls on accommodation remain a driving influence of high-rank rock record cyclicity in this epicontinental foreland basin, while global eustatic

Figure 12: Correlation of Mancos Shale stratigraphy and global eustatic record, calibrated to Gradstein et al. (2012) timescale. Eustatic curves based on Haq et al. (1987), Hardenbol et al. (1998), Miller et al. (2005), Haq and Schutter (2008), and Kominz et al. (2008). Mancos correlations based on available biostratigraphy. Strong correlations exist between the SEPM 98 T-R cycle record and regressive strata in the Mancos Shale. Additional eustatic curves demonstrate high degree of variability and inconsistency in the sea level record.

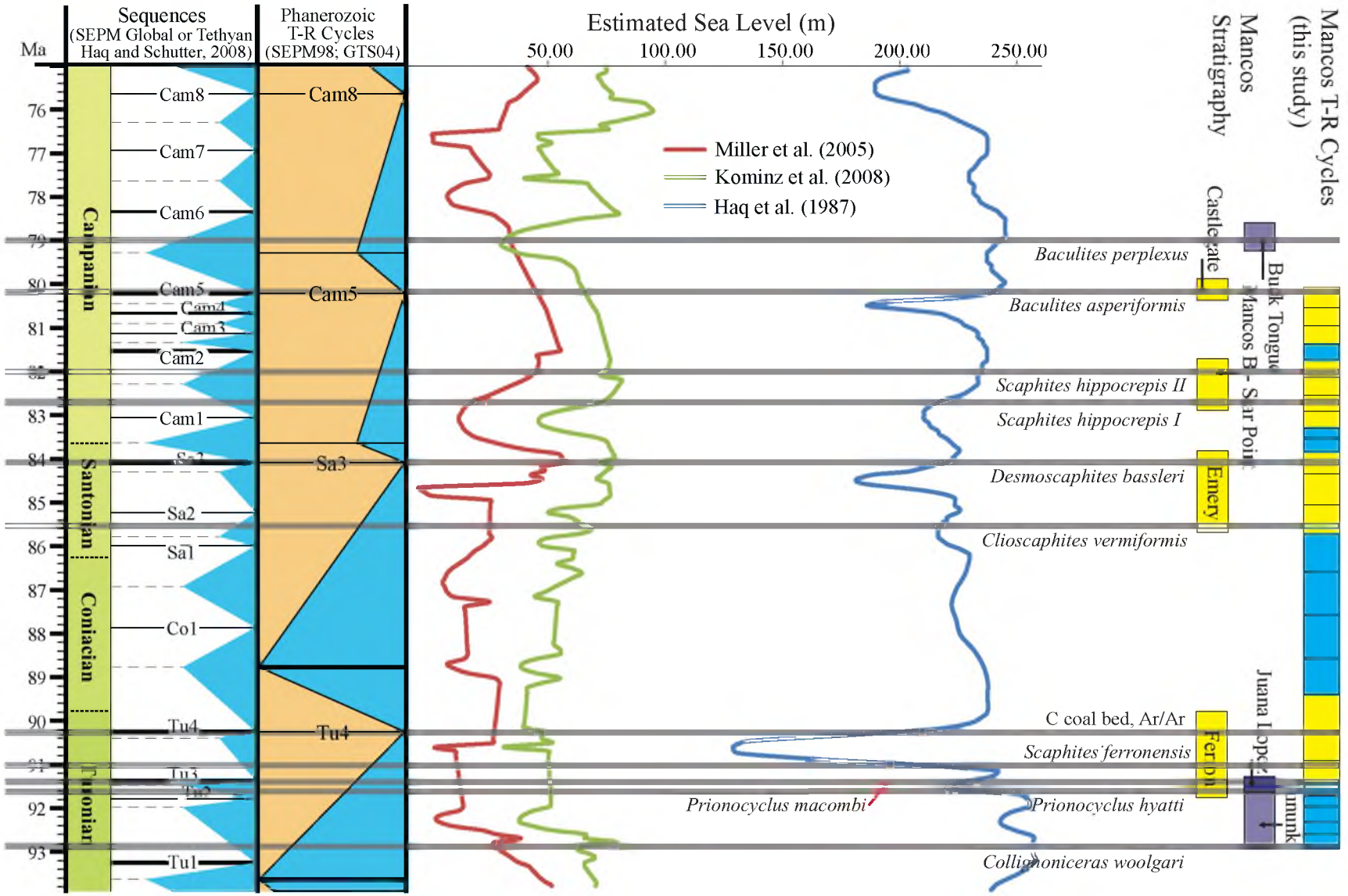
Sequences
(SEPM Global or Tethyan
Haq and Schutter, 2008)
Phanerozoic
T-R Cycles
(SEPM98; GTS04)
Ma
Estimated Sea Level (m)
50.00
100.00
150.00
200.00
250.00
Miller et al. (2005)
Kominz et al. (2008)
Haq et al. (1987)
Mancos T-R Cycles
(this study)
Mancos
Stratigraphy
Campanian
Santonian
Coniacian
Turonian
Cam8
Cam7
Cam6
Cam5
Cam4
Cam3
Cam2
Cam1
Sa3
Sa2
Sa1
Co1
Tu4
Tu3
Tu2
Tu1
Castlegate
Bulk Tongue
Mancos B - Star Point
Emery
Ferron
Juana Lopez
Munk
Baculites perplexus
Baculites asperiformis
Scaphites hippocrepis II
Scaphites hippocrepis I
Desmoscaphites bassleri
Clioscaphites vermiformis
C coal bed, Ar/Ar
Scaphites ferronensis
Prionocyclus macombi
Prionocyclus hyatti
Collignoniceras woolgari

effects are reflected at the 3rd order level. Diecchio and Brodersen (1994) identified similar patterns in Ordovician foreland basin deposits of West Virginia, where five million year, 3rd order cyclicity was tied to a eustatic signal, and longer-lived, more local variations in deposition related instead to tectonic uplifts and basin subsidence. Other Appalachian basin strata display cyclicity on the 3rd, 4th, and lower rank scales, including the Devonian (Brett and Baird, 1996) and Upper Mississippian (Miller and Eriksson, 2000); T-R cycles appear typical of these marine foreland basin deposits, like they do in the Mancos.

Paleoshoreline of the Cretaceous Western Interior Seaway trended roughly north to south, although it may have had a southwest-northeast strike through much of Utah, corresponding roughly to strike of outcrops along the Wasatch Plateau (Franczyk et al., 1992). Uneven deposition driven by sediment source locations, such as the location of Ferron deltas or concentration of sediment by longshore drift, could be causes of stratigraphic thickness changes (Ryer, 2004). However, thickening occurs predominantly in stratigraphy overlying the Ferron, in cycles 13 through 18 (Figure 9), during which time shallow marine strata updip, such as the Emery Sandstone, was wave dominated (Edwards et al., 2005), which limited the influence of sediment point sources on deposit thickness. The dominant thickening trend in the Mancos Shale is from the south to the north, opposite of Western Interior Seaway dominant longshore currents and perpendicular to the strike of paleoshoreline. This suggests thickening from south to north is not controlled by longshore drift or other depositional processes.

It is likely that the thickening of Mancos strata corresponds to tectonically driven differential subsidence along the foredeep of the Sevier foreland basin. Backstripping of

Upper Cretaceous foreland basin deposits by Pang and Nummedal (1995) indicates that through the Turonian, subsidence occurred more rapidly in central Utah than Wyoming, corresponding with a period of along strike onlap to the north in the lowermost Mancos T-R cycles (Figures 10 and 13). However, during the Coniacian and Santonian, subsidence increased in Wyoming, but decreased in central Utah. In the northern portion of the Uinta Basin, additional 4th order T-R cycles thicken the Santonian portion of the Mancos Shale, corresponding to rapid subsidence in the north recognized by Pang and Nummedal (1995). The southern portion of what is now the Uinta Basin likely subsided more slowly, like central Utah, where decreased accommodation corresponds with thinner equivalent strata. The Uinta Basin records the transition between rapid subsidence in Wyoming and slower rates in southern Utah. Local variations in tectonics are the primary driver of regional thickness changes from north to south.

The preservation of organic matter in mudrock is driven by the complex interplay of numerous factors, including ocean anoxia (Demaison and Moore, 1980), and primary production, dilution, and destruction of organic material during deposition (Sageman et al., 2003; Bohacs et al., 2005). Despite the complex and dynamic conditions of marine shale deposition, there appears to be a dominant sequence stratigraphic relationship with the distribution of organic matter, which is most densely preserved at the condensed interval of the transgressive systems tract (Creaney and Passey, 1993; Bohacs, 1998; Slatt and Rodriguez, 2012) and corresponds to the transgressive portion of the T-R cycle. This sequence stratigraphic framework matches trends observed in the Mancos from the San Juan Basin, in which TOC was concentrated most strongly along the condensed intervals at the top of transgressive strata (Pasley et al., 1991; 1993). Similarly, target reservoir

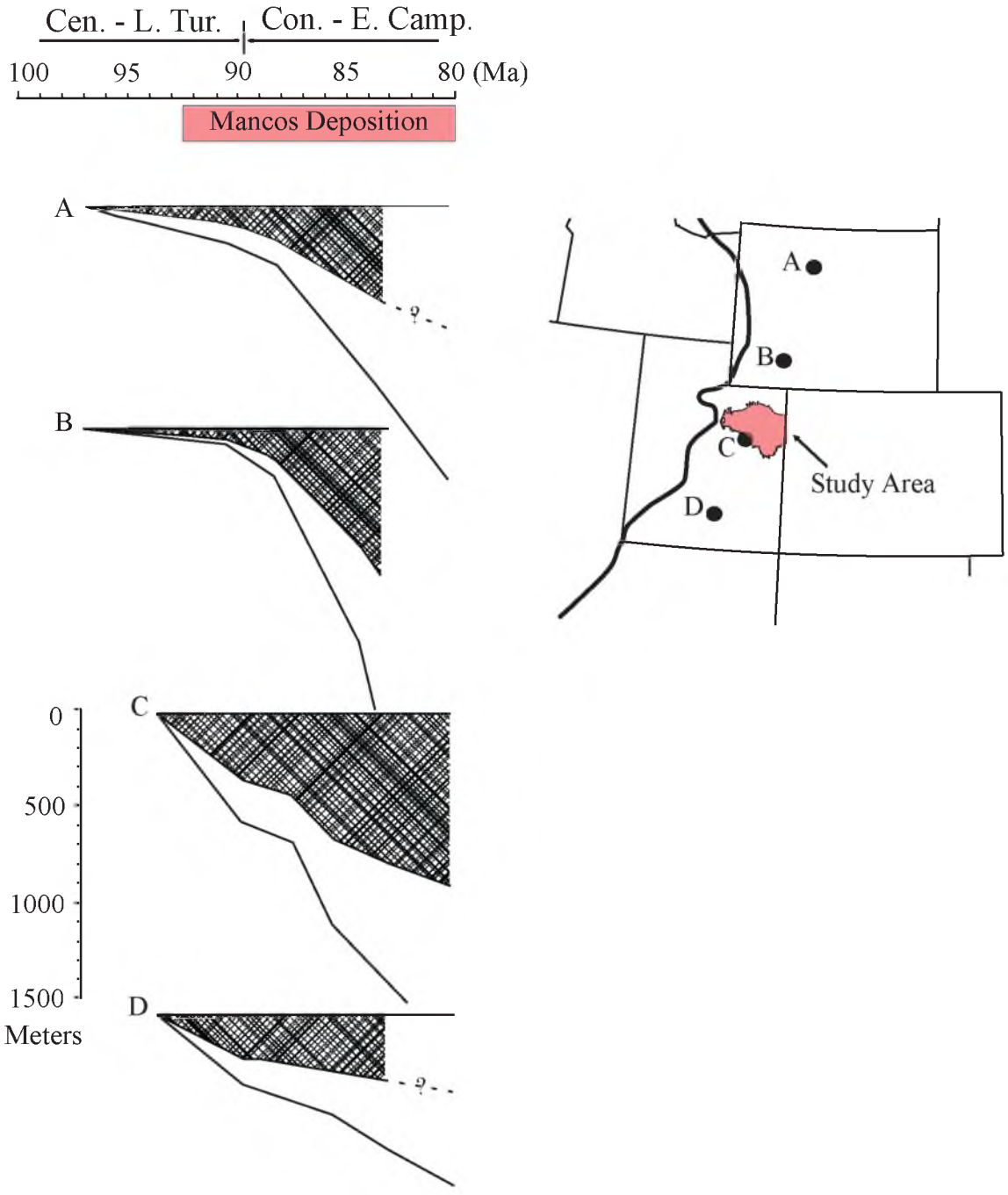

Figure 13: Backstripping analysis of subsidence history along the Sevier foreland basin. Fluctuations in subsidence north (B) and south (C) of the study area reflected in the variable character of Mancos deposition over time.

Modified from Pang and Nummedal (1995).

facies, those with the most TOC and calcite-rich facies, are observed within transgressive deposits from Mancos core (Kennedy, 2011; Horton, 2012).

Shale gas plays require a minimum thickness, generally >200 ft (60 m), and sufficient maturation history, >1.1% Ro (Slatt and Rodriguez, 2012), which can each be estimated by mapping sequence stratigraphic units and building a basin model, respectively. The strong relationship between sequence stratigraphic depositional cycles and production parameters suggests that effective mapping of these units is critical for hydrocarbon evaluation and prospect development, particularly in a unit as thick as the Mancos Shale, where horizontal targets must be highgraded.

The Mancos Shale, which ranges from 3,500 ft (1,070 m) to 5,000 ft (1,525 m) thick across the study area, provides a unique challenge for development as a horizontal petroleum resource play, because there are a wide variety of lithologies within the previously undifferentiated formation. Hydraulic fractures can generally be expected to communicate with several hundred vertical feet of rock (King, 2012), only a small portion of the Mancos thickness. The identification of 2^{nd}, 3^{rd}, and 4^{th} order T-R cycles allows the mapping of strata of relevant production thickness that have been tied to sequence stratigraphy. Both 2^{nd} and 3^{rd} order sequence stratigraphy can be correlated to the lithologic properties of the corresponding strata, so both should be considered when identifying potential production intervals. Cycle 12 represents the most prospective T-R cycle for production based on its correlation to 2^{nd}, 3^{rd}, and dominantly 4^{th} order transgression (Figure 10). Cycle 12 is the most distal expression of the 3^{rd} order transgression, which also includes underlying cycles 9 through 11. Cycles 1 through 5 also correspond to potentially prospective transgressions, with cycle 5 representing the

maximum transgression and most prospective cycle of this lowermost 3rd order cycle (Figure 10). Cycles 1-5 display a regional extent similar to stratigraphically higher transgressive units, like those of cycles 9-12, but likely reflect more proximal depositional environments relative to cycles 9-12 based on the more proximal position of relative shoreline at the beginning of the transgression.

Conclusions

Transgressive-regressive (T-R) cycles can be identified at a number of different scales throughout offshore marine mudstones of the Mancos Shale. In this distal marine shale, traditional sequence stratigraphic correlative conformities are often cryptic; based on detailed core studies (e.g., Kennedy, 2011; Horton, 2012), changes in the relative proportion of claystone versus siltstone and sandstone, as recorded in gamma ray logs, provide an effective tool for determining relative changes in sea level. The relative position of sea level can be determined during deposition by considering the change in claystone content between one T-R cycle and the overlying cycle. Wireline logs taken from the Uinta Basin identify twenty-nine 4th order T-R cycles that are stacked into four 3rd order cycles, which contribute to a single 2nd order cycle of relative sea level change. 4th order cycles can be genetically correlated across the basin, but display some regional variations in stacking patterns, demonstrating the influence of autocyclic processes that modify allocyclic controls (or vice versa) at this scale. The stacking patterns of 2nd and 3rd order T-R cycles in the Mancos are consistent across the basin, suggesting these are controlled by allocyclic processes and are a viable tool for predicting facies changes throughout the formation.

The lower Mancos Shale is dominated by transgression whereas the upper Mancos Shale is largely regressive, a trend which defines the dominant 2nd order T-R cycle of the formation. The four 3rd order T-R cycles each record about four million years of depositional history, the timing of which may be driven by corresponding eustatic fluctuations. This eustatic signal is moderated by tectonically driven temporal changes in subsidence, which define the over-arching cycle of growth and decay of the Western Interior Seaway during the Late Cretaceous. Regional thickness trends within the Mancos also appear to be controlled largely by tectonic activity, specifically a regional increase in tectonic subsidence rate from south to north, and provide insight into the timing and magnitude of changes to basin structure. The evolution of stacking patterns provides a valuable tool for placing the significant facies heterogeneity within the Mancos Shale (Kennedy, 2011; Horton, 2012) in a useful context and within a predictable framework.

By relating the relative hydrocarbon potential of the shale to sequence stratigraphy, T-R cycles can be used as a first-pass tool for identifying prospective target intervals within a thick offshore marine mudstone like the Mancos. In the Mancos Shale, two major transgressions, corresponding to 4th order T-R cycles 5 and 12, offer promising intervals for production because they correspond to the maximum transgression during the lower two 3rd order T-R cycles, which also record the overall deepening of the Cretaceous Western Interior Seaway (a 2nd order cycle). Cycle 12 is likely the most prospective because it also corresponds to the 2nd order T-R cycle maximum flooding surface, the sediment starved shelf facies of the Mancos Shale deposited during the highest relative sea level (Horton, 2012). This differentiation of the 4,000 ft (1,220 m)

thick shale allows the identification of producible intervals, which can be targeted for horizontal drilling and hydraulic fracturing.

CHAPTER 2

DEPOSITIONAL SEQUENCE STRATIGRAPHY AND HYDROCARBON POTENTIAL OF THE MANCOS SHALE, UINTA BASIN, UTAH

Abstract

The Mancos Shale, a marine offshore mudstone that was deposited in the Cretaceous Western Interior Seaway, is a potentially significant hydrocarbon resource. In the Uinta Basin of eastern Utah, the identification of productive sweet spots is critical to efficient economic production from this 4,000 ft (1,220 m) thick formation. However, a unified basin-wide facies and sequence stratigraphic correlation that tests the lateral viability of existing outcrop and core-based geological models to identify reservoir target intervals for the Mancos Shale is still lacking. Furthermore, seminal sequence stratigraphic models were developed from updip shallow marine and fluvial units exposed in the Book Cliffs, but these models have never been extended in detail to the full thickness of correlative offshore deposits of the Mancos Shale. 157 wireline well logs were chronostratigraphically correlated across the basin to build a regional subsurface map and cross sections that highlight facies relationships, illustrate regional stratal architecture, and analyze sequence stratigraphic stacking patterns within a depositional framework.

Previous core analysis in combination with the examination of previously studied outcrops and the new log correlation presented herein suggest reservoir targets correspond with two organic rich facies associations found in two nonadjacent stratigraphic intervals of the Mancos Shale, Uinta Basin, respectively, each corresponding to the transgressive and early highstand sequence sets. These include: 1) organic rich, heterolithic facies of the lowermost Blue Gate and Juana Lopez Members, which contain a high proportion of terrestrial organic matter and were deposited above storm wave base, and 2) sediment starved shelf deposits of the middle Lower Blue Gate, organic-rich (marine organic matter dominant), calcareous claystone to siltstone deposited below storm wave base. Variations in log signature, mudstone facies, and stacking patterns in the distal shale were controlled by fluctuations in relative sea level, basin geometry, and shoreline processes, which varied progressively over the fifteen million years of Mancos deposition. The sequence stratigraphic model presented here clearly defines paleodepositional updip to downdip genetic relationships between key lithostratigraphic units, including the updip Ferron and Emery Sandstones and Mesaverde Group, and downdip Tununk, Juana Lopez, Bluegate, Mancos B, and Buck Tongue members of the Mancos Shale. This study establishes a regionally significant depositional and sequence stratigraphic framework that can be tied to lithologic properties, which is critical for tight shale play evaluation and completion in the Mancos Shale of the Uinta Basin and other analogous offshore deposits of the Cretaceous Western Interior Seaway.

Introduction

The production of natural gas and oil directly from shale reservoirs in North America has provided abundant domestic energy production with the potential to phase out the burning of coal for electricity while decreasing dependence on foreign hydrocarbon imports (US Energy Information Administration, 2013). Between 2007 and 2012, American greenhouse gas emissions have declined by 450 million tons, a greater decline than anywhere else in the world, due in large part to the conversion from coal to natural gas fueled electrical generation (Wright, 2012). In order to continue development of this hydrocarbon resource into the future, identifying and characterizing additional hydrocarbon rich shales is critical to increasing production efficiency and volume.

The Uinta Basin of northeastern Utah has a long history of natural resource development, including extensive natural gas production from a number of Mesozoic sandstones. The Mancos Shale, an Upper Cretaceous marine shale, has long been interpreted as the source for many hydrocarbons in the basin (Kirschbaum, 2003), but has not had strong economic production in its own right (Curtice, 2013). The application of new production techniques, particularly horizontal drilling and hydraulic fracturing, could potentially improve the economics of hydrocarbon production from the Mancos Shale. The Mancos Shale has been the recent target of horizontal drilling for gas and oil in the San Juan Basin, as well as the neighboring Piceance Basin (Durham, 2012; Ridgley et al., 2013). Production from the Uinta Basin is lagging. Detailed formation evaluation is required to identify the most prospective reservoir target intervals in this thick, gray shale.

In the Uinta Basin, the Mancos Shale, which is more than 4,000 ft (1,220 m) thick, relatively organic-lean (1.36% average TOC; Horton, 2012), and was deposited during fifteen million years of the Upper Cretaceous, has not previously been the subject of a detailed, internal stratigraphic analysis. A number of cross sections from the Uinta Basin have been constructed over the last two decades based on well log, core, and outcrop data, although these have not presented a sequence stratigraphic framework for the Mancos Shale. Existing cross sections either focus in detail on a relatively small region and/or stratigraphic interval (e.g., Molenaar and Wilson, 1990; Molenaar and Cobban, 1991; Hampson et al., 1999; Anderson and Harris, 2006) or cover a large region but pick relatively few surfaces of correlation from within the main body of the Mancos Shale (e.g., Johnson, 2003a; Hettinger and Kirschbaum, 2003; Kirschbaum, 2003, Rose et al., 2004; Anna, 2012). Little research has focused on the internal stratigraphy of the Blue Gate Member, the thickest member of the Mancos Shale, which readily weathers in outcrop (Leythaeuser, 1973) and remains undifferentiated with either well log or seismic data.

A sequence stratigraphic and depositional model has been established for the Mancos Shale from detailed core description by Kennedy (2011) and Horton (2012), which needs to be placed in a wider stratigraphic context in order to identify the regional significance of these sedimentary facies relationships. Regional subsurface mapping of the lithofacies distribution within the Mancos Shale allows these strata to be placed in a sequence stratigraphic and depositional framework.

The Mancos Shale in the Uinta Basin provides valuable information regarding the transition in facies from proximal, shallow marine sandstones deposited along the

western margin of the Cretaceous Western Interior Seaway to the deep-water facies typical of Colorado (e.g., chalks and marls) and other more distal marine environments of deposition (Figure 3). The stratigraphy of Upper Cretaceous marine sandstones in Utah has been well documented from many miles of outcrop across the Colorado Plateau (Fouch et al., 1983). To the east, time equivalent marine shales in Colorado, including the Niobrara and Carlile Formations, have been well studied, in part because of their role in petroleum systems of the Denver Basin and other basins across central North America (Longman et al., 1998; Sonnenberg, 2011). Seminal models of sequence stratigraphy were developed in shallow marine lithologies updip of the Mancos Shale, including the Ferron Sandstone (Riemersma and Chan, 1991; Gardner et al., 2004), Panther Tongue member of the Star Point Formation (Posamentier and Morris, 2000), several members of the Blackhawk Formation (e.g., O'Byrne and Flint, 1995; Kamola and Van Wagoner, 1995), the Castlegate Sandstone (Van Wagoner, 1995), and more recent work on the Emery Sandstone (Edwards et al., 2005) (Figure 4). Chronostratigraphic correlation between these shallow marine and downdip mudstone deposits ties a detailed sequence stratigraphic model to the distribution of facies in the distal basin, illuminating an otherwise understudied relationship.

Sequence stratigraphy has proven particularly effective in analysis of most shale hydrocarbon plays, but has not yet been applied to a thick, organic-lean formation like the Mancos Shale. Major shale gas plays, including the Marcellus (Milici and Swezey, 2006), Barnett (Loucks and Ruppel, 2007), and Haynesville Shale (Hammes et al., 2011), are only a few hundred feet thick, so they can be developed with a single horizontal well completion (King, 2012). However, the Mancos is far too thick to be developed in this

way and previous vertical completions have not been economic, typically demonstrating high production decline rates (Curtice, 2013), so identifying and mapping the most prospective reservoir target intervals will be critical for efficient production.

In the Mancos Shale, promising reservoir lithofacies were characterized by sediment starved shelf deposition during the transgressive and early highstand systems tracts (Horton, 2012). The sediment starved shelf includes areas of deposition basinward of the influence of most hyperpycnal flows and instead is dominated by suspension settling (Horton, 2012). Characteristics of this facies include dominantly plane-parallel laminations, relatively fine-grained claystone to siltstone, a lack of bioturbation, the highest documented calcite content (avg. 29.0%), and correspond to indicators of "ideal" brittle deformation behavior observed from Mancos core (Kennedy, 2011). Establishing a sequence stratigraphic framework and depositional model for this formation allows for the predictive mapping of these lithofacies and identification of the most prospective reservoir intervals for production.

This study utilizes a database of several hundred well logs to create a basin-wide subsurface litho- and chronostratigraphic map of the Mancos Shale in the Uinta Basin. Log-based detailed correlations have been tied to various facies descriptions from outcrop (e.g., Molenaar and Cobban, 1991; Edwards et al., 2005; Anderson and Harris, 2006) and core (Kennedy, 2011; Horton, 2012) in order to extend a detailed lithofacies-based model of deposition into the subsurface throughout the Uinta Basin. Identified stratal architecture is placed in a sequence stratigraphic framework and used to identify various basin-wide and local influences on depositional style and corresponding hydrocarbon production potential.

Geologic Background

The Upper Cretaceous Western Interior Seaway of North America was formed in an actively subsiding foreland basin during a global sea level highstand; corresponding strata display the coupled influences of local tectonics and eustasy. Thrusting within the Sevier fold and thrust belt, which trended roughly north to south through central Utah (DeCelles, 1994), thickened the orogenic hinterland (Livaccari, 1991), which shed sediment into the adjacent foredeep (Johnson, 2003b). Episodic thrusting events along this active orogen contributed to uneven rates of subsidence in the adjacent foreland basin (Jordan, 1981; Pang and Nummedal, 1995) and rates of sediment supply from the thrust front. The Mancos Shale was deposited into this foreland basin between the Cenomanian and Lower Campanian, roughly 94 to 79 Ma, synchronous with several thrusting and subsidence events (Schwans, 1995).

The Late Cretaceous was a period of global sea level highstand and included a number of significant eustatic fluctuations (Haq et al., 1987; Miller et al., 2005). High organic carbon preservation during this time is associated with large volumes of off-ridge volcanism and accelerated sea floor spreading (Arthur et al., 1985), including three ocean anoxic events, which record periods of carbon isotope fluctuations and enhanced organic carbon content of sediments (Arthur and Schlanger, 1979; Jenkyns, 1980). Variations in eustasy and global ocean chemistry played important roles in the stratigraphy and lithology of the Mancos Shale and other deposits of the Western Interior Seaway. Palynology from Upper Cretaceous coals and other terrestrial fauna records suggest this was a period of stable, warm, and humid climate (Wolfe and Upchurch, 1987; Howell and Flint, 2003).

In northeastern Utah, the Mancos Shale was deposited overlying a mid-Turonian unconformity above the underlying Cenomanian Dakota Sandstone, Cedar Mountain Formation, or Mowry Shale (Molenaar and Cobban, 1991). The roughly 4,000 ft (1,220 m) thick Mancos Shale is divided into a number of stratigraphic members that reflect varying proportions of sandstone, siltstone, and claystone related to updip fluctuations between proximal shallow marine sandstone and more distal marine siltstone and claystone in present day central Utah (Figure 3). Proximal shoreface sandstones and their downdip equivalent siltstones include, in stratigraphic order, the Frontier and Ferron, Emery, and Mesaverde group sandstones (Molenaar and Cobban, 1991; Johnson, 2003b). These sandstones interfinger and shale out down paleodepositional dip into mudstone dominated members of the Mancos, including the Tununk, Juana Lopez, Blue Gate Shale, and Buck Tongue, in stratigraphic order (Molenaar and Cobban, 1991; Johnson, 2003b) (Figure 4). The Mancos B Member, also known as the Prairie Canyon, is an isolated, heterolithic sandstone and siltstone body that separates the Upper and Lower Blue Gate members across the southeastern portion of the study area. A number of other Blackhawk equivalent isolated sandstone bodies have been identified from outcrop encased in marine shale, suggesting across shelf transport of sands into distal environments during lowstands (Swift et al., 1987; Chan et al., 1991; Pattison, 2005; Pattison et al., 2007; Macquaker et al., 2007).

The Mesaverde group includes the Star Point Sandstone, Blackhawk Formation, and Castlegate Sandstone; the Blackhawk itself is divided into six members, the Spring Canyon, Aberdeen, Kenilworth, Sunnyside, Grassy, and Desert (Young, 1955), which represent cyclical regressive sequences of variable coastal marine environments (Howell

and Flint, 2003). Broadly, the Mancos grades down paleodepositional dip into more calcareous mudstone to the east, where both subsidence and sediment supply were relatively low during deposition so that in present day Colorado, portions of the lower Mancos transition into the chalk and marl-dominated organic-rich Niobrara Formation (Kauffman, 1977).

The Uinta Basin formed during the Laramide Orogeny and postdated Mancos deposition. It is a deep sedimentary basin bounded by Laramide-age uplifts, including the Uinta Mountains to the north and the San Rafael Swell and Uncompaghre Uplifts to the south, and is separated from the Piceance Basin to the east by the Douglas Creek Arch (Johnson, 1992). One of many Laramide basins throughout western North America, the Uinta was a ponded basin, which accumulated a thick package of fluvial and lacustrine sediments during the subsidence and burial of underlying Mesozoic sediments (Dickinson et al. 1988). The Mancos was rapidly buried following deposition until 25 Ma, subsequently uplifted, and in some areas eroded (Anderson and Harris, 2006). Uinta Basin subsidence has asymmetrically favored the northern end of the basin, so the Mancos has not matured uniformly, but has experienced earlier and more extensive thermal maturation in the north than in the south (Nuccio and Roberts, 2003; Quick and Ressetar, 2012). Production from the Mancos will be constrained by both primary depositional processes as well as subsequent burial, maturity, and fracture histories.

Dataset

Data from 453 wells that penetrated the Mancos Shale across the Uinta Basin were compiled into a database. The sources of well data are varied: some data were downloaded from the Utah Department of Natural Resources' Division of Oil, Gas, and Mining database (DOGM, 2013), and a significant amount of data was donated by Anadarko, Bill Barrett Corporation, Del Rio, Gasco, Pioneer Resources, Questar (now QEP), Wind River Resources Corporation, and XTO (now ExxonMobil Corporation). The types of data vary from well to well, but include gamma ray, resistivity, neutron porosity and density, sonic, borehole image, and mud logs. Of the 453 wells, 280 include wireline log data; 157 were used to construct regional cross sections and/or isopach maps (Figure 14; Appendix A). Well log data used here were each collected independently by various well operators over the past half century, so differences in logging tools, borehole conditions, and operator procedures all contribute to variations in absolute values recorded from wells in the dataset. Correlations relied on qualitative visual comparison of stratigraphic trends from well to well rather than quantitative evaluations.

Recent core-based investigations by Kennedy (2011) and Horton (2012) provided useful detailed lithologic descriptions, high-resolution geochemical data, and geomechanical test results. These core data were consulted alongside the wireline log data to provide ground truth from unweathered strata in the subsurface. Kennedy (2011) described core from a 1,712 ft (520 m) interval of the River Gas of Utah #1 (RGU-1) well, from three miles SW of Price, UT, spanning the top of the Tununk Member through the Ferron Sandstone and Lower Blue Gate Shale to the basal Emery Sandstone. Horton (2012) evaluated core taken from four wells, 120 ft (36 m) intervals from three Questar

Figure 14: Distribution of data throughout the Uinta Basin, concentrated primarily in southeast and northeast portions of the basin. Extent of preserved, post-Mancos strata outlined in black. 457 wells included in database (Appendix A) are marked as red (gas), green (oil), or black (dry) circles. Type log (Figure 14) labeled with blue star. Cross sections are marked as heavy red (Figure 20), orange (Figure 21), or purple (Figure 27) lines.

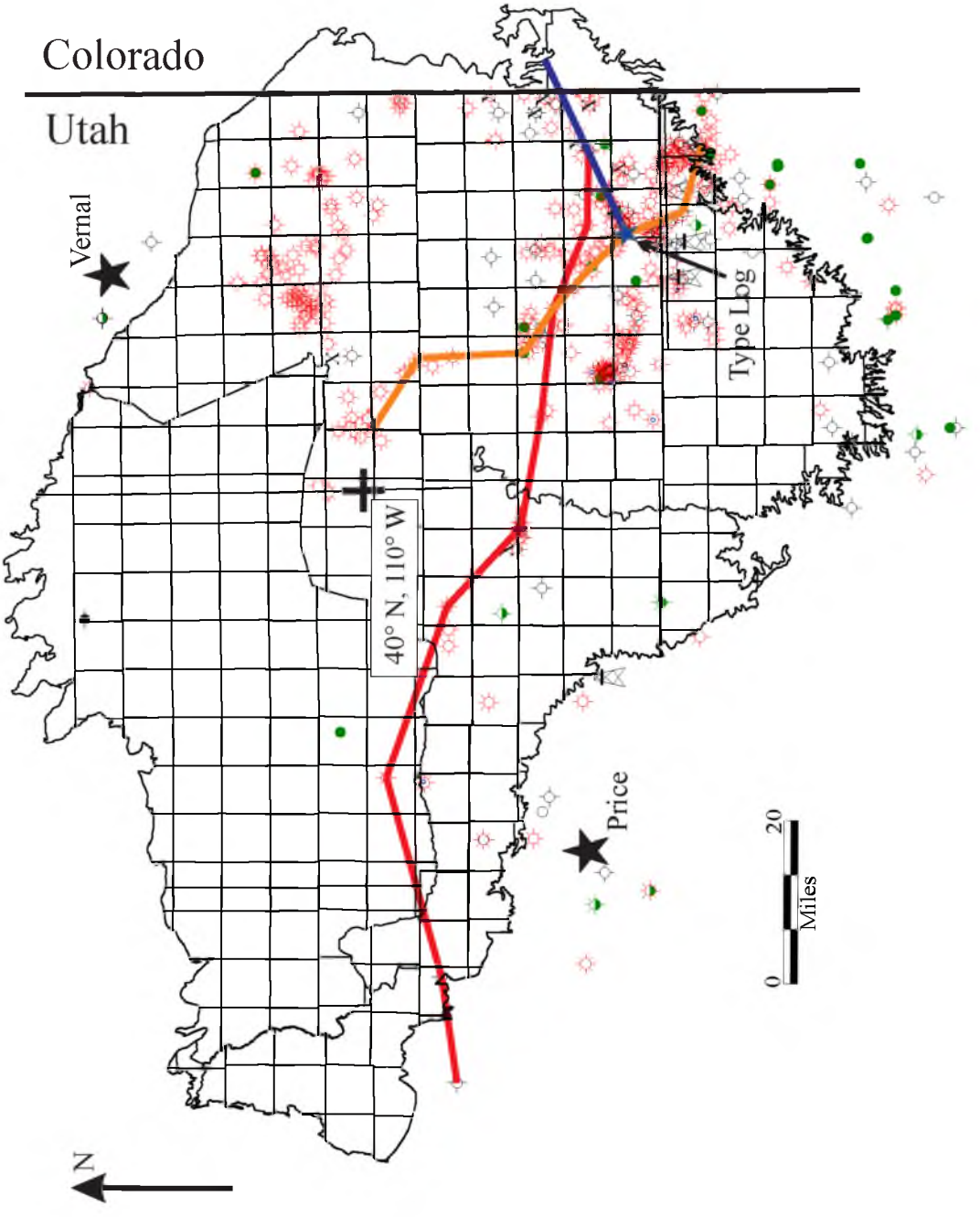
Colorado
Utah
Vernal
Type Log
40° N, 110° W
Price
20
Miles
0
N

wells roughly 25 mi (40 km) south of Vernal, UT, the Glenn Bench 1M-4-8-22R, Red wash 8ML-6-9-24, and Glenn Bench 16M-28-8-21, and two 120 ft (36 m) intervals of the Pioneer Natural Resources Main Canyon Federal 23-7-15S-23E, located roughly 40 mi (64 km) south of the aforementioned Questar wells. These cores were taken from different intervals of the Lower Blue Gate Member and demonstrate the vertical and lateral facies variability of this member. The core descriptions considered details of subsurface lithology, sedimentology, and stratigraphy at the centimeter scale. Geochemical analysis included thin section, x-ray fluorescence, x-ray diffraction, QEMSCAN analysis, and TOC-RockEval pyrolysis (Horton, 2012). The RGU-1 cored interval was sampled to systematically capture facies variability for geomechanical properties, from unconfined compression tests, triaxial compression tests, and indirect tensile strength tests (Kennedy, 2011). Complete descriptions of these core analyses and methods are available from Kennedy (2011) and Horton (2012).

Existing depositional and stratigraphic models developed primarily from outcrop and core by previous workers of different components of the Mancos Shale, including the Lower Blue Gate, Juana Lopez, and Tununk Members (Molenaar and Cobban, 1991; Anderson and Harris, 2006; Kennedy, 2011; Horton, 2012), Frontier Formation (Molenaar and Wilson, 1990), Ferron Sandstone (Riemersma and Chan, 1991; Anderson and Ryer, 2004; Fielding, 2010), Emery Sandstone (Edwards et al., 2005), Mesaverde Group (Yoshida, 2000; Miall and Arush, 2001; Kirschbaum and Hettinger, 2004; Seymour and Fielding, 2013), Mancos B (Cole et al., 1997; Hampson et al., 1999), and other isolated Mesaverde equivalent sandstones such as the Hatch Mesa (Pattison, 2005; Pattison et al., 2007; Macquaker et al., 2007) provided the primary lithologic and

biostratigraphic background for the log-based stratigraphy in this study. Three-dimensional seismic data were available from a portion of the study area, which were valuable for confirming structural continuity between subsurface correlations.

Methods and Approach

PETRA, an industry standard software, was used for this study, in part because it contains correlation, geostatistical, and petrophysical modules that can be applied to formation mapping and evaluation. Well data were loaded as .LAS files, which allow scale manipulation during correlation as well as quantitative petrophysical evaluation. Wells were selected for use in regional correlation based on the quality of available wireline log data, spacing relative to other available wells, penetration through the Mancos, and the availability of core or borehole image data. Some portions of the study area are characterized by a high density of well data, particularly in the east, whereas the western portion has low data density and relatively few total data points. Correlations were based primarily on gamma ray logs, which provide a proxy for claystone content (Bhuyan and Passey, 1994), can be indicative of lithologic stacking patterns (Singh et al. 2008; Passey et al., 2010), and were widely available from wells of different vintage and operators. Where available, resistivity and neutron logs were used to supplement gamma ray log-based correlations. Surfaces were picked during the construction of cross sections, and later mapped regionally as isopach maps using PETRA geostatistical modules.

Well log correlations were critical to establishing the regional extent and stacking patterns of the Mancos across the study area. Major stratigraphic units, including the

Castlegate Sandstone, Blue Gate Shale, Mancos B, Dakota Silt interval of the Tununk, and Dakota Sandstone, were picked from gamma ray logs based on the previous work of Molenaar and Cobban (1991), Johnson (2003a), Rose et al. (2004), and Schamel (2006). From these major surfaces, additional chronostratigraphic packages within the Mancos Shale were identified and correlated regionally based on well log morphology as well as flooding and regressive surfaces. Wherever possible, the top of the Lower Castlegate (Lawton, 1986) was used to hang stratigraphic cross sections because it is regionally extensive and easily identified by a blocky, clean log signature associated with fluvial channels overlain by the Buck Tongue transgression (Yoshida, 2000), is roughly time correlative (Fouch et al., 1983), and is the typical datum of Upper Cretaceous cross sections in the Uinta Basin by other workers (e.g., Yoshida, 2000; Hampson et al., 2001; Kirschbaum, 2003; Johnson 2003b; Pattison, 2005).

Chronostratigraphic correlations were made by identifying maximum regressive surfaces (MRS) and maximum flooding surfaces (MFS) associated with depositional sequences. Despite variations in lithofacies, these surfaces can be traced laterally across the formation, bound genetically related strata, and represent roughly time significant surfaces (Ch. 1). Where available, biostratigraphic data were incorporated in order to corroborate and refine regional correlations. Correlations largely followed the guidelines of Pattison et al. (2009) for shoreface-to-shelf systems, including the gradual basinward thinning of parasequences without clinoforms, rather than abrupt thinning with steeply dipping clinoforms, downlap, and pinch-out. While the latter method has driven correlations for many years, most packages in the Upper Blue Gate and corresponding Blackhawk Formations demonstrate only gradual thinning over more than 25 mi (40 km)

of outcrop (Book Cliffs) and in the subsurface (Pattison et al., 2009). These trends of gradual sequence thinning and shaling out of lithofacies into the basin are also observed throughout the subsurface data of this study.

Facies were mapped within this genetic framework across the basin in order to illustrate the depositional history of the formation; gamma log characteristics were matched with corresponding lithofacies so the distribution of those lithofacies could be interpolated throughout the basin. From intervals with available core analysis, which correspond with intervals of the Lower Blue Gate, the facies association and depositional environment model of Horton (2012) was used to differentiate different styles of offshore deposition. Detailed core analysis of Kennedy (2011) and Horton (2012) was tied directly to gamma ray logs and formed type sections that could be extrapolated around the basin. For other intervals of the Mancos, such as the organic-rich Juana Lopez Member and the sandstone-rich Mancos B, previous facies and depositional environment interpretations in the literature were used to interpret an anticipated log signature, which could be mapped within the basin.

Furthermore, a number of established outcrops, including previously measured sections from the southeast (near junction of I-70 and highway 6), northeast (Steinaker dam) (Molenaar and Cobban, 1991), and southeast (Westwater, UT) (Anderson and Harris, 2006) of the Uinta Basin, as well as heterolithic, sandstone rich units, including the Hatch Mesa Sandstone at Hatch Mesa, UT, the distal Blackhawk at Woodside, UT (Pattison, 2005; Pattison et al., 2007), and the Mancos B at Prairie Canyon, CO (Cole et al., 1997) were visited in order to understand the facies, stacking patterns, and lateral variability of these strata and tie lithologic properties back to gamma ray correlation. The

genetic and chronostratigraphic correlation provides a framework for integrating outcrop, core, and other subsurface data into a comprehensive model for facies distributions throughout the Mancos Shale.

Results

A new type log for the Mancos Shale in the Uinta Basin is developed here (Figure 15) with picks based on previous work in the basin (Molenaar and Cobban, 1991; Kirschbaum, 2003; Anderson and Harris, 2006; Schamel, 2006), as well as new basin-wide correlations presented herein. Eight stratigraphic intervals are identified, including the Tununk Shale, Juana Lopez, Lower and Upper Blue Gate, upper and lower Mancos B, and Buck Tongue Members of the Mancos Shale, and the Mesaverde Group. The variety of facies observed in Mancos outcrop and core are reflected in the diverse gamma log morphologies observed throughout the basin. The Tununk Shale overlies the mid-Turonian unconformity above Lower Cretaceous strata, including the Dakota and Cedar Mountain Sandstones and Mowry Shale (Molenaar and Cobban, 1991). The Juana Lopez member is characterized by a ratty, high gamma ray interval directly overlying the Tununk Shale. This gamma ray pattern reflects the organic-rich but heterolithic interlaminated and interbedded sandstone, siltstone, and claystone deposits of this member (Molenaar and Cobban, 1991; Anderson and Harris, 2006) (Figure 16).

The Lower and Upper Blue Gate members, which constitute the main body of the Mancos, are separated by the Mancos B and are characterized by moderate to high API values, with only subtle stratigraphic variations. This reflects gradual changes between lithologies ranging from claystone to siltstone to sandstone-dominated heterolith

Figure 15: Mancos Shale type log taken from Pioneer Main Canyon Federal 23-7-15S-23E well in the southeastern Uinta Basin. Lithostratigraphic units and sequence sets are labeled on the left, next to gamma ray plotted between 0 and 170 API. Third track overlays resistivity (black) and sonic (blue) logs to identify likely hydrocarbons using the Δ log R method (green shading). Fourth track displays calculated TOC, calibrated with core data and maturity modeling, on 0 to 10% scale (courtesy of R. Hillier). Depth relative to the top of the Lower Castlegate (correlation datum).

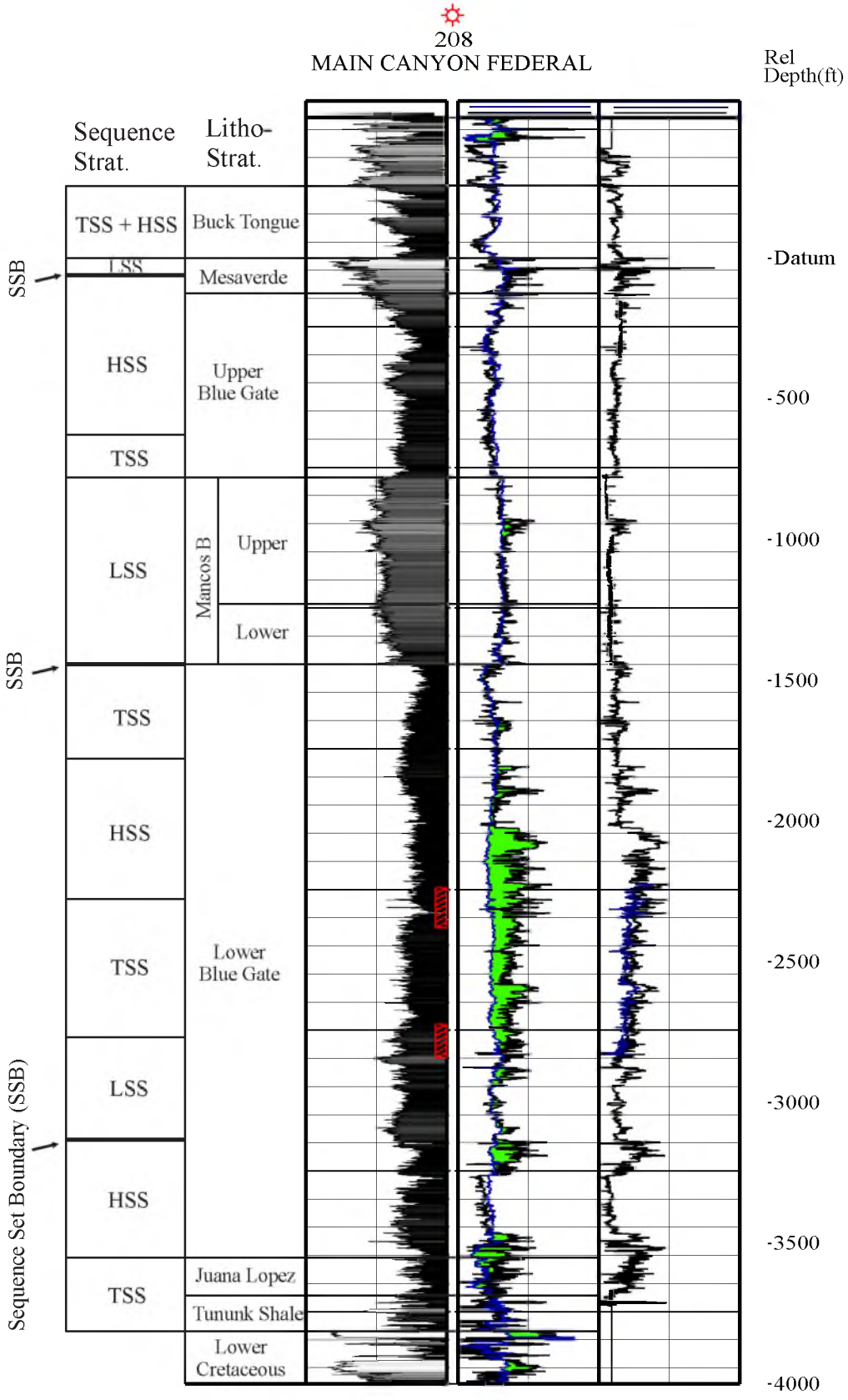
208
MAIN CANYON FEDERAL
Rel Depth(ft)
Sequence Strat.
Litho-Strat.
TSS + HSS
Buck Tongue
LSS
Mesaverde
HSS
Upper Blue Gate
TSS
LSS
Mancos B
Upper
Lower
TSS
HSS
TSS
Lower Blue Gate
LSS
HSS
TSS
Juana Lopez
Tununk Shale
Lower Cretaceous
SSB
SSB
Sequence Set Boundary (SSB)
-Datum
-500
-1000
-1500
-2000
-2500
-3000
-3500
-4000

(Kennedy, 2011; Horton, 2012). The Mancos B is an interval of lower gamma ray values, commonly with sharp upper and basal contacts and multiple internal sharp-based surfaces that provide a basis for internal division of the member into informal upper and lower members herein (Figure 15). The gamma ray character reflects the sandstone-dominated heterolithic lithology of this member (Figures 16 and 17) and its interpreted deposition as subaqueous mass transport deposits (Cole et al., 1997). The Buck Tongue Member displays similar gamma ray signatures to the Blue Gate Shale, but overlies the Castlegate Sandstone.

Thickness and lithofacies of time correlative units within the Mancos vary along both paleodepositional dip and strike according to varying depositional setting and local accommodation. The Mancos Shale and chronostratigraphic equivalents thicken to the west and north in the basin (Figure 18a). This thickening is accommodated primarily in facies of the Lower Blue Gate (Figure 18b). Not all members of the shale follow similar thickness trends; for example, the Mancos B thickens substantially to the southeast (Figure 19). In the southern and eastern portions of the basin, where the Mancos is thinner, vertical facies changes occur more abruptly, characterized by sharp flooding and regressive surfaces (Figures 20 and 21). The most sharp-based surfaces in the Mancos occur at the base and top of more distal portions of the Mancos B, where sandstone-dominated heterolith facies abruptly overlie and underlie the finer-grained siltstone and claystone rich units of the Blue Gate Shale (Figures 20 and 21). Additionally, in the southeastern portion of the basin, distal equivalents of the Ferron and Frontier Sandstones and the thin, high gamma ray shales of the Juana Lopez and lowermost Blue Gate include a number of abrupt facies changes between interbedded finer-grained claystone and

Figure 16: Outcrop photos from exposures of the Mancos Shale in the Uinta Basin. A) Exposure of Juana Lopez Member from road cut along I-70, UT, characterized by alternating organic shale and siltstone bedding with current ripple indicators. B) Ripples preserved in fine sandstone bed of Juana Lopez Member, west of Rt. 191, 16 miles north of I-70 junction, UT. C+D) Exposure of heterolithic facies of Mancos B from Prairie Canyon, CO; C) Interlaminated rippled siltstone and sandstone; D) Mottled and bioturbated interlaminated sandstone and siltstone, burrows highlighted.

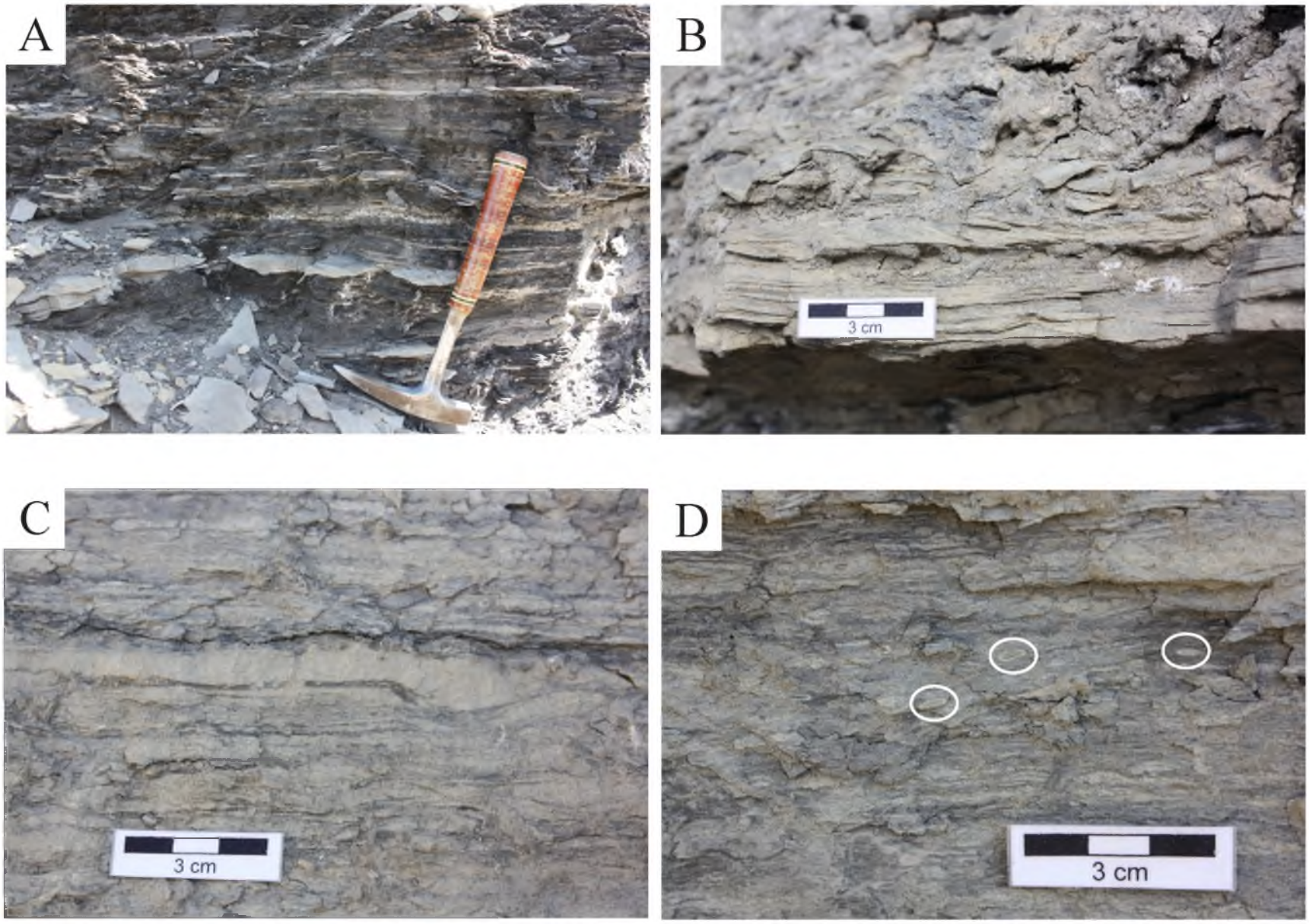
A
B
3 cm
C
3 cm
D
3 cm

Figure 17: Exposure of Mancos B from Prairie Canyon, CO. Note resistant dolomite marker beds near top of hill, which top coarsening up parasequences and correspond with marine flooding surfaces (Hampson, 1999). Stream cut provides relatively unweathered surfaces for observation of heterolithic, fine sandstone interlaminated with siltstone.

Figure 18: Isopach maps of A) full thickness of the Mancos Shale and B) Lower Blue Gate Shale, Uinta Basin based on picks from 150 wells around the basin (black rings). Both intervals thicken strongly to the northwest. Traces of cross sections (Figures 20-red; 21-orange) included for reference.

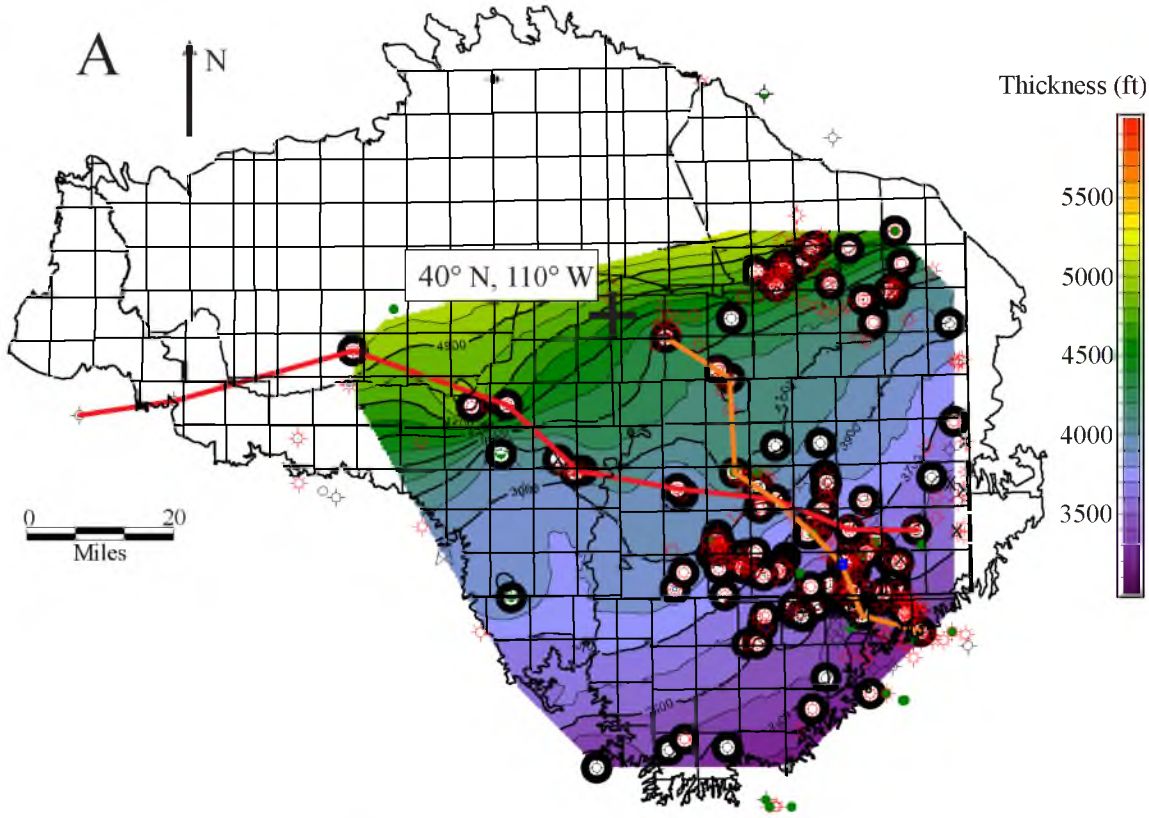
A
N
40° N, 110° W
0
20
Miles
Thickness (ft)
5500
5000
4500
4000
3500

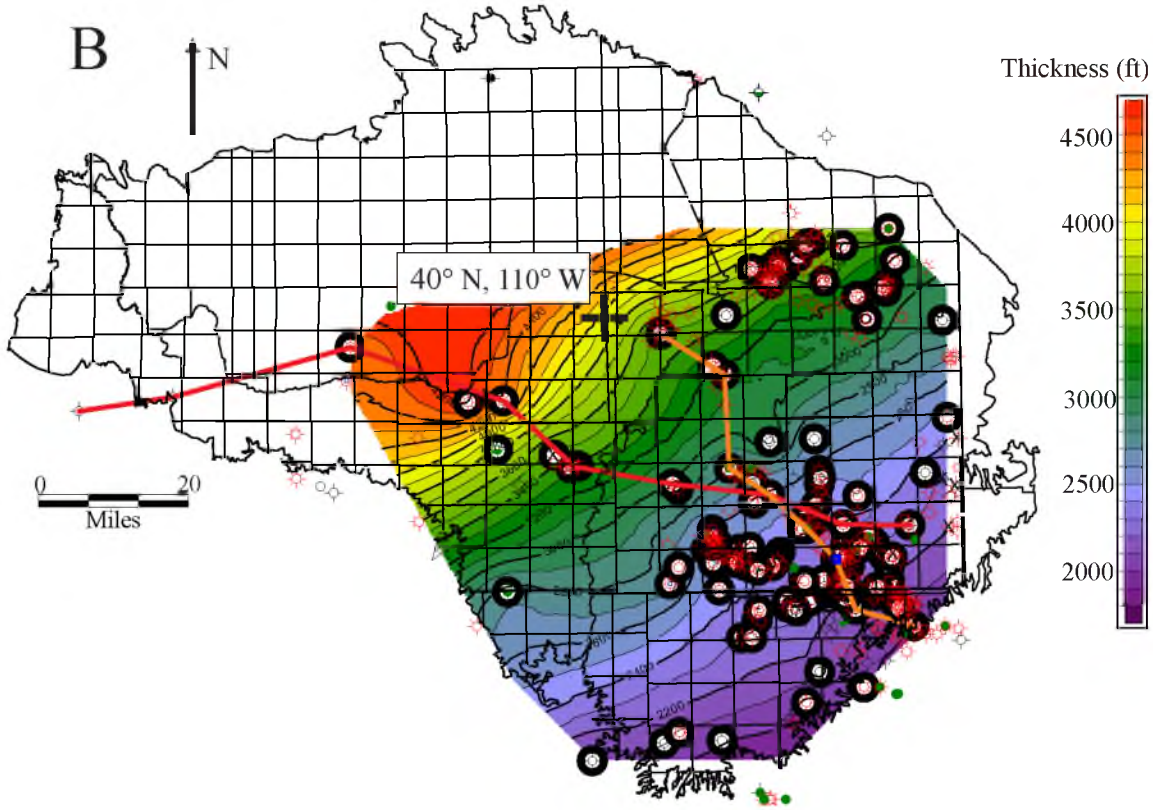
B
N
40° N, 110° W
0
20
Miles
Thickness (ft)
4500
4000
3500
3000
2500
2000

Figure 19: Isopach maps of A) upper and B) lower Mancos B in the Uinta Basin based on picks from 150 wells around the basin (black rings). Traces of cross sections (Figures 20-red; 21-orange) included for reference.

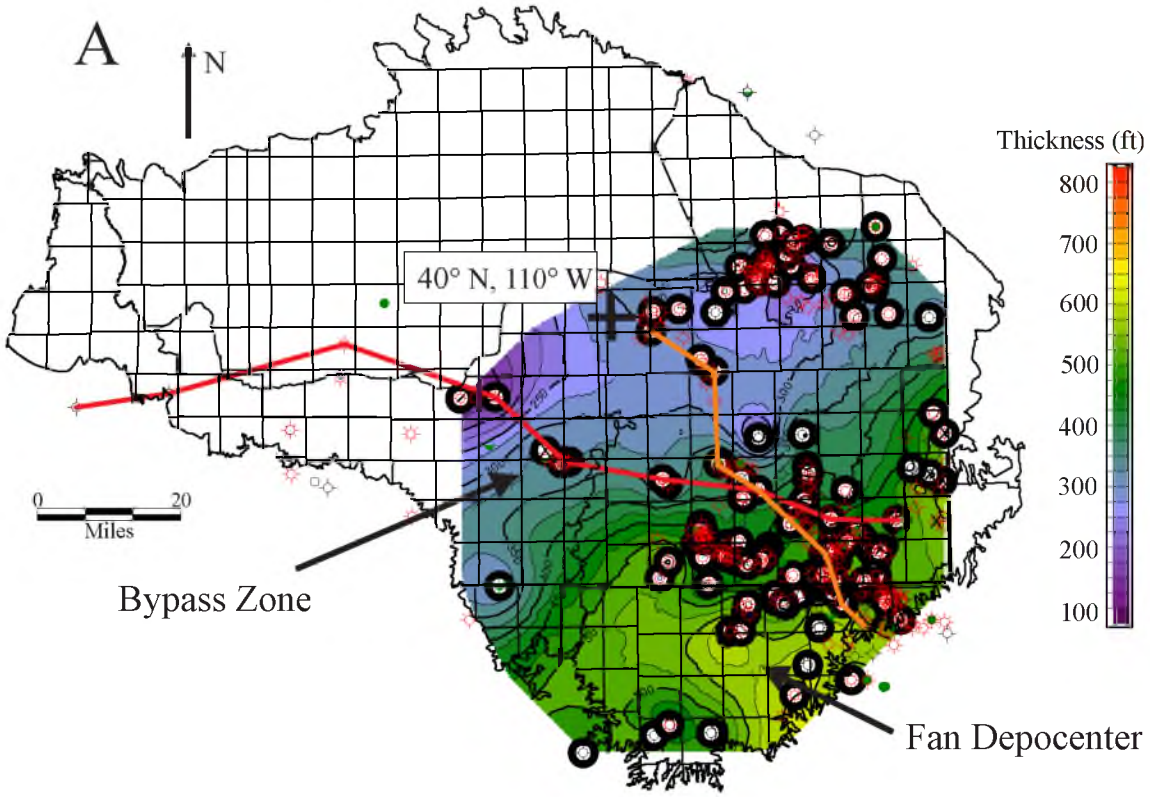
A
N
40° N, 110° W
0
20
Miles
Bypass Zone
Fan Depocenter
Thickness (ft)
800
700
600
500
400
300
200
100

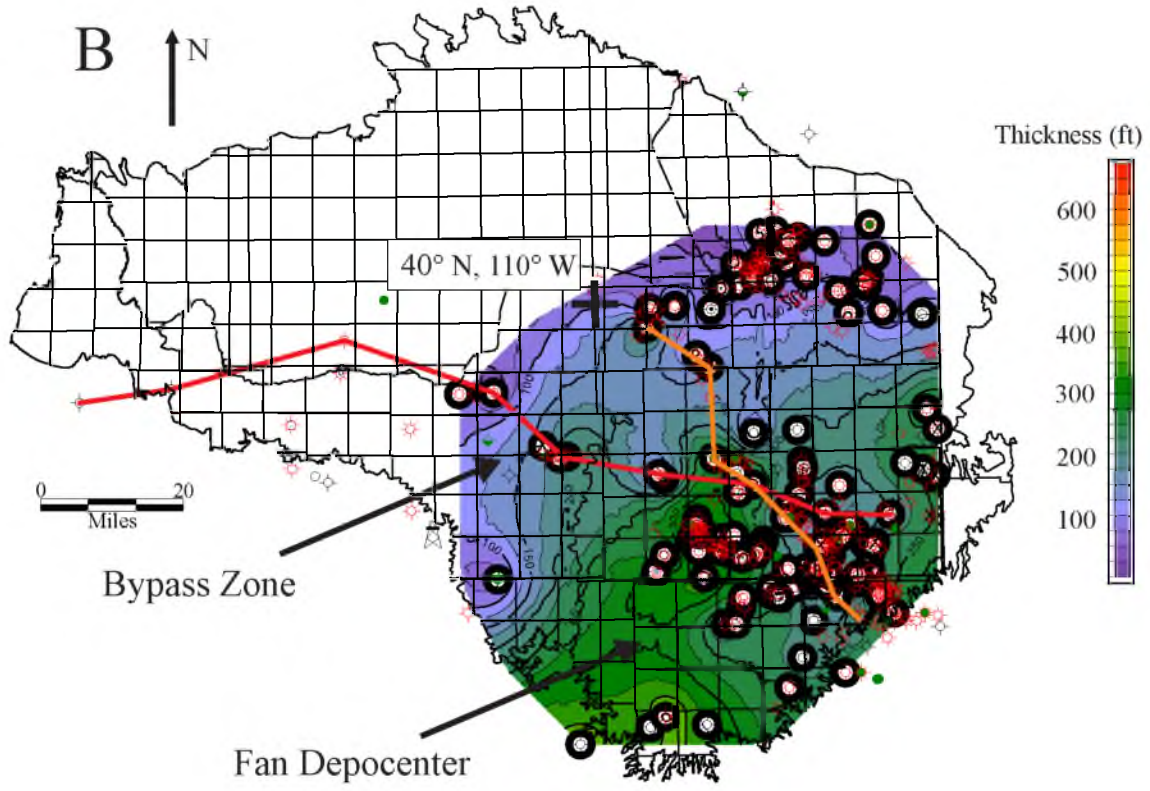
B
N
40° N, 110° W
0
20
Miles
Bypass Zone
Fan Depocenter
Thickness (ft)
600
500
400
300
200
100

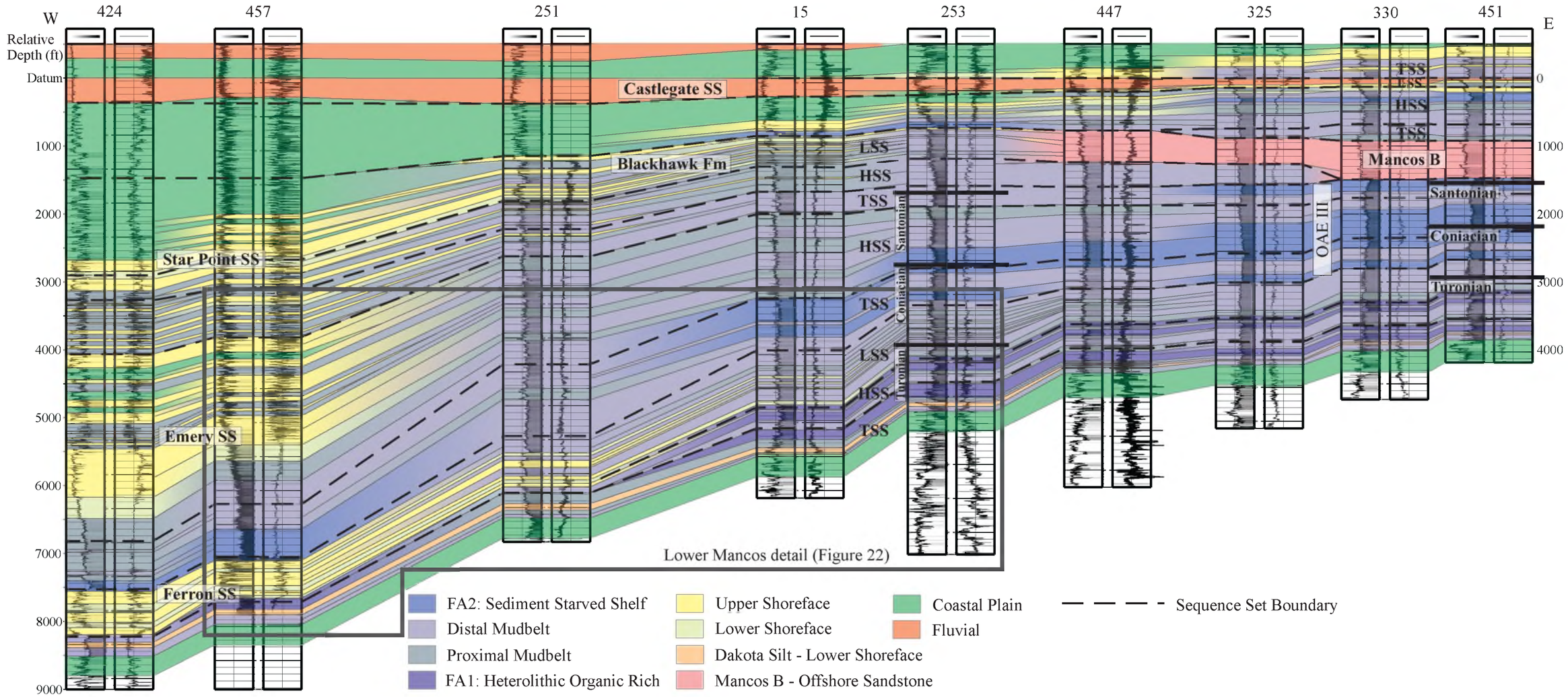

Figure 20: West to east stratigraphic cross section hung on the top of the Lower Castlegate across the Uinta Basin which captures the regional facies variability of the Mancos Shale. Colors indicative of interpretted depositional setting based on core, outcrop, and log data. Correlations from well to well are chronostratigraphic, with estimates of geochronologic ages marked. Interpreted sequence sets labeled HST (highstand sequence set), LST (lowstand sequence set), or TST (transgressive sequence set), and bounded with dashed lines. Stratigraphic position of OAE III (white bar) based on age assignment of Locklair et al. (2011). Gamma ray (0 to 170 API scale, left) and resistivity (2 to 2,000 ohm log scale, right) logs shown for each well. Relative depth from datum is labeled in feet along the sides of the cross section. Cross section trace described on location map (Figure 14).

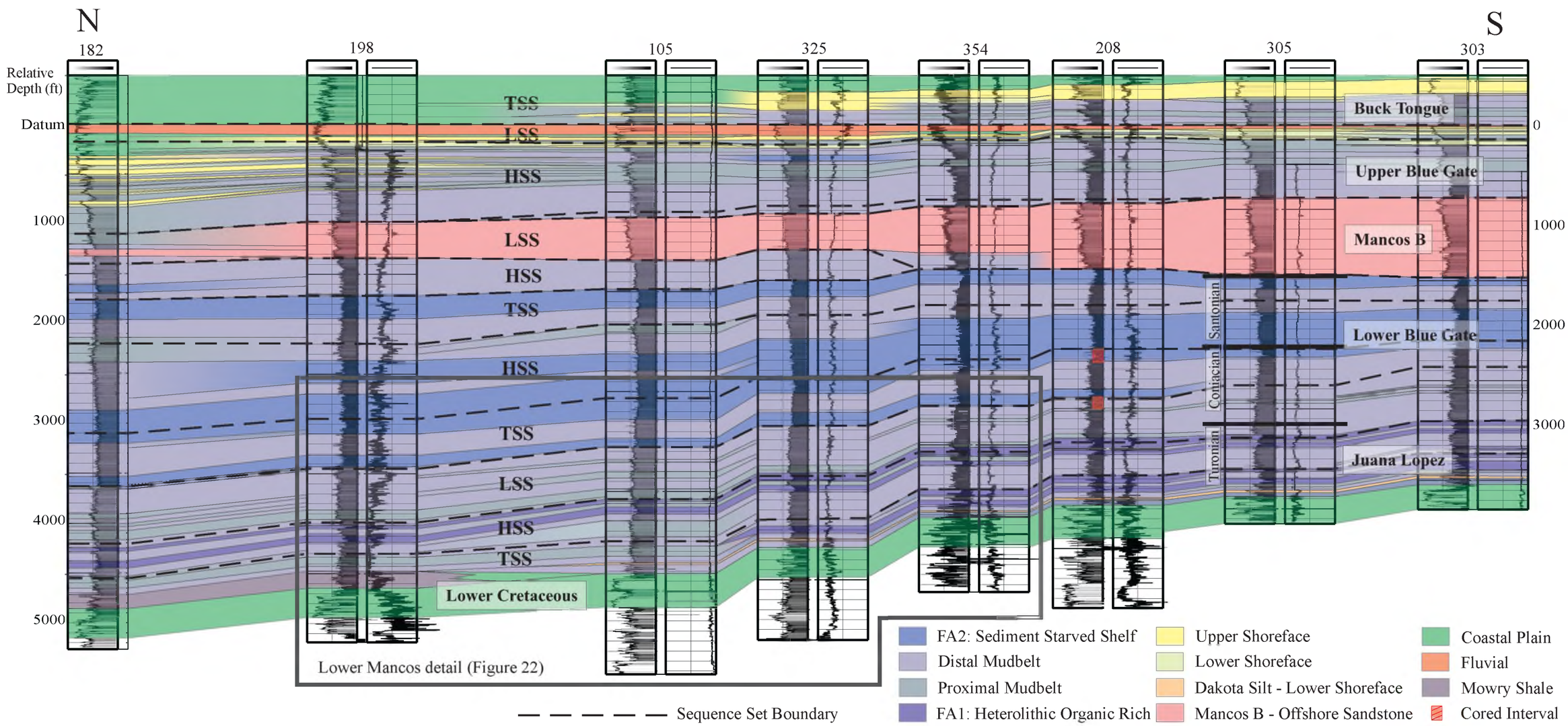

Figure 21: North to south stratigraphic cross section hung on the top of the Lower Castlegate across the eastern Uinta Basin. The distribution of lithofacies of the Mancos Shale are described across the basin. Facies relationships from well to well are chronostratigraphic and reflect the evolution of depositional systems around the basin. Depth relative to the datum is listed along each side of the cross section. The lower Mancos is characterized by alternating packages of thin organic-rich and poor strata, while the upper Mancos includes only a few, thicker intervals of more consistent strata. Gamma ray (0 to 170 API scale, left) and resistivity (2 to 2,000 ohm log scale, right) logs shown for each well. Cross section trace described on location map (Figure 14).

siltstone and coarser-grained siltstone to sandstone lithologies. In general, the gamma ray changes across most sharp-based surfaces suggest proximal coarser-grained facies overlie more distal, fine-grained facies, or vice versa, and record abrupt facies transitions interpreted as abrupt changes in the relative distance to shoreline. Intervals from the northern, central, and western portions of the basin tend to display more gradual, bow-shaped vertical gamma ray, and hence more gradual lithofacies transitions (Figures 20 and 21).

There are two major facies associations of relatively high gamma ray, organic, and clay-rich facies identified from the distal portions of the Mancos Shale. These two associations do not occur along the same depositional profile but instead occur in discrete intervals of the stratigraphy. Facies Association 1 (FA1) corresponds with sharply interbedded high and low gamma ray intervals of the Tununk, Juana Lopez, and lowermost Blue Gate. In outcrop, these facies are organic-rich heterolith (Figure 16), which contain dominantly organic-rich mudstone (>2% TOC over 50 ft [15 m]; Anderson and Harris, 2006) with thinly interbedded and interlaminated fine sandstone. The sandstone displays hummocky cross stratification and current ripples, sedimentary structures which suggest episodic energetic deposition above storm wave base (Figure 16). Visual inspection of outcrop, palynology, and kerogen analysis suggests this interval contains relatively abundant terrestrial organic matter, including peat swamp and lacustrine signatures (Anderson and Harris, 2006; G. Waanders, personal communication, 2006). Across the basin, this interval is characterized by high gamma ray, laterally continuous shales (claystone to siltstone dominated), often 100 ft (30 m) or less thick, separated by low gamma ray intervals (siltstone to sandstone dominated), the distal

equivalents of deltaic deposition from the Dakota Silt, Frontier Formation, or Ferron Sandstone.

In contrast, Facies Association 2 (FA2) corresponds with the consistently high gamma interval of the Lower Blue Gate, a stratigraphically more uniform lithology dominated by siltstone and claystone with only minor sandstone interlaminations. Core analysis indicate this interval, particularly the sediment starved shelf facies (*sensu* Horton, 2012), is characterized by low energy deposition near or below storm wave base, with relatively high proportions of carbonate (29% Ca, n=24) and organic carbon (up to 2.17 % TOC) (Horton, 2012), with a stronger marine organic signature (Anderson and Harris, 2006; G. Waanders, personal communication, 2006). This interval of consistently high gamma ray characterizes much of the Lower Blue Gate across the basin, with higher, more claystone-rich facies to the east and south and lower gamma ray generally to the west and north, corresponding to more distal and proximal expressions, respectively.

The Dakota Silt, Frontier Formation, and Ferron Sandstone are sandstone-dominated intervals which stratigraphically interfinger with organic-rich heterolith of FA1 in the lowermost Mancos (Figures 20 and 21). The Dakota Silt interval of the Tununk Shale, characterized by cleaning upward gamma, or a coarsening upward package, topped by an abrupt flooding surface, is most pronounced in the southern portion of the basin. The Frontier Formation, a coarsening upward package below the Lower Blue Gate, is prominent in the north and transitions to mudstone to the south, where it is chronostratigraphically equivalent to the Juana Lopez member (Figure 22). The Ferron Sandstone interfingers with and overlies the upper most organic-rich shale of FA1, and corresponds with low gamma ray sandstone and siltstone-rich beds well into the

Figure 22: Detail of lower Mancos (Tununk and Juana Lopez Members, Frontier Formation, and Ferron Sandstone) correlations from regional cross sections (Figures 20 and 21). A) 70 mi interval west to east through basin (Figure 20) describing the distal expression of the Ferron Sandstone stratigraphically overlying high gamma, heterolithic shales of the Juana Lopez. B) 30 mi interval north to south on eastern side of basin (Figure 21) depicts time correlative facies transition between Frontier Formation and Juana Lopez, both underlying low gamma ray strata of distal Ferron Sandstone.

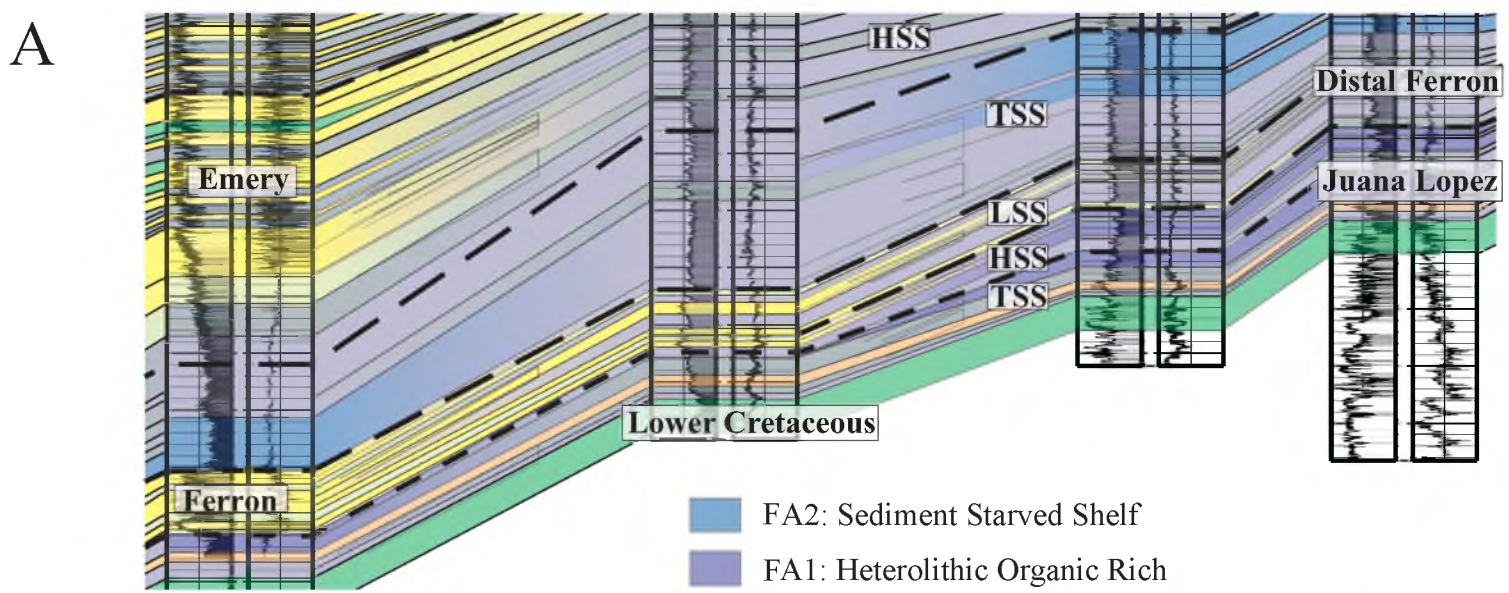
A
HSS
TSS
LSS
HSS
TSS
Emery
Distal Ferron
Juana Lopez
Lower Cretaceous
Ferron
FA2: Sediment Starved Shelf
FA1: Heterolithic Organic Rich

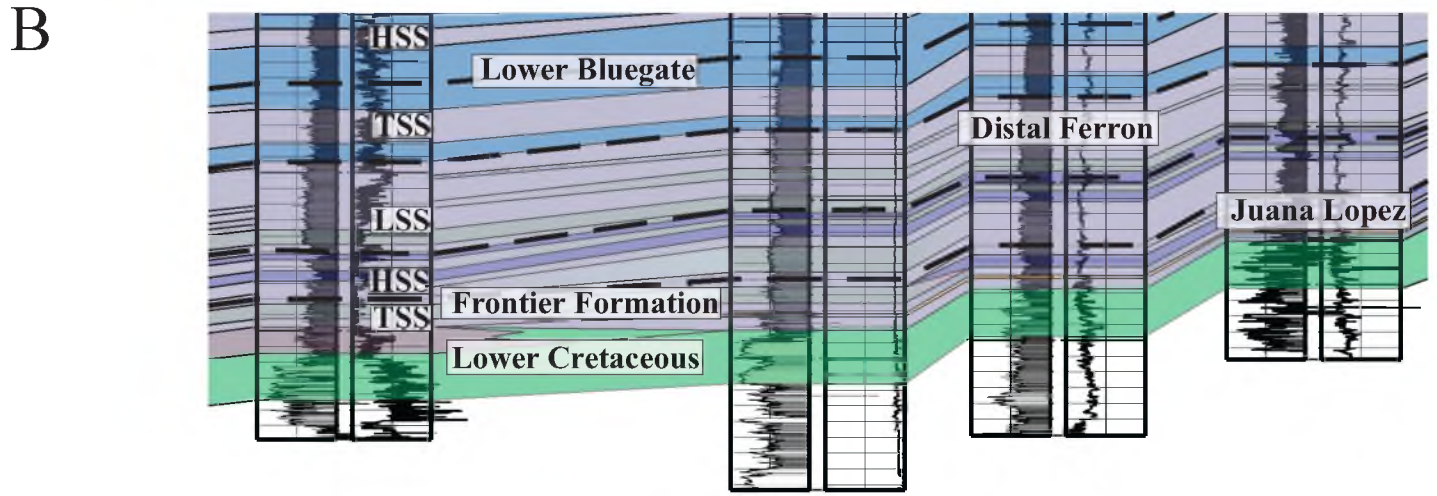
B
HSS
Lower Bluegate
TSS
Distal Ferron
LSS
Juana Lopez
HSS
Frontier Formation
TSS
Lower Cretaceous

distal basin (80 mi [130 km]; Figures 20 and 22; Appendix B). These dominantly deltaic facies correspond with distal deposits of relatively coarse-grained strata which vary along strike and are interbedded with laterally continuous deposits of organic-rich, high gamma ray shales.

In contrast, the Emery Sandstone corresponds with distal deposits of FA2 that lack resolved beds and significant interlaminations of coarse siliciclastic material. The Emery, characterized by thick packages of wave-dominated shoreface (Edwards et al., 2005) and a dominantly aggradational (with minor progradation) shoreline trajectory, does not dramatically interfinger with mudstone downdip (Figure 20). Instead there is a rapid downdip facies transition from sandstone-dominated facies to organic-rich, claystone-dominated facies within 30 mi (50 km) of paleoshoreline (Figure 20). Whereas FA1 is extensively interbedded with coarse-grained deposits periodically delivered a significant distance into the basin, FA2 is starved of this coarse-grained material during Emery deposition.

The sandstone- and siltstone-rich heterolithic facies of the Mancos B (Figures 16 and 17) correlate laterally to, but are isolated from, the prograding deltaic and wave-dominated shorefaces of the Star Point and Blackhawk Formations, respectively. The compensational stacking of the upper and lower Mancos B illustrated in the isopach maps (Figure 19) suggests a progressive deposition and infilling of sediment to the east, with younger strata deposited further into the paleobasin (i.e., progradation). Some sediment bypass of the muddy shelf during deposition of the Mancos B accounts for the isolated sandstone body characteristics of the Mancos B.

This interpretation of a sediment bypass zone with downdip fan depocenter (Figure 19) is further supported by evidence of sediment bypass and winnowing in preferential cementation observed from Mancos outcrops that are distal equivalents of the Blackhawk Formation in the Book Cliffs (Macquaker et al., 2007). The overall progradation of shorefaces of the Mesaverde Group transition in a relatively short distance down paleodepositional dip to offshore mudbelt facies (*sensu* Horton, 2012). Only the Star Point Sandstone and lower members of the Blackhawk Formation, including the Spring Canyon and Aberdeen Members, correlate with thick offshore sandstone bodies of the Mancos B down dip, although smaller isolated sandstone bodies have been correlated updip with other Blackhawk members, such as the Kenilworth (Pattison, 2005). In outcrop, members of the Blackhawk Formation are characterized by low clinoform dip angles (Hampson, 2000) and display gradual facies changes over 1–3 mi (2–5 km) down paleodepositional dip from upper shoreface into offshore mudstone (Pattison et al., 2009).

Discussion

Depositional Framework

The depositional environment of the Mancos Shale evolved over the fifteen million years of deposition as a product of tectonically driven fluctuations in basin structure and global eustatic changes. The distal deposits of the Mancos evolved from heterolithic organic-rich mudstone with interbedded and interlaminated sandstone typical of FA1, which was deposited along a low gradient, shallow ramp in a low tectonic subsidence and accommodation regime where fluvial dominated delta systems delivered

an abundance of terrestrial organic matter. Later, sediment was delivered from multiple source wave-dominated deltas along the coast to the deeper, basinal claystone to siltstone, specifically sediment starved shelf deposits of FA2, during Coniacian-Santonian highstand under a high tectonic subsidence, high accommodation regime. Basin-floor fans of the Mancos B then dominated the basin deposition, sourced from the prograding shoreline of the Mesaverde group. These facies transitions reflect the tectonically driven evolution of the foreland basin from a shallow ramp during the Early Turonian into a deeper physiographic feature between the Middle Turonian and Upper Santonian, which was subsequently infilled with shallow marine and then terrestrial sediments during the early Campanian (Figures 23 and 24). Changing depositional conditions affected the lateral and vertical distribution of lithofacies throughout the formation, including corresponding proportions of quartz, clay, and carbonate, the preservation and source of organic carbon, and the permeability and porosity of the formation.

The transition between energetic (above storm wave base), heterolithic deposition of FA1 and low energy deposition (below storm wave base and basinward of most hyperpycnal flows) of FA2 reveals a fundamental change in depositional environment over this period. FA1 suggests relatively shallow water deposition with a significant component of terrestrial organic matter and other sediment, but retains relatively high organic matter content, with primary production likely driven by river fed nutrients (Kosters et al., 2000). Recent work suggests that in broad, low gradient ramp settings, the distance from shore maintains a greater influence on average grain size than water depth, and mud transport is dominated by hyperpycnal flows and bedload transport rather than suspension settling (Varban and Plint, 2008; Bhattacharya and MacEachern, 2009;

Figure 23: Schematic illustration of the contrasting depositional settings of the Mancos B (A), FA2 (B), and FA1 (C). Horizontal scale based on characteristic intervals from interpreted cross section (Figure 20).

A **Mancos B**

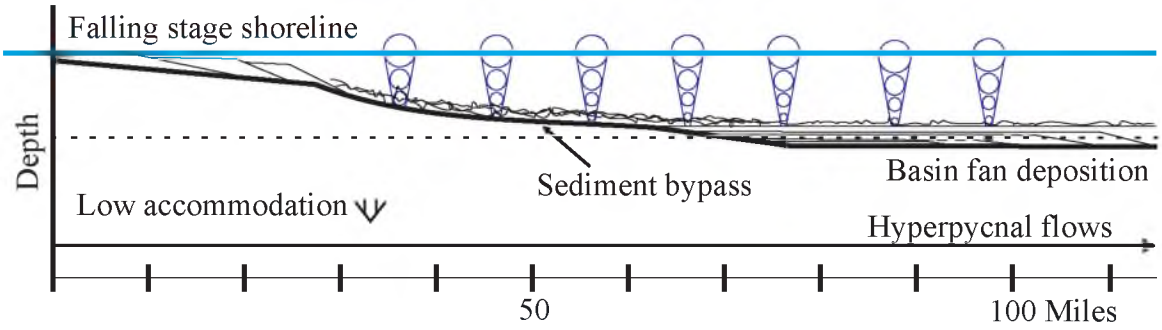

B **Facies Association 2**

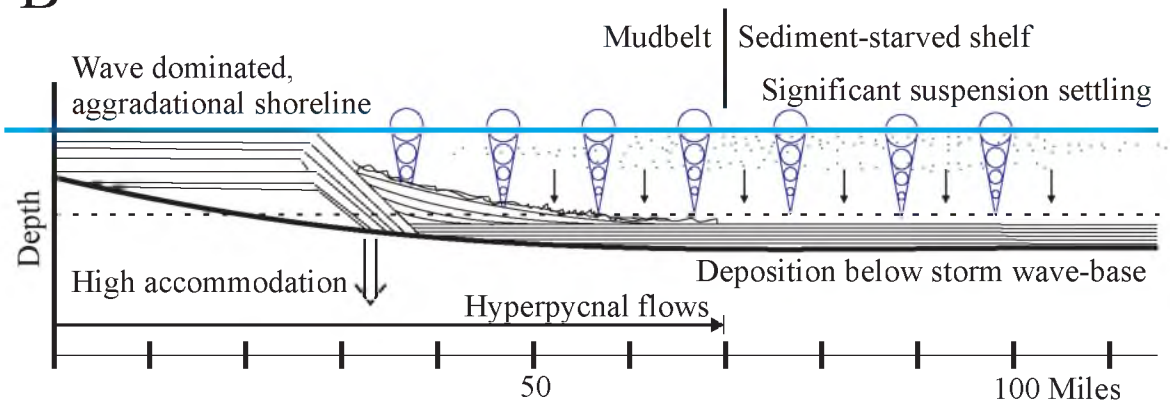

C **Facies Association 1**

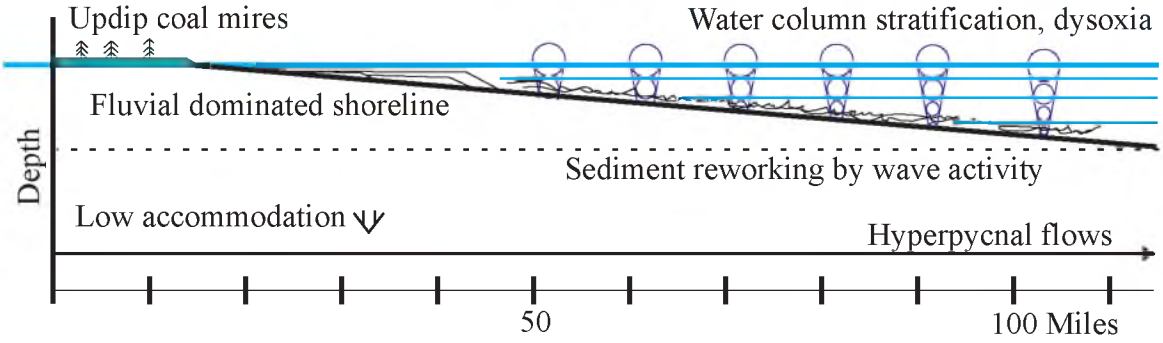

Figure 24: Paleogeographic maps of the study area from various times during the Upper Cretaceous. Representative lithostratigraphy for each is labeled. Maps have been ordered from oldest to youngest (A to G).

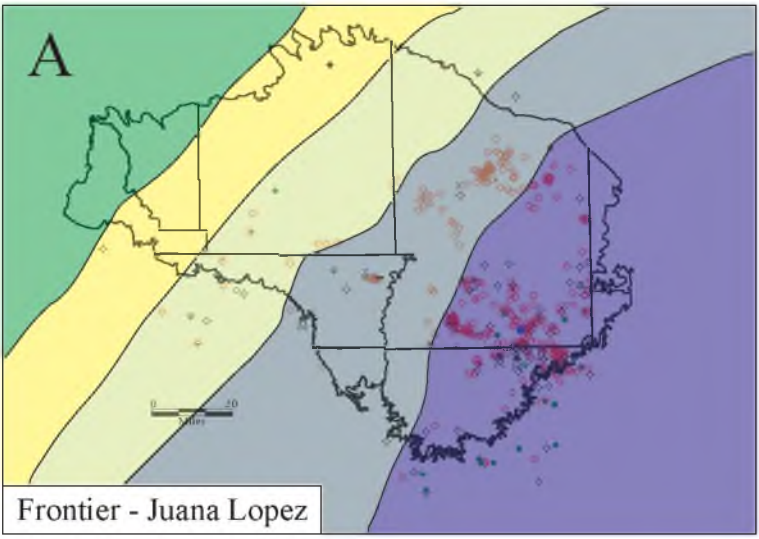
A
Frontier - Juana Lopez

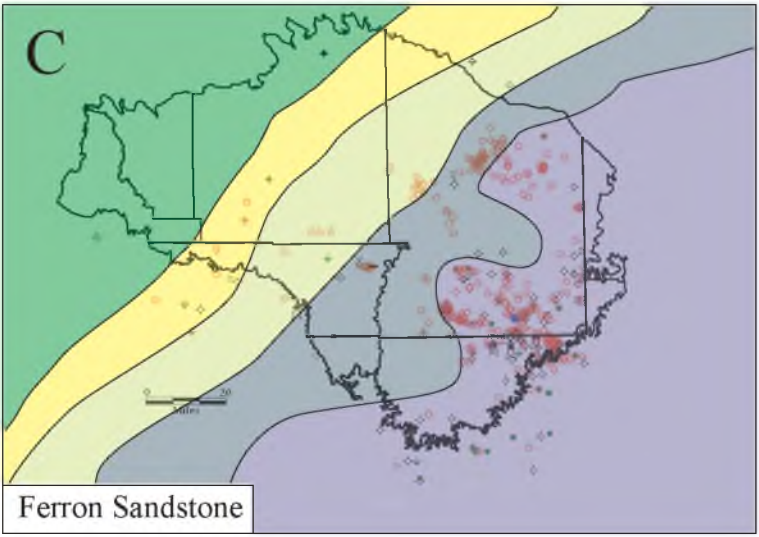
C
Ferron Sandstone

B
Facies Association 1

D
Emery Sandstone

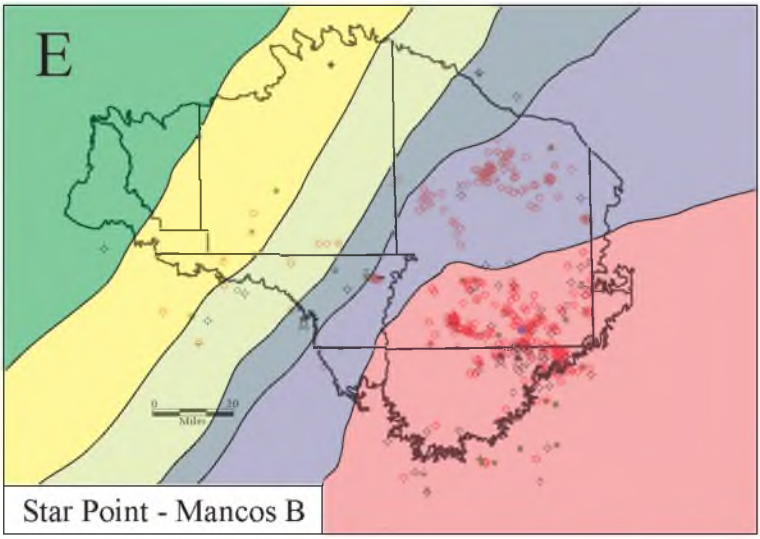

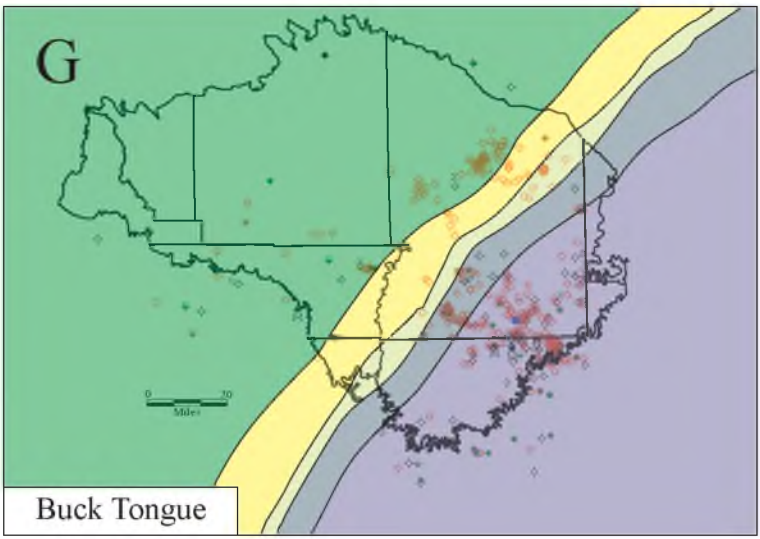

Figure 24: Continued

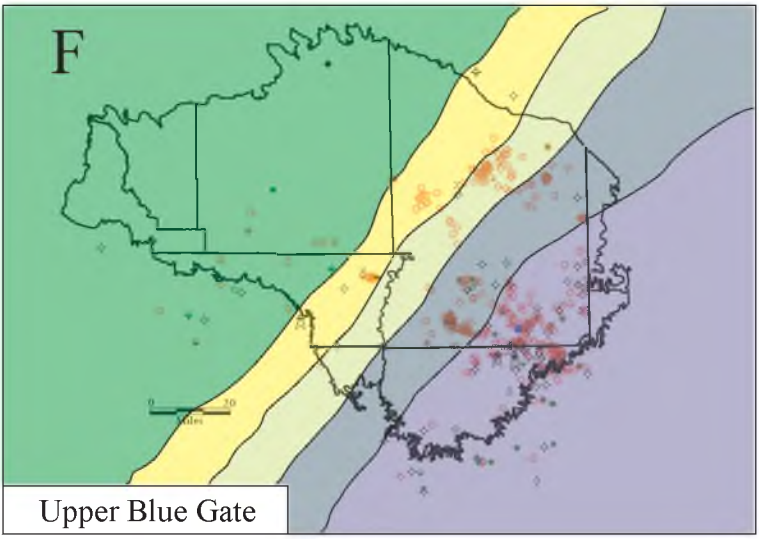

Coastal Plain

Upper Shoreface

Lower Shoreface

Proximal Mudbelt

Distal Mudbelt

FA1: Heterolithic Organic Rich

FA2: Sediment Starved Shelf

Mancos B - Offshore Sandstone

Macquaker et al., 2010; Plint et al., 2012). Largely unbioturbated facies of FA1 observed from outcrop (Figure 16) suggest this was a very stressed environment for burrowers, typical of delta front deposits (Bann and Fielding, 2004; MacEachern et al., 2005), potentially related to brackish (Bhattacharya and MacEachern, 2009) or euxinic (Algeo et al., 2004) water conditions, reducing the destruction of organic matter in sediments and allowing for relatively high organic carbon preservation despite shallow water deposition. In outcrop analysis that evaluated distal equivalent marine deposits of the Frontier and Ferron from Westwater, UT, Anderson and Harris (2006) identified multiple sequences of turbidite and delta front deposits interbedded with regionally extensive organic-rich shales. Sandstone bodies within the sequences display variable paleocurrent directions, suggestive of multiple sediment sources (Anderson and Harris, 2006). Modern analogues for FA1 include broad shelves of the Po, Orinoco, Rhône, and Mississippi deltas, which include organic-rich sediments with high organic content and abundant plant material (Kosters et al., 2000).

In contrast, sedimentary structures of FA2 in the Lower Blue Gate indicate the most carbonate and organic carbon-rich facies were deposited near or below storm wave base and basinward of the influence of most hyperpycnal flows (Kennedy, 2011; Horton, 2012). These facies were deposited in a deeper basin than earlier or subsequent Mancos strata, made possible by enhanced tectonic subsidence. At this time sandstone and siltstone of the Emery was accommodated near to paleoshoreline, so the offshore dispersal distance of terrestrial organic matter and coarse-grained siliclastics was limited. Distal deposition of FA2 was dominated by clay and carbonate suspension settling, including coccolithophores and silicious diatoms (Figure 25) rather than bedload

Figure 25: Scanning electron microscope images of Mancos Shale. Images A–C of sediment starved shelf facies (FA2) from Pioneer 23-15 well (#208, Appendix A), D from mudbelt facies of Questar 16 well (#181). All images taken under high voltage (20.00 kV) conditions. A) 7,101 ft (2,164 m) sample displays fecal pellet (pe) composed of coccolith fragments. Sodium rich feldspar (F) and sparry dolomite (do) are highlighted. B) Same sample as A, higher magnification reveals coccolith tubes within fecal pellet which contribute to 3.77% effective porosity. C) 7,118 ft (2,170 m) sample of admixed calcareous and organic material in fecal pellet. Yellow arrows indicate fine amorphous kerogen and red arrows indicate intercrystalline pore space which contribute to 4.34% effective porosity. D) 15,178 ft (4,626 m) depth sample with siliceous microfossil (si) filled with framboidal pyrite (py), in matrix of calcite cement (ca) and authigenic clays (arrows).

B
5 μm
D
ca
sl
py
sl
sl
py
20 μm

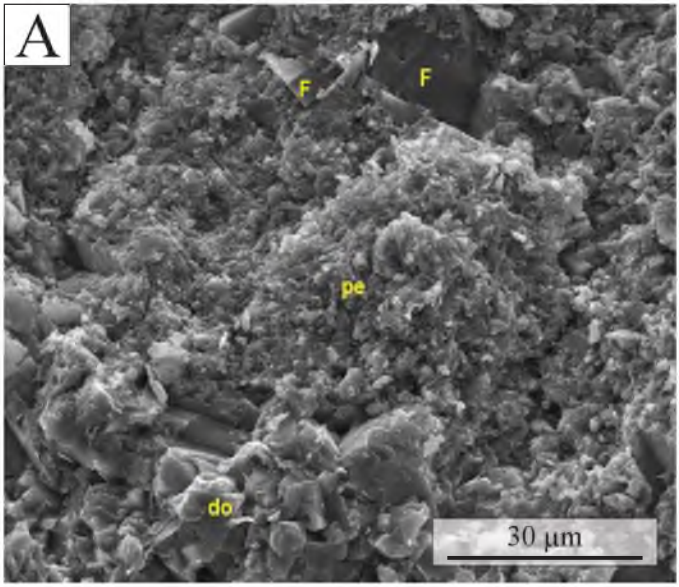
A
F
F
pe
do
30 µm

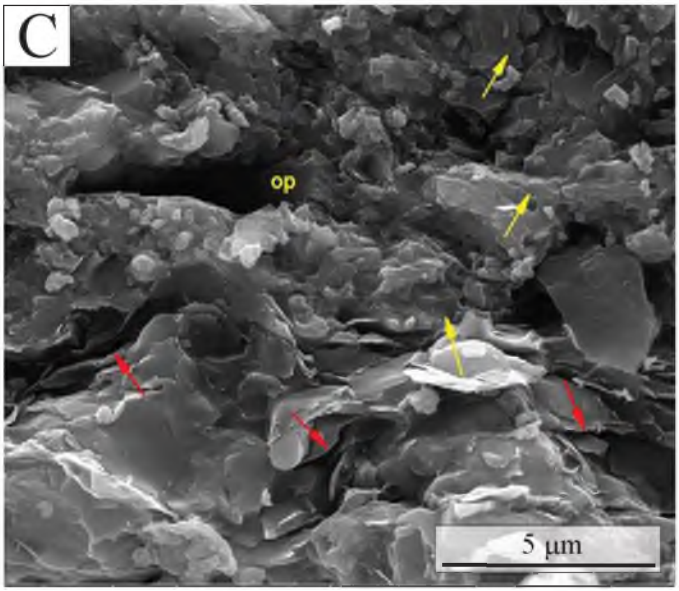
C
op
5 µm

transport and lacked the frequent lamination to bed-scale fluctuations in lithofacies between organic-rich mudstone and sandstone typical of FA1. These facies heterogeneities typical of FA1 were controlled by shoreline processes, including individual fluvial-deltaic sedimentation events, rapid depositional lobe shifting or relative sea level change along a low gradient ramp system.

The offshore isolated sandstone bodies of the Mancos B have been variously interpreted as the product of across shelf mass transport deposits (Cole et al., 1997) and nearshore, tidally influenced fluvial channels and fluvial-dominated delta fronts with some storm influence (Hampson et al., 1999) and share many characteristics of other isolated offshore sandstone bodies identified within the distal Blackhawk of the Upper Blue Gate Shale (Creaney and Passey, 1993; Pattison, 2005; Pattison et al., 2007). However, to date, a unified detailed genetic stratigraphic and depositional interpretation of the Mancos B is lacking. The Mancos B clearly represents an anomalously sandstone dominated, heterolithic interval, physically isolated from updip, shallow marine sandstone, with evidence of bioturbation and a moderately energetic depositional environment (Figure 16) (Cole et al., 1997). Significant bioturbation and low organic contents are characteristics shared by other Upper Mancos strata, particularly Blackhawk formation sandstones and their offshore equivalents (Macquaker et al., 2007) in contrast to FA1, indicating a more hospitable environment for burrowing activity. As reflected in the regional chronostratigraphic correlations presented here (Figure 20), the onset of Mancos B deposition (*Scaphites hippocrepis II*, 82.00–81.53) Ma, Anna, 2012) coincided with the falling stage deposition (Posamentier and Morris, 2000) of the Star Point Formation (Anna, 2012), and global eustatic fall (Miller et al., 2003) (Figure 12). The

Mancos B corresponds with falling sea level and represents lowstand basin floor fan deposition, which infilled the deep basin formed during deposition of the Blue Gate in the Coniacian and Santonian to a level above storm wave base. It is possible that sediment was transported to more distal portions of the shelf either through small incised channel forms like those observed in the distal Blackhawk of the Upper Blue Gate (Figure 26) or through net across shelf transport driven by geostrophic currents as suggested by Cole et al. (1997). Distinct bodies of regional extent are correlated within the Mancos B suggesting multiphase deposition that correlates to multiple shallow marine sandstone members updip (Figures 20 and 21).

Sequence Stratigraphy

Mancos equivalent strata in northeastern and central Utah have been the subject of extensive sequence stratigraphic analysis, and provide ground truth for evaluation of the sequence stratigraphy in more distal lithologies. Transgressive-regressive (T-R) cycles provide a useful framework for identifying genetic stratigraphic context for the distal Mancos Shale in the eastern portion of the Uinta Basin, where stratigraphy is fairly layer-cake and relative proportions of claystone and sandstone provide an effective proxy for relative sea level (Embry, 2002; Ch. 1). However, T-R cycles are unable to distinguish the nature of regression. They cannot distinguish between highstand and lowstand conditions. These distinctions have significant impacts on the distribution of lithofacies, influencing the relative abundance of sandstone, carbonate, and organic matter in strata across the basin (Bohacs, 1998; Slatt and Rodriguez, 2012). Furthermore, shallow marine sandstone units that are the paleodepositional updip equivalents of the Mancos

Figure 26: Dolomite concretions highlight depositional channel forms from Upper Blue Gate outcrop at Woodside, UT. Interval is roughly equivalent to the Kenilworth Member of the Blackhawk Formation (Pattison, 2005). Interpreted as possible feeder channels for isolated offshore sandstone deposition. Channel fills consists of heterolithic interlaminated sandstone and siltstone.

Shale such as the Ferron, Emery, Star Point Sandstones and Blackhawk Formation have largely been interpreted using an Exxon-style sequence stratigraphic framework (e.g., Van Wagoner and Bertram, 1996), so there is an existing need to test these models in the downdip equivalent offshore deposits of the Mancos Shale using a similar framework.

Across the basin, mapping at the sequence set scale provides the most appropriate rank for the analysis of allocyclic controls. For lower rank mapping, local variability, likely due to depositional systems, such as lobe shifting, or regional variations in accommodation due to nonuniform thrusting and subsidence, interfere with consistent models. Regionally correlative sequences were stacked to form sequence sets, packages which demonstrate stacking patterns of sequence stratigraphic significance. Sequence sets have been labeled based on the stacking patterns of constituent sequences (Figure 20); transgressive sequence sets (TSS) are characterized by a retrogradational stacking pattern (a stepped upward increase in gamma ray), highstand sequence sets (HSS) record aggradation followed by progradation (an accelerating upward stepped decrease in gamma ray), and lowstand sequence sets (LSS) are characterized by an abrupt basinward stepping pattern overlain by dominant aggradation to minor progradation (abrupt upward decrease in gamma ray overlain by consistent values), and ultimately transition to a TSS.

The abrupt shallowing of facies at the base of each LSS (i.e., distal Ferron and Mancos B) (Figure 20) is interpreted as a sequence set boundary, a correlative conformity which should correspond to a significant subaerial unconformity associated with base-level fall somewhere up paleodepositional dip. The sharp facies change at these surfaces, particularly in the distal Mancos B (Figures 19 and 20), suggests that they may be incisional; however, the deposition of relatively coarse-grained sediments associated with

lowstand fans and turbidity flows would not require significant erosion or base level change in order to sharply juxtapose relatively clean sandstones and siltstones with mudstones in a distal setting. The Emery Sandstone and its distal equivalents are interpreted as an HSS, with an overlying TSS, lacking a well-defined incisional sequence set boundary and LSS (Figure 20). This is not unexpected, as unconformities and their correlative conformities are often cryptic in distal marine environments (Embry, 1990). Transgressive surfaces, located at the base of each TSS, occasionally correspond with abrupt facies changes indicative of possible wave ravinement and erosion, particularly overlying the distal Mancos B and Ferron, as well as overlying more proximal (western) expressions of the Ferron and Emery Sandstones (Figures 20 and 21). However, generally these surfaces correspond with a gradual facies change and corresponding fluctuations of relative sea level.

There is a strong relationship between facies distributions and sequence stratigraphy in distal intervals of the Mancos Shale. The two relatively coarse-grained, sandstone- and siltstone-rich intervals of the distal Mancos are the distal Ferron and the Mancos B, both significant lowstand sequence sets (Figure 20). More fine-grained and organic-rich intervals of the Mancos Shale, FA1 and FA2, correspond with highstand and transgressive sequence sets, including distal expressions of the Emery Sandstone (Figure 20). The transgressive systems tract has been recognized as the most organic-rich interval in marine mudstone in general (e.g., Bohacs, 1998; Slatt and Rodriguez, 2012) and the Mancos Shale in particular (Pasley et al., 1991, 1993), and appears here to be driving the variations in organic content in offshore deposition. The lower Mancos, including organic-rich FA1 and FA2, was deposited amidst high rank transgression while

the organic-lean upper Mancos is characterized by regression (Ch. 1); these contrasting sea level trajectories are likely contributing to variations in the distribution of organic-rich facies. Of note, FA1 and FA2 correspond updip to intervals with distinct shoreline trajectory angles. The Frontier and Ferron, which correlate downdip to FA1, have fairly shallow shoreline trajectory, dominantly progradational and in some cases downstepping. The Emery Sandstone, which correlates downdip to FA2, has a steep shoreline trajectory, dominantly aggradational.

The defined sequence sets create a framework for further detailed stratigraphic subdivision of the Mancos Shale according to the anticipated distribution of lithofacies throughout the formation. The Lower Blue Gate Member includes five sequence stratigraphic subunits based on stacking patterns, including in stratigraphic order a lowermost HSS, a distal Ferron equivalent LSS, a lower TSS, an Emery equivalent HSS, and an upper TSS (Figure 20). These divisions are regionally correlative and indicative of regional facies distributions based on models established from core (Horton, 2012). FA1 corresponds with the basal TSS and HSS below the Ferron LSS, whereas FA2 corresponds with the Emery equivalent HSS and underlying TSS. The relatively thick packages of lowstand and transgressive strata in the distal basin observed here fit the model developed by Posamentier and Allen (1993) for foreland ramp-type basins. The concentration of organic material in the transgressive and lower highstand systems tracts documented in core analysis (Kennedy, 2011; Horton, 2012) is also recorded at the sequence set scale by petrophysical evaluation (Figure 15) (Hillier et al., 2013) and provides validation of the anticipated tie between lithofacies distribution and sequence stratigraphy as well as a sequence stratigraphic division of the Blue Gate.

Driving Mechanisms

The correlation of chronostratigraphic markers provides a framework for understanding the stratigraphic evolution of the Mancos Shale in the Uinta Basin. However, absolute age control is required in order to relate this formation to the global geological record. Ash beds are located within the Mancos, but these have not been well dated, and geochronology is based primarily on biostratigraphy, which is well constrained for the Cretaceous Western Interior Seaway (Kauffman et al., 1993). Age control for the Mancos Shale in northeastern Utah has been reported largely by Fouch et al. (1983) and Molenaar and Cobban (1991), with more recent work by Anderson and Harris (2006) and Anna (2012), and a compilation of Ferron biostratigraphy is reported in Gardner et al. (2004). The base of the Tununk Shale is younger to the west, near Farnham Dome, where the Early Turonian *Mytiloides* was identified, whereas the Late Cenomanian *Pycnodonte newberryi* was found south of Green River. The Dakota Silt, near the base of the Mancos, includes Middle Turonian *Collinoniceras woolgari*, (92.90 Ma, Molenaar and Cobban, 1991). These lower Mancos intervals suggest a roughly four million hiatus exists between the Mancos and underlying Cenomanian Dakota, Cedar Mountain, and Mowry strata (Molenaar and Cobban, 1991). Middle Campanian *Baculites perplexus* (79.01–78.34) Ma) from the Buck Tongue (Anna, 2012) and *Baculites asperiformis* (80.21–79.64) Ma) from the Castlegate Sandstone (Fouch et al., 1983) constrain the end of Mancos deposition.

Late Cretaceous eustasy has been the subject of study from European and North American strata (e.g., Haq et al., 1987; Hancock, 1993; Sahagian et al., 1996; Miller et al., 2003) and can be used to separate the relative influence of eustasy and tectonics in sea

level changes recorded in the rock record. Several major eustatic regressions are identified from multiple records during the time of Mancos deposition; at 90, 84, and 80 Ma (Miller et al., 2003), which correspond with the timing of Ferron (Ar/Ar, 90.25 ± 0.45 Ma, Gardner, 1995a), Emery (*Clioscaphites vermiformis*, 85.56–85.23 Ma to *Desmoscaphites bassleri*, 84.08–83.64 Ma, Fouch et al., 1983), and Mesaverde Group Star Point – Mancos B (*Scaphites hippocrepis I*, 82.7–81.94 Ma, Fouch et al., 1983; Anna, 2012) , and Castlegate (*Baculites asperiformis*, 80.21–79.64 Ma, Fouch et al., 1983) deposition, respectively (Figure 12). Furthermore, stratigraphic unconformities updip, in the Indianola group of the terrestrial hinterland, correspond with these regressions and their correlative conformities (Schwans, 1995). These relationships suggest the timing of these regressive events is controlled at least in part by global eustatic change. However, recent work suggests that mantle flow-induced dynamic topography can cause fluctuations of up to 100 m of vertical change along otherwise stable crust (e.g., Moucha et al., 2008; Müller et al., 2008; Conrad and Husson, 2009), suggesting that confidently isolating a eustatic signal at any particular location is nearly impossible.

Tectonically driven subsidence in the Sevier foredeep was neither spatially nor temporally uniform, and this variation had a significant impact on basin and Mancos Shale stratigraphy. Variations in the position of the forebulge over time affected the deposition of lower Mancos strata. During the Late Cretaceous, the Western Interior Seaway was an overfilled basin, so the forebulge was buried by sediment and did not restrict sedimentation to the foredeep (Flemings and Jordan, 1989). However, stratigraphic evidence and modeling suggests the forebulge likely contributed to

sedimentation bypass and erosion and was responsible for nondeposition during the early Turonian across northeastern Utah (White et al., 2002; Kirschbaum and Mercier, 2013). This contributed to the mid-Turonian unconformity of progressively younger age to the east at the base of the Mancos Shale in the Uinta Basin. Variable subsidence along the thrust front caused uneven subsidence along strike, further complicating basin geometry over time. Backstripping analysis suggests subsidence in southern Wyoming accelerated rapidly after 90 Ma, whereas central Utah experienced only moderate subsidence (Pang and Nummedal, 1995) (Figure 13). Furthermore, variations in stacking patterns of the Star Point sandstone through central Utah indicate increasing tectonic subsidence to the north during its deposition (Hampson et al. 2011). The relative thickening of the Mancos Shale in the northern portion of the basin relative to the south (Figures 9, 18, and 21) appears to correspond to a transition between more rapid subsidence in Wyoming and the more subdued tectonic activity of central Utah. Tectonically driven increases in sediment supply, weathered from the hinterland, and subsidence driven increases in accommodation drive the thickening of this interval and its generally coarser-grained character to the north.

Thrusting in the Sevier hinterland occurred episodically, alternating between periods of activity and quiescence. The Turonian was a period of relative quiescence between the Charleston-Nebo-Pavant I event and active Coniacian and Santonian thrusting along the Tintic Valley-Pavant II thrust (Schwans, 1995). The rapid subsidence during this Coniacian–Santonian thrusting is evident in the thick highstand, dominantly aggradational to slightly progradational (high angle shoreline trajectory) packages of the Emery Sandstone (Edwards et al., 2005) and the correlative distal, sediment starved

deposits (FA2) of the Blue Gate Shale. Rapid subsidence during this time may have outpaced eustatic fall, created significant accommodation relative to sediment supply, and resulted in net relative sea level stasis (i.e., no relative sea level fall), eliminating the expression of sequence set boundaries in the succession. Emery deposition during active thrusting and associated subsidence (Schwans, 1995), created unique stratigraphic relationships predicted by Swift et al. (1987) in which subsidence that increased landward prevented incision during lowstand and ensuing transgression. Similarly, paralic to shallow marine strata deposited during the time equivalent rapid Santonian subsidence in the Kaiparowits Plateau of southern Utah also record almost exclusively transgressive and highstand sedimentation, and preserve complete T-R cycles in marginal marine strata (Shanley and McCabe, 1995; Allen and Johnson, 2010, 2011; Dooling, 2012).

Deposited during tectonic quiescence, the Ferron Sandstone, Mancos B, and Star Point Sandstone display stacking patterns in outcrop typical of a forced regression in relative sea level (Riemersma and Chan, 1991; Hampson et al., 1999; Posamentier and Morris, 2000) and correspond with sequence set boundaries visible from wireline logs (Figures 15 and 20). In a low accommodation setting, coarse-grained sediments are deposited in increasingly distal portions of the basin, rather than accumulating in thicker packages adjacent to shore. Modeling work of foreland basin stratigraphy suggests that periods of rapid subsidence will preserve regressive and transgressive facies without erosive surfaces (Karner, 1986; Posamentier and Allen, 1993), which is typical of the Emery Sandstone, but contrasts with the low accommodation deposition of the Ferron and Star Point Sandstones. While eustatic fluctuations influenced the timing of regressions along the coast, the basin-wide stacking patterns of shallow marine sandstone

bodies and their distal equivalent regressive strata are controlled in large part by tectonically driven subsidence histories and associated accommodation.

Variations between downdip mudstone deposits of FA1 and FA2 were largely controlled by the interplay of tectonically driven accommodation, shoreline trajectories, and coastal processes. Shallow, sharply progradational shoreline trajectories of the lower Mancos distribute coarse-grained sediments widely across the basin. Both fluvial-dominated deltaic deposition and the continued influence of storm energy are effective for distributing material downslope along the shallow depositional ramp (Varban and Plint, 2008; Bhattacharya and MacEachern, 2009; Plint et al., 2012) (Figure 23). Terrestrial organic matter and coarse-grained deposits were readily added to distal mudstones of FA1, which remain interbedded with well-developed deltas on the low gradient ramp. The position of deltas along the coast changed with time, tending to young to the south (Gardner, 1995b) which is reflected in stratigraphy presented here (Figures 20, 21, and 22; Appendix B) and previous biostratigraphy (Molenaar and Cobban, 1991). With multiple point sources, the influence of regressive deltaic deposits is subject to significant local variability and suggests the role of coastal processes is subject to temporal and spatial variability during the shallow ramp deposition of FA1.

In contrast, the sediment starved deposits of FA2 correspond with a steep, dominantly aggradational shoreline trajectory and wave-dominated coastlines during tectonic activity and high accommodation. Coarse grained deposits and terrestrial organic matter were trapped by wave activity along the coastline and accommodated by tectonic subsidence, starving the distal basin of this detritus. In addition, storm energy was less effective at mobilizing and redistributing sediment along the deeper basin

seafloor (Figure 23). The sediment starved shelf setting isolated FA2 from the dynamics of coastal processes and eustatic changes, so this interval of organic rich mudstone is far thicker and more stratigraphically lithologically uniform than the earlier FA1.

The Middle Coniacian–Santonian ocean anoxic event (OAE) III corresponds to Niobrara deposition in distal portions of the Western Interior Seaway (Locklair et al., 2011) and the transgressive and highstand sequence sets of the Lower Blue Gate in the Uinta Basin (Figures 20 and 27). OAE III lacks typical $\delta^{13}C$ excursion of OAE II, although this appears to be a result of dilution caused by increased carbonate production alongside organic matter preservation which was on par with previous ocean anoxic events (Locklair et al., 2011). Lithofacies of FA2 identified in cores taken from Mancos strata of this age in the Pioneer Main Canyon Federal 23-7-15S-23E well (Figure 27) are characterized by significantly increased TOC and carbonate content (Horton, 2012) and contain dispersed coccolithophores that are visible in SEM (Figure 25), suggesting oceanic conditions supportive of organic matter preservation, and chalk deposition in more distal environments of the Niobrara also had some more depositionally proximal record in the facies of the Mancos Shale. The Coniacian–Santonian was characterized by subsidence driven deep-water conditions and increasingly anoxic ocean chemistry, factors that contributed to the deposition of highly carbonate and organic-rich, sediment starved mudstone deposits.

Hydrocarbon Production Implications

Though organic-lean and relatively clay-rich, the significant volume of source rock in the Mancos Shale suggests the potential development of this resource and similar

Figure 27: Detailed correlation of Mancos Shale in the Uinta Basin to Niobrara on the Douglas Creek Arch, cross section trace described on location map (Figure 13). CO picks (in italics on right) based on Kuzniak (2011). OAE III stratigraphic interval based on age assignment by Locklair et al. (2011). Colors indicate interpreted depositional setting. See regional cross sections (Figures 20 and 21) for key.

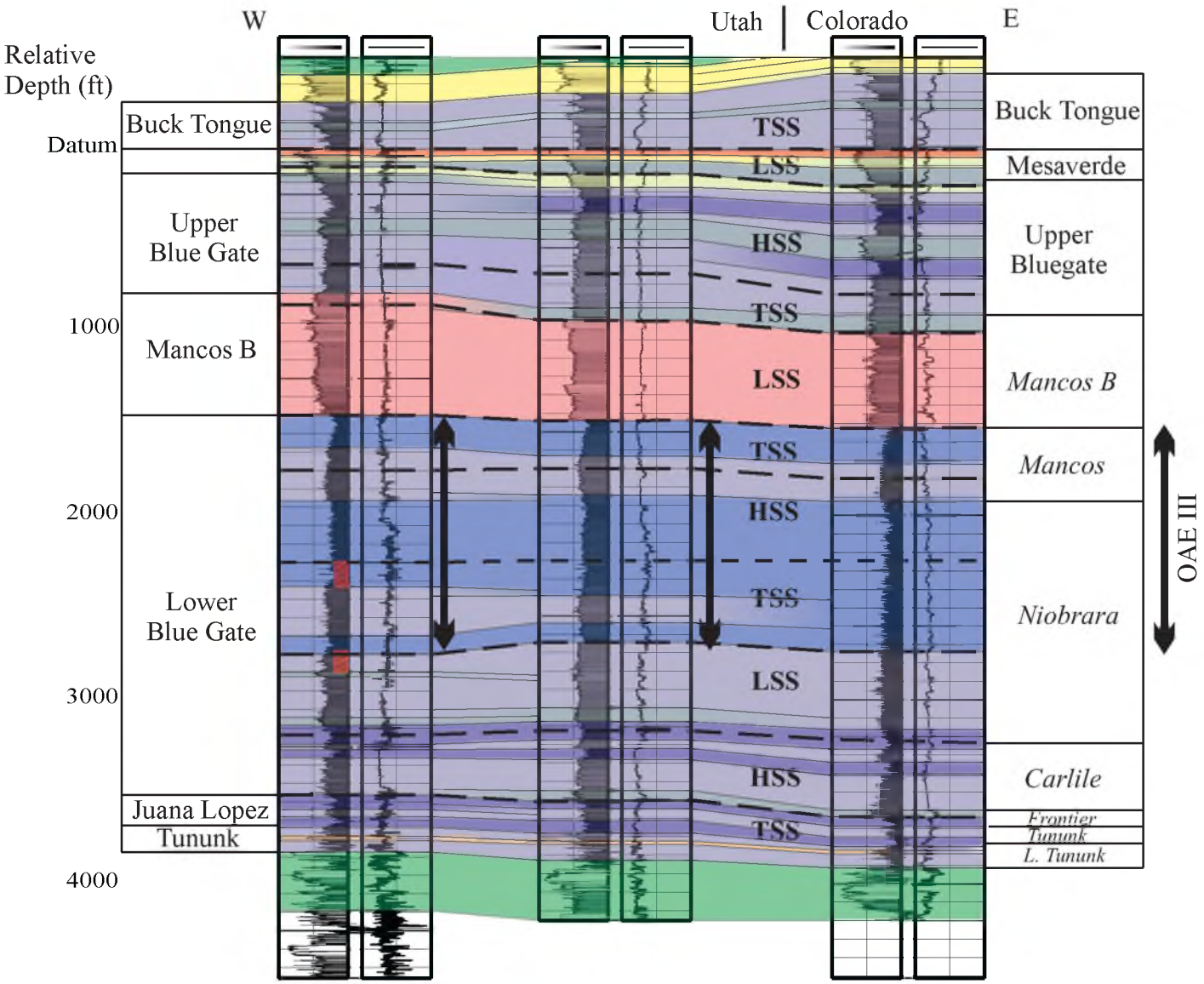
W
Utah
Colorado
E
Relative Depth (ft)
Datum
1000
2000
3000
4000
Buck Tongue
Upper Blue Gate
Mancos B
Lower Blue Gate
Juana Lopez
Tununk
TSS
LSS
HSS
TSS
LSS
TSS
HSS
TSS
LSS
HSS
TSS
Buck Tongue
Mesaverde
Upper Bluegate
Mancos B
Mancos
Niobrara
Carlile
Frontier
Tununk
L. Tununk
OAE III

lithologies of the Cretaceous Western Interior Seaway should not be ignored as the development of tight oil and gas continues to expand across North America. The composition of the most prospective lithofacies in the Mancos do not vary considerably from those of other tight shale plays currently in production (Horton, 2012) (Figure 28). The Mancos has long been identified as a significant source rock, and the Mancos/Mowry petroleum system in the Uinta basin has been assessed with 3.1 TCF gas potential (Kirschbaum, 2003). The first horizontal well was drilled in the Mancos Shale in the Uinta Basin in 2010. It targeted an interval of the upper Lower Blue Gate and came on with 1,234 BBLS oil and 69,638 MCF gas in the first month of production and produced 5,135 BBLS oil and 401,958 MCF gas over the first year (DOGM, 2013). Potential for development of this resource has been demonstrated, although maximizing the economics for development requires targeting only those intervals with the best opportunities for success.

Petrophysical evaluation using the Δ log R technique on eleven wells from the eastern Uinta Basin, calibrated with available core data, has illustrated a few intervals of the Mancos with calculated TOC values of 3–4% that are regionally extensive across the dataset available (Figure 15). The calculated highest TOC intervals correspond to FA1 (organic rich heterolithic intervals of the Juana Lopez and lowermost Blue Gate) as well as FA2 (distal, claystone to siltstone sediment-starved shelf deposits of the Lower Blue Gate) (Hillier et al., 2013) (Figure 15). These two intervals each correspond to transgressive and early highstand sequence sets, during which dilution from siliclastics are anticipated as relatively low and the preservation potential of organic material relatively high (e.g., Pasley et al., 1991; Posamentier and Weimer, 1993; Bohacs et al.,

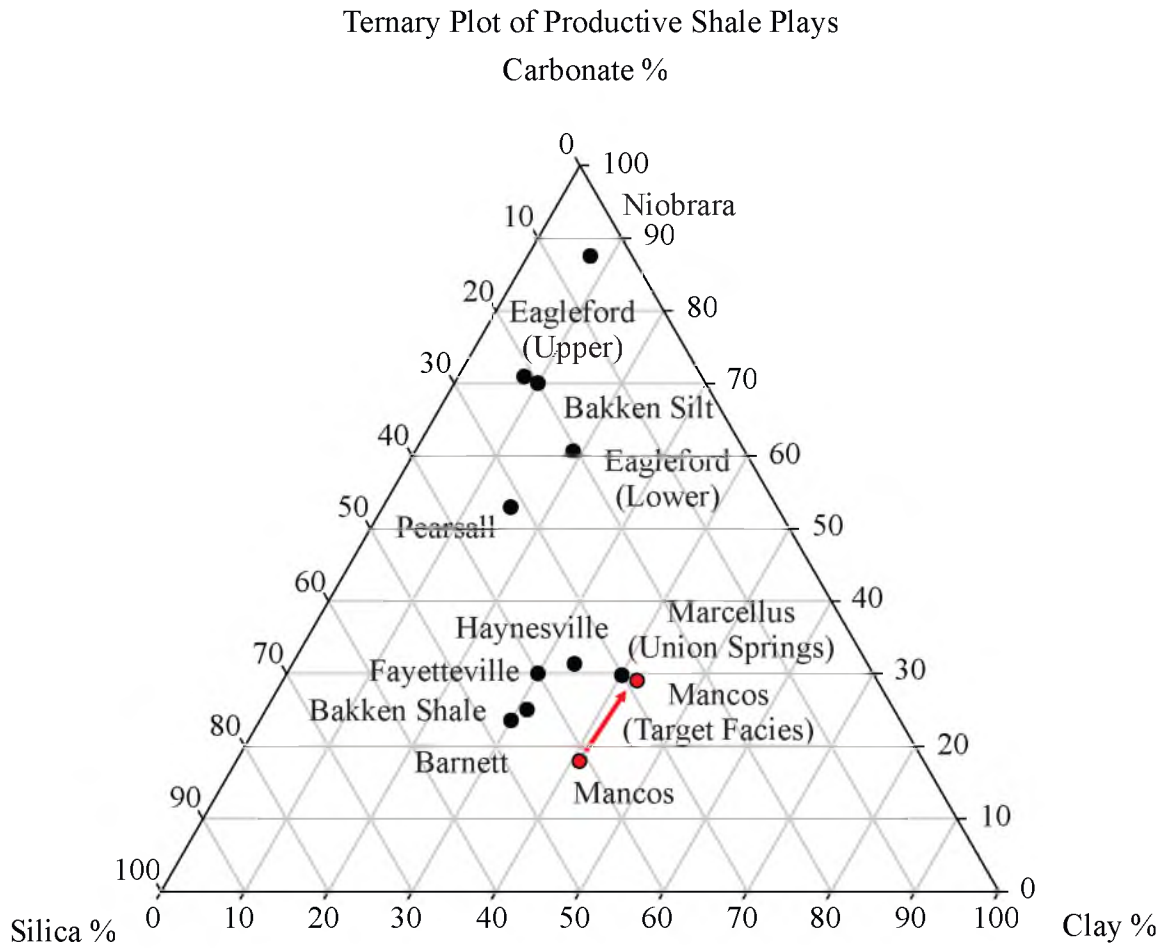

Figure 28: A ternary diagram plotting productive shale plays of North America based on relative proportions of clay, carbonate, and silica content. The bulk composition of the Mancos Shale is the most carbonate poor and clay rich of any of these producing shales, but reservoir target facies include higher proportions of carbonate, in line with the productive Marcellus Shale.

Modified from Anderson (2012), Boyce and Carr (2009), Bruner and Smosna (2011), and Horton (2012).

2005; Slatt and Rodriguez, 2012). The distal sediment-starved shelf deposits (FA2) described in detail from core are believed to offer the greatest potential for production based on an abundance of organic material and calcite cement, which lends a natural brittleness to the otherwise clay-rich formation (Horton, 2012).

Furthermore, Kennedy's (2011) findings support the conclusion that the sediment starved shelf deposits display the most ideal geomechanical failure behavior and, hence, potentially favorable hydraulic fracture potential. It is unlikely that the organic-rich heterolith typical of the Juana Lopez formation contains similar quantities of calcite as the sediment starved shelf deposits, largely because it was deposited in a shallower setting above storm wave base relative to FA2. A higher abundance of detrital fine sandstone and siltstone could displace claystone from the facies and provide a certain amount of brittleness for hydraulic fracture and higher porosity and permeability for increased hydrocarbon storage and production. Other intervals of the Mancos Shale are less prospective, characterized by similar porosity and permeability values (Figure 29) but a lower organic content (Horton, 2012) (Figure 30).

Laramide tectonic activity played a major role in the rapid burial of the Mancos Shale into the oil and gas window in various portions of the asymmetric Uinta Basin. In the northern Uinta Basin, the Mancos entered the gas to the overmature window, but was less deeply buried to the south, where much of the formation entered the condensate and oil windows (Nuccio and Roberts, 2003; Quick and Ressetar, 2012) (Figure 31). The majority of the Mancos in the Uinta Basin provides opportunities for natural gas production, as has been undertaken to date by one horizontal and numerous vertical wells. However, success with liquids production from the Mancos in the San Juan Basin

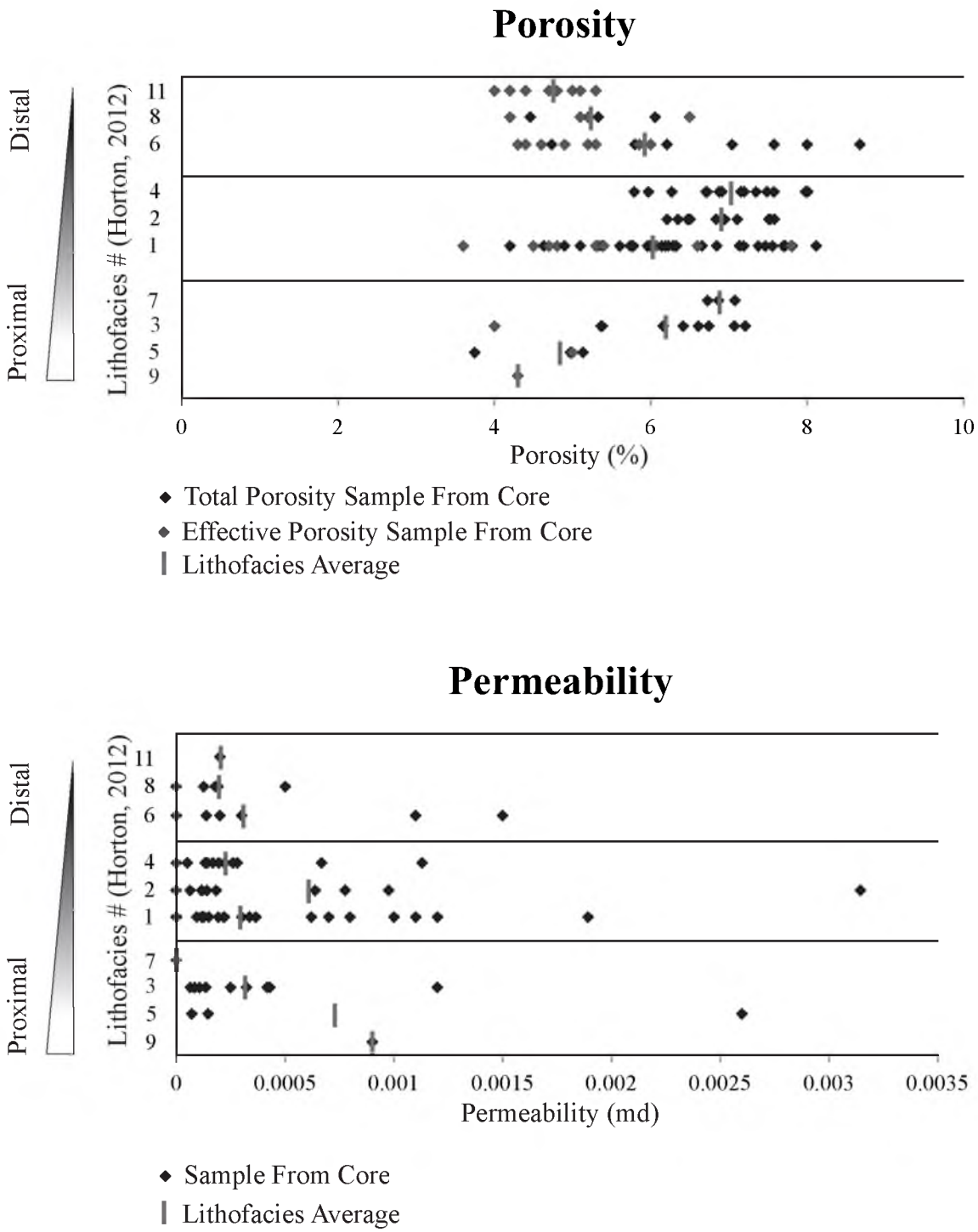

Figure 29: Distribution by lithofacies of porosity and permeability measurements from Mancos core. Lithofacies described by Horton (2012) and organized by position relative to shoreline.

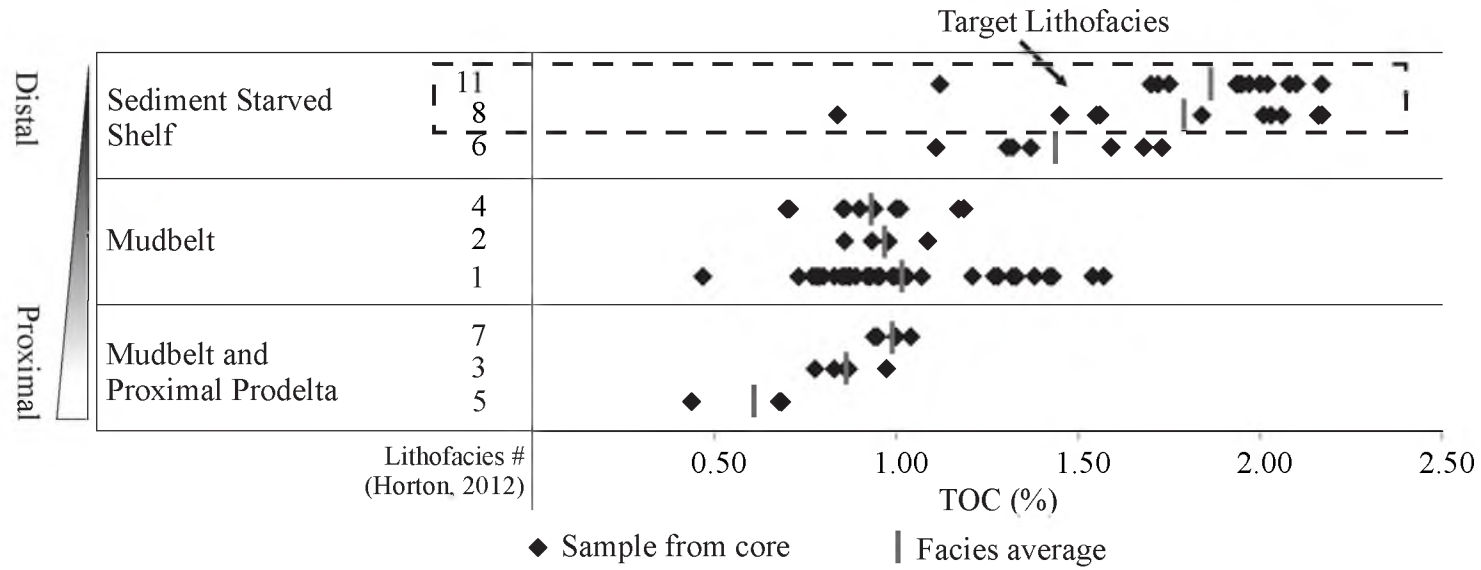

Figure 30: Distribution of TOC measurements from Mancos core. Lithofacies described by Horton (2012) and organized by depositional environment and position relative to shoreline. Evident correlation between distance from shoreline and TOC. Most prospective facies for tight hydrocarbon development indicated.

Figure 31: Thermal maturity of the Mancos Shale in the Uinta Basin at the A) middle (Nuccio and Roberts, 2003; Kirschbaum, 2003) and B) base (Quick and Ressetar, 2012) of the formation.

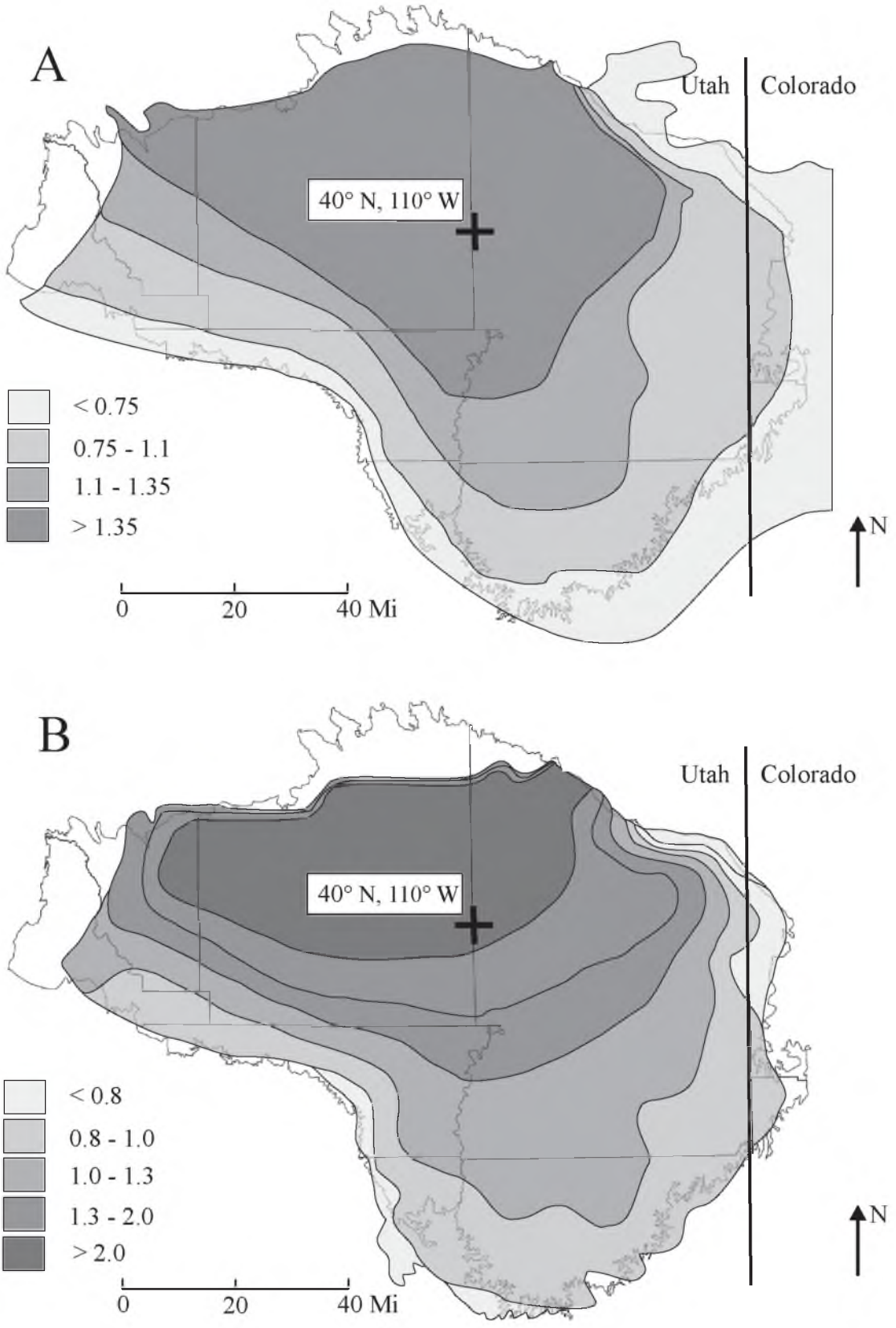
A
Utah
Colorado
40° N, 110° W
< 0.75
0.75 - 1.1
1.1 - 1.35
> 1.35
0
20
40 Mi
N
B
Utah
Colorado
40° N, 110° W
< 0.8
0.8 - 1.0
1.0 - 1.3
1.3 - 2.0
> 2.0
0
20
40 Mi
N

(Slothower, 2012; Ridgely et al., 2013) and oil and condensate window maturation histories in the Uinta Basin suggest liquids production may also be possible from particular combinations of geographic and depth or stratigraphic zones in the Uinta Basin.

Conclusions

The Mancos Shale was deposited across what is now the Uinta Basin during fifteen million years of the Late Cretaceous into the foreland basin of the Sevier fold and thrust belt. This heterolithic to mudstone-dominated marine shale represents the depositional transition between shallow marine sandstones currently exposed in central Utah and distal marine shales of the eastern Western Interior Seaway. The mudstone-dominated, organic-rich, distal deposits of the Mancos in the eastern Uinta Basin can be divided into two major facies associations. FA1 is typified by interbedded and interlaminated organic rich mudstone and fine sandstone deposited along a low-gradient shallow ramp above storm wave base with more abundant terrestrial organic matter input. FA1 corresponds stratigraphically to the distal Tununk, Juana Lopez, and lowermost Blue Gate Members. FA2 is composed of relatively marine organic-rich claystone to siltstone facies with relatively higher calcite content deposited on the sediment starved shelf below storm wave base during a period of high accommodation. As a result of higher subsidence rates, FA2 was deposited during active thrusting and reflects higher maximum water depth than more typical shallow ramp facies deposited in other Mancos strata, including FA1. During a period of relative tectonic quiescence in the early Campanian

which corresponded with eustatic fall, the basin filled with increasingly coarse-grained deposits transported away from the coast.

Both tectonics and eustasy demonstrate influence on the evolution of lithofacies in the Mancos Shale. Whereas the stratigraphic occurrence of shoreface sandstones appears to correlate with eustatic falls, the way these eustatic falls are expressed in facies of more distal strata is variable and is dominantly controlled by tectonically driven accommodation variations through space and time. The major sandstone-rich components of the Mancos Shale, the Ferron/Frontier, Emery, Star Point-Mancos B, and Blackhawk, each appear to correspond to eustatic falls identified from a variety of additional sea level records around the world. Whereas the Ferron/Frontier and Star Point-Mancos B correspond with sea level lowstand and are characterized by sandstone and siltstone-rich facies in relatively distal portions of the basin which interfinger with organic-rich deposits of FA1 in the lower Mancos, the Emery Sandstone corresponds with sea level highstand and mudstone-dominated facies in the distal realm (FA2). This depositional pattern appears to be the product of active subsidence in the Coniacian and Santonian, which outpaced the synchronous eustatic fall during Emery deposition in order to maintain a high relative sea level. Both eustasy and tectonic factors strongly affect sedimentation in an active foreland basin like the Western Interior Seaway.

While the use of T-R cycles produces a robust record of relative sea level change, the addition of detail from outcrop and stratal stacking patterns in the subsurface allow the creation of a more detailed sequence stratigraphic framework that distinguishes between highstand and lowstand sequence set conditions and clearly identifies sequence set boundaries, or more commonly their correlative conformities in the offshore

environment, through correlation to their expression in proximal shallow marine environments. The Mancos Shale includes two major sequence set boundaries, one corresponding with the base of the Ferron Sandstone and a second corresponding to the base of the Mancos B. There is a clear association between sequence sets and lithofacies distributions in the distal, eastern portion of the basin; lowstand sequence sets correspond with increased coarse-grained detrital components, whereas transgressive and highstand sequence sets are dominated by increasing organic and calcareous components. This relationship between distal facies and sequence stratigraphy allows it to be used for the predictive mapping of lithofacies throughout the formation.

Economic production of hydrocarbons from the Mancos Shale is dependent upon the identification of "sweet spots" based on primary and secondary characteristics of units in the formation. Core-based analysis has identified intervals of the formation compositionally similar to other successful resource plays of North America in an otherwise clay-rich, organic-lean shale (Horton, 2012). Primary lithological characteristics can be predicted using sequence stratigraphy to identify facies with suitable geomechanical and production potential, which appear to correlate with organic and calcite-rich facies of the transgressive and lower highstand systems tracts (Horton, 2012). Two potential target intervals are identified that correspond to FA1 and FA2. These two facies associations are each relatively high in organic content and correspond with transgression and early highstand, but reflect different depositional settings. Variations in the proportion of calcite and detrital quartz suggest each would likely behave differently during production. A thorough consideration of primary depositional characteristics alongside subsequent burial history is critical for efficient hydrocarbon

production from relatively organic lean tight shale plays like the Mancos Shale and other Upper Cretaceous shales of the Western Interior Seaway.

APPENDIX A

WELL DATABASE

Appendix A summarizes all of the well data available for use in this study. Wells are ordered randomly, and this well order is used to identify select wells throughout the study. Any wells with an "x" in the last column were incorporated into cross sections and/or isopach maps.

Well log abbreviations:

gr	gamma ray
rho	density
dphi	porosity from density
nphi	porosity from neutron
sp	spontaneous potential
ohm	resitivity
dt	sonic
pe	photoelectric factor
calc	calculated petrophysics – geomechanics, mineralogy, and/or water saturation

#	API	Well Label	Operator	Completion	Latitude	Longitude	.LAS	Other	
1	43007104810000	PETERS POINT-HUMBLE 8	RESERVE OIL & GAS CO	10/16/1964	39.7248457	-110.1120829			
2	43007104810001	PETERS POINT-HUMBLE 8	RESERVE OIL & GAS CO	7/19/1978	39.7248457	-110.1120829			
3	43007107530000	KEEL RANCH 1	MOUNTAIN FUEL SUPLY	1/10/1964	39.7771291	-110.4666056	gr	dst	
4	43007107530001	KEEL RANCH UNIT 1-16	TRIGG DRLG CO INC	10/23/1981	39.7771291	-110.4666056			
5	43007300780000	STATE 18-1A	MOSBACHER PROD CO	7/30/1982	39.6024109	-111.071113	gr, rho, dphi		
6	43007301290000	STATE OF UTAH RGU1	RIVER GAS CORP THE	3/13/1991	39.5693974	-110.85971	gr, nphi	core (220-1,932')	x
7	43007307860000	JENSON 7-15 DEEP	WILLIAMS PROD RMT CO	10/21/2001	39.7866338	-110.7844743			
8	43007307860001	JENSEN DEEP 7-15-12-10	PIONEER NAT RES USA	12/23/2007	39.7866338	-110.7844743			
9	43007311670000	CORDINGLY CANYON 15-5	MARION ENERGY	12/4/2006	39.6965144	-110.7820731			
10	43007312520000	COTTONWOOD FED 23-13	PETRO-CANADA RES USA	9/8/2008	39.6809985	-110.2025203			
11	43007312610000	PETERS POINT UNIT FE 15-6D-13-17	BARRETT BILL CORP	7/4/2008	39.7211563	-110.0554674	sp, gr, ohm, nphi		x
12	43007312800000	PETERS POINT STATE 8-2D-13-16	BARRETT BILL CORP	9/20/2007	39.7204595	-110.0859977			
13	43007312800001	PETERS POINT STATE 8-2D-13-16D	BARRETT BILL CORP	11/28/2010	39.7204595	-110.0859977			
14	43007313360000	STATE 7-16-14-13	BARRETT BILL CORP	2/16/2010	39.6086916	-110.4645617	gr, calc		
15	43013326850000	GATE CANYON STATE 23-16-11-15	GASCO PRODUCTION CO	2/15/2009	39.8551438	-110.2409273	sp, gr, ohm, dt, calc	FMI log	x
16	43013334370000	RYE PATCH FED 22-21	PETRO-CANADA RES USA	2/16/2009	39.8487164	-110.3349003	gr, ohm, nphi		x
17	43013334430000	RYE PATCH 24-21	PETRO-CANADA RES USA	9/16/2008	39.8486047	-110.2969876	gr, nphi		

#	API	Well Label	Operator	Completion	Latitude	Longitude	.LAS	Other	#
18	43013337580000	RESERVATION RIDGE-ST 42-2	WILLIAMS PROD RMT CO	9/18/2008	39.8934702	-110.6510284	gr		
19	43019102740000	CISCO 5	CRYSTAL CARBON CO	6/11/1928	39.0426067	-109.5618101			
20	43019104620000	GOVT 5	HANCOCK B W	10/16/1960	39.3568467	-109.0644106			
21	43019107810000	WESTWATER UNIT 3-C	OIL INCORPORATED	4/15/1959	39.3460007	-109.3232683			
22	43019159010000	SAN ARROYO 21	SINCLAIR OIL & GAS C	5/11/1963	39.3851973	-109.1043708			
23	43019159010001	SAN ARROYO 21	SINCLAIR OIL & GAS C	3/29/1964	39.3851973	-109.1043708			
24	43019302460000	J D M-VANOVER 1	MEZO J D	10/30/1975	38.9712246	-109.3116999			
25	43019303610000	FEDERAL-258 2	ANSCHUTZ CORP	6/11/1978	39.2648543	-109.2769561			
26	43019304920000	FEDERAL 30-2	NP ENERGY	10/25/1979	39.0426555	-109.5241718	sp		
27	43019305090000	FEDERAL 24-2	JACOBS R L O&G	9/29/1979	39.0532846	-109.3278768			
28	43019305670000	UTON 1	UTON ENERGY INC	8/15/1983	39.4417608	-109.2877932			
29	43019305670001	UTON 1	COCHRANE RES INCORP		39.4417608	-109.2877932			
30	43019305820000	FEDERAL 26-3	ADAK ENERGY	1/1/1982	39.043126	-109.5660142			
31	43019305820001	ADCO FEDERAL 26-3	BOWERS OIL & GAS INC	1/27/1990	39.043126	-109.5660142			
32	43019306650000	FEDERAL 22-3	ADAMS FRANK B	4/14/1981	39.0570481	-109.5898316	gr		
33	43019306650001	FEDERAL 22-3	BOG INCORPORATED	12/20/1985	39.0570481	-109.5898316			
34	43019306960000	CAPANSKY-BUSH 11-2	BUSH WILLIAM G	5/7/1981	39.2509808	-109.2349403			
35	43019307030000	WILSON 33-2	TENNECO OIL CO	5/6/1981	39.3777712	-109.2687609			
36	43019307150000	TUMBLEWEED 27-5	AMBRA OIL & GAS CO	7/18/1982	39.0419983	-109.5799743	sp		
37	43019307150001	TUMBLEWEED 27-5	BOG INCORPORATED	4/17/1987	39.0419983	-109.5799743			
38	43019307640000	WESTERN FEDERAL 14-5	EXIT INCORPORATED	6/26/1981	39.0932564	-109.4029875	sp		

#	API	Well Label	Operator	Completion	Latitude	Longitude	.LAS	Other	#
39	43019307890000	CAPANSKY-BUSH 11-1	BUSH WILLIAM G	7/20/1981	39.2506324	-109.2299476			
40	43019308530000	WESTWATER UNIT 3	ODEGARD RESOURCES	1/30/1982	39.3326342	-109.3266955	gr		
41	43019308530001	WESTWATER UNIT 3	THOMPSON J C	10/5/1994	39.3326342	-109.3266955			
42	43019309230000	MIDDLE CANYON 24 13-13-16	COSEKA RES (USA) LTD	10/20/1982	39.4208952	-109.2228606	gr		x
43	43019309340000	WESTERN FEDERAL 15-5A	EXIT INCORPORATED	1/26/1983	39.091509	-109.4022281			
44	43019309470000	CAPANSKY 11-3	BUSH WILLIAM G	6/29/1982	39.2504476	-109.2310952			
45	43019309560000	CAPANSKY 11-4	BUSH WILLIAM G	6/8/1983	39.2497274	-109.2340259			
46	43019310770000	USA 1-34	F & M OIL CO INC	11/1/1983	39.3701508	-109.2479987	gr		
47	43019310800000	CAPANSKY 11-5	BUSH WILLIAM G	7/13/1983	39.2509685	-109.2306467			
48	43019310810000	BUSH 11-6	BUSH WILLIAM G	7/22/1983	39.2509033	-109.229372			
49	43019311000000	BUSH 11-7	BUSH WILLIAM G	11/26/1983	39.2514126	-109.2302088			
50	43019311390000	CC CO 26-7	CC COMPANY	7/23/1985	39.0427853	-109.5614004	gr		
51	43019311650000	TUMBLEWEED 27-8	AMBRA OIL & GAS CO	11/4/1984	39.0430755	-109.5806003	gr		
52	43019311770000	GOVERNMENT BUSH 258-6A	BUSH WILLIAM G	2/5/1985	39.2651501	-109.2762485	gr		
53	43019311780000	BUSH 11-8	BUSH WILLIAM G	12/15/1984	39.2504542	-109.2317943			
54	43019313980000	MOON CANYON 1	ROYALE ENERGY	12/2/2003	39.3688257	-109.6318876	gr, rho, dt		x
55	43019313980001	MOON CANYON DEEPENIN 1	ROYALE ENERGY	8/24/2005	39.3688257	-109.6318876			
56	43019314020000	CACTUS ROSE MSC 2-1	TIDEWATER OIL&GAS CO	11/1/2005	39.0107611	-109.8941981	gr		
57	43019314020001	CACTUS ROSE MSC 2-1	NAE LLC	5/8/2009	39.0107611	-109.8941981			
58	43019314570000	THREE PINES 14-17-16-23	WIND RIVER II CORP		39.4107661	-109.4044529	sp, gr, rho, nphi		
59	43019314580000	KELLY CANYON 5 8-16-22	WIND RIVER II CORP	2/27/2006	39.4319187	-109.5167582	sp, gr, rho, nphi		
60	43019314580100	KELLY CANYON 10-8-16-22	WIND RIVER II CORP	8/1/2007	39.4319187	-109.5167582	sp, gr, rho, nphi		

#	API	Well Label	Operator	Completion	Latitude	Longitude	.LAS	Other	#
61	43019314690000	TIDEWATER STATE 32-3	SAMSON RESOURCES CO	8/31/2006	38.9478223	-109.8398508	gr, nphi		x
62	43019314690001	TIDEWATER 32-3	SAMSON RESOURCES CO	10/9/2007	38.9478223	-109.8398508			
63	43019315100000	SHOWSHOE 4-15-16-22	WIND RIVER II CORP		39.4213946	-109.4857183	sp, gr, nphi		x
64	43019315150000	CISCO 4-12-3	RUNNING FOXES PET	9/7/2010	39.0928007	-109.2734059	gr		
65	43019315460000	CACTUS ROSE 16-11-2118	TIDEWATER OIL&GAS CO	9/2/2008	38.9922245	-109.9461679	gr		
66	43047114200000	OAKES ESTATE 1	GEOTRONIC DEV	4/22/1959	40.4640426	-109.5646244			
67	43047114200001	W H OAKS ESTATE 1	VERNAL INTERMTN PET	3/22/1966	40.4640426	-109.5646244			
68	43047114210000	W H OAKS ESTATE 2	VERNAL INTERMTN PET	3/22/1966	40.464477	-109.5656415			
69	43047204660000	R R LEONARD 1	CARTER OIL COMPANY	4/6/1955	40.1061666	-109.1360194			
70	43047301650000	TEXACO-SKYLINE-GOVT 1	TEXACO INCORPORATED	12/23/1974	39.7024963	-109.4240809	gr, ohm, dphi		x
71	43047301650001	CHORNEY NCT 1	TEXACO INCORPORATED	10/15/1976	39.7024963	-109.4240809			
72	43047302450000	FEDERAL 12-7	HOUSTON OIL&MIN CORP	2/23/1977	40.4876907	-109.7269011			
73	43047302480000	BLACK HORSE CANYON 2	COSEKA RES (USA) LTD	3/13/1979	39.478041	-109.2465039	gr, ohm		x
74	43047302700000	BITTER CREEK 1	TAIGA ENERGY INC		39.6083562	-109.1739405	sp		
75	43047303250000	RAT HOLE CANYON 1	TAIGA ENERGY INC	11/19/1977	39.6131148	-109.1388181	gr		x
76	43047303310000	DRY BURN UNIT 1	COSEKA RES (USA) LTD	10/13/1978	39.6545661	-109.1366731	gr		x
77	43047303320000	FEDERAL 1-L-23	TAIGA ENERGY INC	4/14/1978	39.5891486	-109.1943728	gr		

#	API	Well Label	Operator	Completion	Latitude	Longitude	.LAS	Other	#
78	43047303910000	RED WASH UNIT 250 41-29C	CHEVRON U S A INC	10/3/1981	40.1863007	-109.2306243	gr		x
79	43047303910001	RED WASH UNIT 25041-29C	CHEVRON U S A INC	2/13/1995	40.1863007	-109.2306243			
80	43047304450000	DRY BURN UNIT 2-35-13-25	COSEKA RES (USA) LTD	10/23/1985	39.6473025	-109.0834108	gr		
81	43047304600000	SWEETWATER CANYON 1	COSEKA RES (USA) LTD	9/27/1979	39.6013311	-109.2041363	gr		x
82	43047305970000	RAT HOLE UNIT 3	CHANCELLOR&RIDGEWAY	10/9/1980	39.5767843	-109.0687124			
83	43047305980000	RAT HOLE UNIT 4	CHANCELLOR&RIDGEWAY	10/10/1980	39.5933334	-109.0676336			
84	43047306740000	MAIN CANYON FEDERAL 15-8-15-23	PIONEER NAT RES USA	4/10/1981	39.5318924	-109.3647132	sp, gr, ohm, rho, nphi		x
85	43047306740001	MAIN CANYON 15-8-15-23	PIONEER NAT RES USA	10/14/2007	39.5318924	-109.3647132			
86	43047307080000	CROOKED CANYON 10-10-14-23	COSEKA RES (USA) LTD	12/2/1980	39.6161876	-109.3267775	gr		
87	43047307350000	MAIN CANYON UNIT 2-8-15-23	COSEKA RES (USA) LTD	12/19/1980	39.5225757	-109.3624291	gr, ohm, dphi		
88	43047307350001	MAIN CANYON FED 2-8-15-23	PIONEER NAT RES USA	11/8/1998	39.5225757	-109.3624291			
89	43047307460000	WOLF UNIT 11-2-15-22	COSEKA RES (USA) LTD	11/27/1980	39.5438489	-109.4242016	gr		
90	43047308600000	LAMCO 3-24	CHAMPLIN PETRO CMPNY	5/14/1981	39.6690094	-109.6225373	gr		
91	43047309440000	TRAP SPRINGS-STATE 8-36-14-23	COSEKA RES (USA) LTD	7/9/1981	39.5548515	-109.2837534	gr		
92	43047309750000	TRAPP SPRINGS UNIT 1-25-14-23	COSEKA RES (USA) LTD	8/11/1981	39.5650102	-109.2858629	gr, ohm		
93	43047310440000	MAIN CANYON-FEDERAL 8-8-15-23	COSEKA RES (USA) LTD	7/30/1981	39.5254797	-109.3583295			

#	API	Well Label	Operator	Completion	Latitude	Longitude	.LAS	Other	#
94	43047310450000	BLACK HORSE CANYON 14-15-15-24	COSEKA RES (USA) LTD	1/28/1982	39.5181005	-109.2179396			
95	43047310550000	TRAPP SPRINGS 6-13-14-23	COSEKA RES (USA) LTD	10/14/1981	39.5982311	-109.2932385			
96	43047310720000	MAIN CANYON 6-3-15-23	COSEKA RES (USA) LTD	12/18/1981	39.5406993	-109.3302765	sp, gr, ohm, rho		
97	43047310720001	MAIN CANYON 6-3-15S-23E	PIONEER NAT RES USA		39.5406993	-109.3302765			
98	43047310740000	PINE SPRINGS UNIT 13-26-14-22	COSEKA RES (USA) LTD	12/23/1981	39.5764989	-109.4287104	gr, ohm		
99	43047310740001	PINE SPRINGS 13-26-14-22	BONNEVILLE FUELS	10/22/2001	39.5764989	-109.4287104			
100	43047310910000	22 FEDERAL 2-18-15	COSEKA RES (USA) LTD	11/25/1981	39.5076937	-109.4939606			
101	43047311040000	BLACK HORSE CANYON 12-8-15-24	COSEKA RES (USA) LTD	12/16/1981	39.5295021	-109.2607808	sp, gr, ohm, rho, nphi, dt, calc		x
102	43047311110000	MAIN CANYON 16-4-15-23	COSEKA RES (USA) LTD	11/12/1982	39.5473257	-109.3400875	sp, gr, ohm, rho, nphi	dst	x
103	43047311110001	MAIN CANYON FED 16-4-15-23	PIONEER NAT RES USA	8/1/2003	39.5473257	-109.3400875			
104	43047311350000	STATE OF UTAH 8-2-15-22	COSEKA RES (USA) LTD	9/11/1981	39.5399279	-109.4146105			
105	43047315100000	AGENCY DRAW 16-3	CELERON O&G CO	3/11/1985	39.710179	-109.6569544	sp, gr, ohm, rho, nphi, dt		x
106	43047325870000	DRAGON CANYON 27-12- 1	AMOCO PROD CO	6/24/1996	39.7483922	-109.0999466	gr, ohm, rho, nphi		x
107	43047325870001	DRAGON CANYON 27-12- 1	MEDALLION EXPL	5/5/1998	39.7483922	-109.0999466			
108	43047325920000	BLACK HORSE 9-15-24 1	AMOCO PROD CO	5/17/1996	39.5325858	-109.2323155	gr, ohm, rho, nphi		x
109	43047325920001	BLACK HORSE 9-15-24 1	CDX ROCKIES LLC		39.5325858	-109.2323155			
110	43047325930000	TPC STATE 23-36-14-24	AMOCO PROD CO	8/14/1996	39.5602282	-109.1769119			

#	API	Well Label	Operator	Completion	Latitude	Longitude	.LAS	Other	#
111	43047325930001	TPC STATE 36-14-241	RETAMCO OPERTNG INC	6/13/2005	39.5602282	-109.1769119			
112	43047326020000	ATCHEE RIDGE 24-13-2 1	AMOCO PROD CO	10/15/1996	39.6667779	-109.0685037	gr, ohm, rho, nphi		x
113	43047326020001	ATCHEE RIDGE 24-13-2 1	CDX ROCKIES LLC		39.6667779	-109.0685037			
114	43047326050000	EVACUATION CREEK 24-12-25	AMOCO PROD CO	9/15/1995	39.7633332	-109.0604833	gr		x
115	43047326050001	EVACUATION CREEK 24-12-25	RETAMCO OPERTNG INC		39.7633332	-109.0604833			
116	43047326180000	DAVIS CANYON 12-13-2 1	AMOCO PROD CO	4/18/1996	39.7030853	-109.0589977			
117	43047326180001	DAVIS CANYON 12-13-2 1	PIONEER NAT RES USA	6/5/2006	39.7030853	-109.0589977			
118	43047326570000	ATCHEE RIDGE 35-13-2 1	AMOCO PROD CO	8/7/1996	39.6449808	-109.0828729			
119	43047326590000	ATCHEE RIDGE 34-15-13-25	AMOCO PROD CO	7/10/1996	39.6813147	-109.1013649	gr, ohm, rho, nphi		x
120	43047326590001	ATCHEE RIDGE 15-13-2 1	CDX ROCKIES LLC		39.6813147	-109.1013649			
121	43047326600000	SEEP CANYON STATE 24-19-12-25	AMOCO PROD CO	8/14/1996	39.755123	-109.1624319			
122	43047326600001	SEEP CANYON STATE 19-12-25	MEDALLION EXPL	4/27/1998	39.755123	-109.1624319			
123	43047327050000	RAT HOLE CANYON 23-1 1	AMOCO PROD CO	6/6/1996	39.5847482	-109.0866425	sp, gr, ohm, nphi		x
124	43047327050001	RAT HOLE CANYON 23-1 1	CDX ROCKIES LLC		39.5847482	-109.0866425			
125	43047333420000	STATE 1	TULLY F M	10/26/1995	40.3747148	-109.3881807			
126	43047339240000	WEEKS 6-154	EL PASO PROD O&G CO	10/4/2002	40.0629283	-109.5301832	sp, gr, rho, nphi, dt		
127	43047339240001	WEEKS 6-154	WESTPORT O&G CO LP	10/11/2003	40.0629283	-109.5301832			
128	43047339240002	WEEKS 6-154	WESTPORT O&G CO LP	1/18/2005	40.0629283	-109.5301832			

#	API	Well Label	Operator	Completion	Latitude	Longitude	.LAS	Other	#
129	43047340140000	TUMBLEWEED UNIT 14-16-15-21	BARRETT BILL CORP	7/11/2003	39.5078689	-109.5729936	sp, gr, rho, nphi		
130	43047340190000	PAWWINNEE 3-181	EL PASO PROD O&G CO	4/27/2002	40.0638996	-109.5448551	sp, gr, rho		
131	43047340190001	PAWWINNEE 3-181	WESTPORT O&G CO LP	7/6/2004	40.0638996	-109.5448551			
132	43047340530000	STAGECOACH UNIT 66-8N	EOG RESOURCES INC	1/6/2003	40.0450685	-109.4703295			
133	43047340530001	STAGECOACH UNIT 66-8N	EOG RESOURCES INC	2/10/2003	40.0450685	-109.4703295			
134	43047340600000	WONSITS STATE 9-32	COASTAL O&G CORP	11/6/2001	40.1656684	-109.465471	sp, gr, rho, nphi, dt		
135	43047340770000	CHAPITA WELLS UNIT 804-18	EOG RESOURCES INC	6/25/2003	40.0304682	-109.3758464			
136	43047340770001	CHAPITA WELLS UNIT 804-18	EOG RESOURCES INC	9/1/2003	40.0304682	-109.3758464			
137	43047341370000	ISLAND UNIT 86	WEXPRO COMPANY	2/10/2008	39.9673228	-109.7436783	gr, ohm		x
138	43047341370001	ISLAND UNIT 86	WEXPRO COMPANY	10/21/2009	39.9673228	-109.7436783	gr, ohm		
139	43047341660000	FENCE CANYON ST 32 2	DOMINION EXPL&PROD	6/7/2002	39.4755443	-109.3730435	gr, ohm, rho, nphi		
140	43047341660001	FENCE CANYON ST 32 2	XTO ENERGY INC	11/9/2010	39.4755443	-109.3730435			
141	43047342800000	WONSITS VALLEY 14W-11-8-21	QEP UINTA BASIN INC	3/28/2005	40.1326846	-109.5231253	sp, gr, rho, nphi		x
142	43047342800001	WONSITS VALLEY WV 14M-11-8-21	QEP UINTA BASIN INC	8/4/2006	40.1326846	-109.5231253			
143	43047343840000	WONSITS VALLEY 14W-30-7-22	QEP UINTA BASIN INC	7/19/2003	40.1768926	-109.485205	sp, gr, rho, nphi		x
144	43047345100000	CHAPITA WELLS UNIT 810-23	EOG RESOURCES INC	5/21/2003	40.025314	-109.4134797			
145	43047345100001	CHAPITA WELLS UNIT 810-23	EOG RESOURCES INC	1/27/2006	40.025314	-109.4134797			

#	API	Well Label	Operator	Completion	Latitude	Longitude	.LAS	Other	#
146	43047345810000	CHAPITA WELLS UNIT 819-15	EOG RESOURCES INC	3/9/2003	40.0376776	-109.432321			
147	43047345810001	CHAPITA WELLS UNIT 819-15	EOG RESOURCES INC	10/8/2003	40.0376776	-109.432321			
148	43047346750000	PINE SPRINGS FED 3-23-14S-22E	CARBON ENERG CORP US	11/1/2002	39.5795589	-109.4233885	sp, gr, ohm, rho		
149	43047347190000	OVER & UNDER SAGE GR 10W-15-8-22	QEP UINTA BASIN INC	4/16/2003	40.1210983	-109.4228745	rho, nphi		
150	43047347190001	OVER & UNDER SAGE GR 10W-15-8-22	QEP UINTA BASIN INC	5/23/2003	40.1210983	-109.4228745			
151	43047347190002	OVER & UNDER SAGE GR 10W-15-8-22	QEP UINTA BASIN INC	8/25/2003	40.1210983	-109.4228745			
152	43047347280000	BONANZA 10-3	WESTPORT O&G CO LP	11/22/2003	39.9679081	-109.3101837			
153	43047347420000	HILL CREEK NORTH 1-9-15-20	WIND RIVER RES CORP	4/6/2003	39.532841	-109.677898	ohm, rho, nphi		
154	43047347510000	BONANZA 4-6	WESTPORT O&G CO LP	11/30/2003	39.9761319	-109.3330073			
155	43047347530000	WHITE RIVER UNIT 5M-9-8-22	QEP UINTA BASIN INC	8/11/2005	40.1389238	-109.4517736	sp, gr, rho, nphi		
156	43047348250000	DIRTY DEVIL 22X-27	THURSTON ENERGY OPER	3/9/2006	40.0085755	-109.2011872	gr		x
157	43047348300000	HILL CREEK NORTH 10-10-15-20	WIND RIVER RES CORP	4/28/2003	39.526092	-109.6616092	sp, gr, rho, nphi		x
158	43047348780000	DUCK CREEK NORTH 214-33	EOG RESOURCES INC	11/2/2003	40.0815772	-109.5611997			
159	43047349000000	OVER & UNDER GLEN BE 3M-27-8-21	QEP UINTA BASIN INC	5/25/2005	40.099726	-109.5417101	sp, gr, rho, nphi		x
160	43047349020000	DUCK CREEK NORTH 11M-22-8-21	QUESTAR EXPLOR&PROD	11/8/2007	40.1081129	-109.5422345	gr, ohm, rho, nphi		x
161	43047349220000	HILL CREEK NORTH 4-1-15-20	WIND RIVER RES CORP	12/6/2003	39.547129	-109.6340143	sp, gr, rho, nphi		x

#	API	Well Label	Operator	Completion	Latitude	Longitude	.LAS	Other	#
162	43047349410000	BONANZA FEDERAL 15-27-10-25	CARBON ENERG CORP US	9/23/2003	39.925744	-109.083529			
163	43047349530000	HILL CREEK NORTH 14-11-15-20	WIND RIVER RES CORP	9/5/2003	39.5217194	-109.6481919	sp, gr, rho, nphi	RockEval	x
164	43047349540000	HILL CREEK NORTH 8-13-15-20	WIND RIVER RES CORP	11/16/2003	39.5149321	-109.6203777	sp, gr, rho, nphi		x
165	43047349550000	HILL CREEK NORTH 2-14-15-20	WIND RIVER RES CORP	5/15/2005	39.5186246	-109.6434546	gr, rho, nphi		x
166	43047349570000	GLEN BENCH 1D-27-8-21	QEP UINTA BASIN INC	9/5/2006	40.0993222	-109.5314412	sp, gr, rho, nphi		
167	43047350540000	HILL CREEK NORTH 4-13-15-20	WIND RIVER RES CORP	11/19/2003	39.5178504	-109.6340494	gr, rho, nphi		
168	43047351400000	HILL CREEK NORTH 1-6-15-20	WIND RIVER RES CORP	2/16/2004	39.5477164	-109.7100529	sp, gr, ohm, rho, nphi		x
169	43047352460000	GLEN BENCH 4D 28-8-21	QEP UINTA BASIN INC	6/9/2006	40.100068	-109.5654108	sp, gr, rho, nphi		x
170	43047352470000	GLEN BENCH 7M-28-8-21	QEP UINTA BASIN INC	8/11/2005	40.0960133	-109.55562	sp, gr, rho, nphi		
171	43047352830000	HILL CREEK NORTH 2-12-15-20	WIND RIVER RES CORP	2/26/2004	39.5315776	-109.6235319	sp, gr, rho, nphi		
172	43047353900000	HILL CREEK NORTH 9-11-15-20	WIND RIVER RES CORP	3/20/2004	39.5237489	-109.6397132	sp, gr, rho, nphi		
173	43047354420000	HILL CREEK NORTH 3-6-15-20	WIND RIVER RES CORP	10/18/2004	39.5518647	-109.7202353	gr, rho, nphi		x
174	43047355550000	PINE SPRINGS STATE 6-36-14-22	PIONEER NAT RES USA	9/2/2005	39.5555654	-109.4042086			
175	43047355670000	LINDISFARNE 1-26	EOG RESOURCES INC	12/18/2006	39.4802909	-109.3146843			
176	43047359970000	UTE TRIBAL 10-21-1319	FIML NATURAL RES LLC	6/2/2005	39.6695637	-109.7908138	gr		x
177	43047359970001	UTE TRIBAL 10-21-1319	FIML NATURAL RES LLC	3/3/2006	39.6695637	-109.7908138			
178	43047360940000	FEDERAL 32-20-9-19	GASCO PRODUCTION CO	10/25/2007	40.0191231	-109.8028637			

#	API	Well Label	Operator	Completion	Latitude	Longitude	.LAS	Other	#
179	43047360940001	FEDERAL 32-20-9-19	GASCO PRODUCTION CO	2/27/2008	40.0191231	-109.8028637			
180	43047361360000	SUBW 14M-7-7-22	QUESTAR EXPLOR&PROD	1/12/2007	40.2208533	-109.4852088	gr, ohm, rho, nphi		x
181	43047362600000	GLEN BENCH 16M-28-8-21	QEP UINTA BASIN INC	3/14/2006	40.0892924	-109.5513445	sp, gr, ohm, rho, nphi, calc	core (15,145-15,265'); RockEval	x
182	43047362710000	FEDERAL 14-31-9-19	GASCO PRODUCTION CO	8/10/2007	39.9816531	-109.8301644	sp, gr	FMI log	x
183	43047363510000	RED WASH 34-34 AMU	QEP UINTA BASIN INC	3/25/2008	40.163138	-109.4228578	sp, gr, rho		x
184	43047364680000	FEDERAL 9-12-9-18	NEWFIELD EXPL CO	2/14/2009	40.0436088	-109.8342985			
185	43047366200000	NBE 10ML-26-9-23	QEP UINTA BASIN INC	5/19/2007	40.0050959	-109.2916694	sp, gr, rho, nphi		x
186	43047368960000	LITTLE CANYON UNIT 11-9H	XTO ENERGY INC	9/26/2008	39.8737818	-109.6857456	gr, ohm, rho, nphi, dt, calc		
187	43047369090000	NHC 1-8-15-20	WIND RIVER RES CORP		39.5298841	-109.6882079	sp, gr, rho, nphi		
188	43047369100000	NORTH HILL CREEK 1-25-14-19	WIND RIVER RES CORP	11/4/2006	39.57409	-109.7281891	sp, gr, rho, nphi		
189	43047369110000	HILL CREEK NORTH 15-31-14-21	WIND RIVER RES CORP	5/27/2007	39.5504346	-109.6070611	sp, gr, rho, nphi		x
190	43047369160000	LAMB TRUST 14-14-9-19	GASCO PRODUCTION CO	12/16/2008	40.0257957	-109.7557783	gr, ohm		x
191	43047369620000	PINE SPRINGS STATE 15-36	PIONEER NAT RES USA	7/12/2006	39.5603301	-109.4007372			
192	43047372380000	NBZ 8D-31-8-24	QEP UINTA BASIN INC	2/4/2008	40.082038	-109.2512543	sp, gr, rho, nphi		
193	43047372770000	CWD 14D-32-8-24	QEP UINTA BASIN INC	8/1/2007	40.0733259	-109.2390603	sp, gr, rho, nphi		
194	43047373100000	RWS 14D-5-9-24	QUESTAR EXPLOR&PROD	6/26/2008	40.0600241	-109.2403895	sp, gr, ohm, rho, nphi, dt		x
195	43047373470000	CWD 10D-32-8-24	QUESTAR EXPLOR&PROD	3/11/2008	40.0761477	-109.2344542	sp, gr, ohm, rho, nphi, dt		x

#	API	Well Label	Operator	Completion	Latitude	Longitude	.LAS	Other	#
196	43047373500000	RWS 6D-5-9-24	QUESTAR EXPLOR&PROD	7/2/2007	40.0671377	-109.2402832	gr, ohm, rho, nphi		x
197	43047373520000	RWS 8D-6-9-24	QEP UINTA BASIN INC	2/28/2007	40.0671082	-109.2492124	sp, gr, ohm, rho, nphi	core (9,630-9750'); RockEval	x
198	43047374440000	HILL CREEK UNIT 15-33F	XTO ENERGY INC	12/15/2008	39.89881	-109.6658929	gr, ohm, rho, nphi, calc		x
199	43047374440001	HCU 15-33F	XTO ENERGY INC	8/16/2009	39.89881	-109.6658929			
200	43047374720000	WEAVER RIDGE 26-3	BAYLESS R L PROD LLC	8/4/2006	39.9235839	-109.0699388			
201	43047374730000	WEAVER RIDGE 26-5	BAYLESS R L PROD LLC	8/4/2006	39.9209488	-109.0751097			
202	43047375220000	STATE 6-36-13-22	DEL RIO RES INC	12/8/2007	39.6449382	-109.405897			
203	43047375410000	WOLF FLAT 14C-29-15-19	QUESTAR EXPLOR&PROD	9/1/2006	39.4777688	-109.8151103	sp, gr, ohm, rho, nphi, calc		x
204	43047376210000	FEDERAL 21-19-9-19	GASCO PRODUCTION CO	10/27/2007	40.0214167	-109.8244677	sp, gr	FMI log	x
205	43047376210001	FEDERAL 21-19-9-19	GASCO PRODUCTION CO	9/10/2010	40.0214167	-109.8244677			
206	43047376650000	GLEN BENCH 8D-20-8-22	QEP UINTA BASIN INC	6/2/2007	40.1104006	-109.456857	sp, gr, rho, nphi		x
207	43047376710000	BZ 10ML-16-8-24	QUESTAR EXPLOR &PROD	9/1/2007	40.121086	-109.2159558	sp, gr, ohm, rho, nphi		x
208	43047377050000	MAIN CANYON FEDERAL 23-7-15S-23E	PIONEER NAT RES USA	2/27/2007	39.5240412	-109.3844732	gr, ohm, rho, nphi, dt, calc	core (6,995-7,135'; 7,480-7,600'); RockEval	x
209	43047380280000	UTELAND STATE 34-2-10-18	GASCO PRODUCTION CO	9/1/2008	39.9669681	-109.85759			
210	43047380280001	UTELAND STATE 34-2-10-18	GASCO PRODUCTION CO	6/21/2010	39.9669681	-109.85759			
211	43047380490000	WONSITS VALLEY 11AML-14-8-21	QEP UINTA BASIN INC	6/9/2008	40.1235361	-109.5207694	sp, gr, rho, nphi		
212	43047382670000	GYPSUM HILLS 7D-19-8-21	QUESTAR EXPLOR &PROD	9/18/2008	40.1102357	-109.5935749	sp, gr, ohm, rho, nphi, calc		x

#	API	Well Label	Operator	Completion	Latitude	Longitude	.LAS	Other	#
213	43047384690000	SHEEP WASH FEDERAL 12-25-9-18	GASCO PRODUCTION CO	3/21/2008	40.0034939	-109.849067			
214	43047386370000	WHITE RIVER UNIT EIH 7AD-26-8-22	QUESTAR EXPLOR&PROD	3/18/2008	40.0972385	-109.401995			
215	43047386400000	WHITE RIVER UNIT EIH 6DD-35-8-22	QUESTAR EXPLOR &PROD	3/7/2008	40.0795941	-109.4072183	sp, gr, ohm, rho, nphi		
216	43047386410000	WHITE RIVER UNIT EIH 7AD-35-8-22	QEP UINTA BASIN INC	9/29/2007	40.0827122	-109.401968	sp, gr, rho, nphi		x
217	43047386620000	GH 6MU-20-8-21	QUESTAR EXPLOR &PROD	12/7/2008	40.1105308	-109.5811472	gr		
218	43047386630000	WV 6ML-24-8-21	QUESTAR EXPLOR &PROD	10/27/2008	40.1110326	-109.5039893	sp, gr, rho, nphi, calc		x
219	43047387370000	WONSITS VALLEY 16CML-14-8-21	QUESTAR EXPLOR &PROD	12/16/2008	40.1165712	-109.5151239	sp, rho		
220	43047389630000	SCS 5C-32-14-19	QUESTAR EXPLOR &PROD	7/31/2008	39.5583107	-109.8208931			
221	43047389900000	GB 1M-4-8-22R	QUESTAR EXPLOR &PROD	8/11/2007	40.157633	-109.4364575	sp, gr, ohm, rho, nphi, dt, calc	core (13,375-13,495'); RockEval	x
222	43047389940000	WHITE RIVER UNIT EIH 6D-5-8-23	QUESTAR EXPLOR &PROD	1/23/2008	40.1533643	-109.3518291	sp, gr, ohm, rho, nphi, calc		x
223	43047389950000	TU 3-35-7-21	QUESTAR EXPLOR &PROD	6/2/2008	40.1726596	-109.5249453	gr		
224	43047390400000	WONSITS VALLEY UNIT 8D-15-8-21	QUESTAR EXPLOR&PROD	10/27/2008	40.1234715	-109.5314677	gr		
225	43047390410000	WONSITS VALLEY UNIT 4BD-23-8-21	QUESTAR EXPLOR &PROD	10/12/2008	40.1158023	-109.5300726	sp, gr, ohm, rho, nphi, calc		x
226	43047390440000	WONSITS VALLEY UNIT 7BD-23-8-21	QUESTAR EXPLOR &PROD	8/18/2008	40.1125054	-109.5202763	sp, gr, ohm, rho, nphi		x
227	43047391700000	STATE 21-32B	GASCO PRODUCTION CO	6/25/2008	39.9905783	-109.8063133			
228	43047391720000	STATE 21-32A	GASCO PRODUCTION CO	6/20/2008	39.9906035	-109.8062707			

#	API	Well Label	Operator	Completion	Latitude	Longitude	.LAS	Other	#
229	43047392990000	TUMBLEWEED 18-9	STEWART PETROLEUM CO	1/15/2008	39.5104353	-109.601536	sp, gr, ohm		x
230	43047393210000	WONSITS VALLEY UNIT 13AD-8-8-22R	QUESTAR EXPLOR &PROD	11/19/2007	40.1347448	-109.469082	sp, gr, ohm, rho, nphi, calc		x
231	43047393410000	NBE 8CD-10-9-23	QUESTAR EXPLOR &PROD	2/23/2008	40.0509341	-109.3066371	sp, gr, ohm, rho, nphi		x
232	43047393460000	NBE 5DD-10-9-23	QUESTAR EXPLOR &PROD	3/30/2008	40.0509953	-109.3172348	gr, ohm, rho, nphi		x
233	43047393480000	NBE 4DD-17-9-23	QUESTAR EXPLOR &PROD	6/2/2008	40.0399219	-109.356162	sp, gr		
234	43047394450000	RED WASH UNIT 34-27ADR	QUESTAR EXPLOR &PROD	2/28/2008	40.1774097	-109.4235984	gr, rho		
235	43047394450001	RED WASH UNIT 34-27ADR	QUESTAR EXPLOR &PROD	1/17/2009	40.1774097	-109.4235984			
236	43047394990000	HILL NORTH CREEK 12-33-15-20	WIND RIVER RES CORP	2/15/2008	39.4644552	-109.6905186	sp, gr, nphi		
237	43047395950000	WEAVER CANYON 26-2	BAYLESS R L PROD LLC	11/3/2008	39.9266248	-109.0670861	sp, gr, rho		
238	43047395980000	HILL CREEK NORTH 1-11-15-20	WIND RIVER RES CORP	5/14/2008	39.5334275	-109.6398891	sp, gr, nphi		
239	43047396110000	HCU 12-29F	XTO ENERGY INC	8/14/2009	39.9157241	-109.6951662	gr, ohm, rho, nphi, calc	FMI log; RockEval	x
240	43047396110001	HCU 12-29F	XTO ENERGY INC	1/22/2011	39.9157241	-109.6951662			
241	43047396460000	HILL CREEK NORTH 14-8-15-20	WIND RIVER RES CORP	5/13/2008	39.5192944	-109.7025524	sp, gr, nphi		x
242	43047396620000	GB 15D-27-8-21	QUESTAR EXPLOR &PROD	8/3/2008	40.0891413	-109.5374428	sp, gr, ohm, rho, dphi, calc		x
243	43047396640000	WV 15D-23-8-21	QUESTAR EXPLOR &PROD	9/27/2008	40.1035623	-109.5180507	gr		
244	43047396830000	SCS 10C-16-15-19	QUESTAR EXPLOR &PROD	7/7/2008	39.5105721	-109.7921226	gr		x
245	43047397720000	STATE 23-2T-9-17	NEWFIELD EXPL CO	4/30/2009	40.0615541	-109.9767013			

#	API	Well Label	Operator	Completion	Latitude	Longitude	.LAS	Other	#
246	43047398090000	FR 6P-20-14-20	QUESTAR EXPLOR &PROD	12/2/2008	39.5861314	-109.7030869	gr, ohm		x
247	43047399620000	STATE 4-36TA-8-17	NEWFIELD PRODUCTION	1/29/2009	40.0804409	-109.960718			
248	43047403450000	GB 3D-4-8-22R	QUESTAR EXPLOR &PROD	12/10/2008	40.156975	-109.4472812	sp, gr, ohm, rho, nphi, calc		x
249	43047403960000	HILL CREEK UNIT 1-30F	XTO ENERGY INC	10/26/2010	39.9238435	-109.6997272	gr, calc		x
250	43013303860000	INDIAN CYN14-1	GULF OIL CORPORATION		40.04292	-110.53476	gr		
251	43013305380000	INDIAN CANYON 2	BHP PETROLEUM (AMERICAS)		39.96047	-110.64089	sp, gr, ohm, rho, nphi, dt		x
252	43007300240000	3	PEASE OIL & GAS COMPANY		39.68102	-110.72019	gr		x
253	43007308590000	PETERS POINT 6-7D-13-17	BILL BARRETT CORP		39.7178	-110.06019	gr, ohm, rho		x
254	43019108040000	CHERRY CANYON UNIT 1	PACIFIC NATURAL GAS	8/17/1964	39.4393677	-109.4515459	sp, gr, ohm, dt		
255	43019108060000	MRU 22-22	PACIFIC NATURAL GAS	7/4/1963	39.4031993	-109.5907203	sp, gr, rho		x
256	43019110110000	EAST CANYON FED 2	SHAMROCK O&G CORP	6/12/1962	39.4039944	-109.2162017	gr		
257	43019110120000	EAST CANYON-FED 3	SHAMROCK O&G CORP	8/1/1963	39.3860073	-109.24132	gr		
258	43019112940000	EAST CANYON UNIT 1-8	TIDEWATER OIL CO	8/27/1963	39.4271973	-109.1809221			
259	43019113190000	FED-GIBBS 1-29	UNDERWOOD RIP C	10/6/1962	39.393108	-109.2930426	ohm		
260	43019113200000	MURPHY STATE 1-16	UNDERWOOD RIP C	7/1/1962	39.4148776	-109.2770794			
261	43019156710000	MOON RIDGE 31-15	PACIFIC NATURAL GAS	10/20/1963	39.4212028	-109.5861651	sp, gr, ohm, nphi		x
262	43019156720000	SEGUNDO CANYON 2	PACIFIC NATURAL GAS	2/25/1963	39.366914	-109.6048994	sp, gr, ohm, rho, nphi		

#	API	Well Label	Operator	Completion	Latitude	Longitude	.LAS	Other	#
263	43019160460000	FENCE CANYON UNIT 3	TEXACO INCORPORATED	9/15/1970	39.4552283	-109.379949	sp, gr, ohm		
264	43019162020000	EAST CANYON UNIT 1-17	TIDEWATER OIL CO	8/5/1963	39.4188444	-109.1827915			
265	43019162030000	FED-SEAGULL 1-18	UNDERWOOD RIP C	10/3/1962	39.4156428	-109.1985384			
266	43019162050000	EAST CANYON UNIT 44-12	TIDEWATER OIL CO	10/13/1963	39.4263512	-109.2091011			
267	43019201550000	HORSE POINT UNIT M-5	OIL INCORPORATED	7/17/1968	39.3624052	-109.2758545			
268	43019301350000	ANDERSON-FEDERAL 1	PEASE WILLARD O&G CO	8/1/1973	39.4248436	-109.1835415			
269	43019301360000	ANDERSON-FEDERAL 2	PEASE WILLARD O&G CO	7/25/1973	39.4265798	-109.2220847			
270	43019301690000	STATE 428-1	ANSCHUTZ CORP	6/10/1976	39.4398734	-109.5117178	sp, gr, ohm, rho, nphi		
271	43019301720000	FEDERAL 051-1	ANSCHUTZ CORP	12/4/1973	39.3966228	-109.3674346	sp, ohm		
272	43019301790000	FEDERAL 33-11	PACIFIC TRNSMSN SPLY	11/30/1973	39.4288464	-109.2326831			
273	43019301930000	STATE 913 1-A	ANSCHUTZ CORP	8/23/1974	39.4265969	-109.4912906	gr, ohm, rho		
274	43019304210000	TEN MILE-STATE 921-1	ANSCHUTZ CORP	10/6/1978	39.3772545	-109.5907868	sp, gr, ohm, rho, nphi		
275	43019304600000	FEDERAL 1-20	NAT GAS CORP OF CALI	7/9/1979	39.4002841	-109.1779157	gr, ohm, dt		
276	43019305190000	FEDERAL 29-15	TENNECO OIL CO	11/20/1979	39.3815683	-109.2899395			
277	43019305450000	FEDERAL 28-15	TENNECO OIL CO	9/2/1980	39.3805499	-109.2747052			
278	43019305520000	TXO-ARCO-FEDERAL-B 1	TEXAS O&G CORP	2/18/1980	39.4397119	-109.19259			
279	43019306040000	DIETLER-STATE 2-7	TENNECO OIL CO	8/2/1980	39.3599437	-109.2292079			
280	43019306240000	TXO-ARCO-FEDERAL-G 1	TEXAS O&G CORP	5/10/1980	39.404965	-109.2036712			
281	43019306530000	CHERRY CANYON UNIT 16-1	BEARTOOTH O&G CO	8/14/1981	39.4215326	-109.4914428	sp, gr, ohm, rho		x
282	43019306690000	ICE CANYON UNIT 16-9	ODEGARD RESOURCES	5/10/1982	39.4172793	-109.6022278	sp, gr, ohm, rho		

#	API	Well Label	Operator	Completion	Latitude	Longitude	.LAS	Other	#
283	43019306970000	REINAUER 1-5	TENNECO OIL CO	6/23/1981	39.3608757	-109.215957			
284	43019307210000	FEDERAL 23-1	FORTUNE OIL COMPANY	9/9/1982	39.4425478	-109.2204506			
285	43019307500000	BUSHER CANYON 21-11	NAT GAS CORP OF CALI	9/23/1982	39.4352927	-109.238696			
286	43019307550000	FEDERAL 21-7	FORTUNE OIL COMPANY	10/9/1982	39.4356359	-109.2008056			
287	43019307580000	UTAH-STATE 1	NORTHWEST EXPL CO	4/12/1981	39.3669313	-109.1846977			
288	43019307520000	FEDERAL 1-15	MEGADON ENT INC	9/10/1993	38.8085047	-110.0387035			
289	43019307880000	THREE PINES UNIT 32-10	ODEGARD RESOURCES	8/10/1981	39.3715086	-109.3996044	sp, gr, ohm, rho, nphi		x
290	43019307900000	ARCO-FEDERAL 1	ODEGARD RESOURCES	11/23/1981	39.454692	-109.2311543			
291	43019307940000	TEXACO-STATE 1	TEXAS O&G CORP	7/7/1982	39.4548008	-109.4063918	sp, gr, ohm, rho		x
292	43019308380000	WALL-FEDERAL 1	TEXAS O&G CORP	1/8/1983	39.3853543	-109.1998565			
293	43019308410000	BAUMGARTNER-FEDERAL 2	TXO PROD CORP	11/10/1981	39.3821913	-109.2220326			
294	43019308560000	ARCO-FEDERAL 2	ODEGARD RESOURCES	5/18/1982	39.4556269	-109.239471			
295	43019308570000	CALLISTER-FEDERAL 1	TXO PROD CORP	8/2/1983	39.3998039	-109.2158323			
296	43019308590000	LAUCK-FEDERAL 1	TXO PROD CORP	6/23/1983	39.3893942	-109.1802005			
297	43019309910000	FEDERAL 43-7	FORTUNE OIL COMPANY	10/14/1982	39.4281011	-109.1972623			
298	43019310300000	FEDERAL 31-1	FORTUNE OIL COMPANY	8/31/1983	39.4393767	-109.2111673			
299	43019310340000	TXO-USA-A 1	TXO PROD CORP	8/23/1983	39.3949918	-109.1880701			
300	43019310350000	FEDERAL 42-8	FORTUNE OIL COMPANY	11/11/1983	39.4245668	-109.1765746			
301	43019310460000	FEDERAL 34-31	FORTUNE OIL COMPANY	10/4/1983	39.4537185	-109.2069808			

#	API	Well Label	Operator	Completion	Latitude	Longitude	.LAS	Other	#
302	43019310750000	LITTLE BERRY-STATE 1	TXO PROD CORP	11/23/1983	39.4390382	-109.3547007	gr, rho		x
303	43019311090000	LAUCK FEDERAL 2	TXO PROD CORP	12/13/1983	39.3848613	-109.1852442	gr, ohm		x
304	43019311510000	LITTLE BERRY STATE 1	TXO PROD CORP	6/12/1985	39.4485861	-109.3528521	gr, ohm, rho, nphi		x
305	43019311530000	MIDDLE CANYON UNIT 13-3	TXO PROD CORP	7/29/1984	39.4203388	-109.3355196	sp, gr, ohm		x
306	43019311600000	LITTLE BERRY STATE B-1	TXO PROD CORP	8/4/1984	39.4431868	-109.3611871	gr, ohm, rho		x
307	43019311620000	ARCO STATE 36-7	ARCO OIL & GAS CORP	10/19/1984	39.4534329	-109.2134076			
308	43019311670000	SAGE-FEDERAL 31-31	SAGE ENERGY CO	10/9/1984	39.3774173	-109.1969852			
309	43019311920000	ARCO-STATE 36-8	ARCO OIL & GAS CORP	9/27/1985	39.4545447	-109.2235413			
310	43019314130000	DIVIDE 1	COCHRANE RES INCORP	12/28/2005	39.4490461	-109.2765435	sp, gr, nphi, dt		x
311	43019315260000	TEN MILE CANYON 22-1	ROYALE ENERGY	11/16/2008	39.3993163	-109.5820286			
312	43047100180000	WINTER RIDGE 1	ALPINE OIL & ROYALTY	6/25/1962	39.4968678	-109.5544886	sp, gr		
313	43047105770000	UTE TRIBAL 32-5A	WHITING OIL & GAS	12/8/2009	39.5540295	-109.6943517	sp, gr, ohm, nphi, pe	dst	
314	43047107640000	MAIN CANYON 1	MOUNTAIN FUEL SUPLY	9/10/1960	39.4822619	-109.3401289	ohm	dst	
315	43047111170000	UINTAH-FED-122 1	SINCLAIR OIL & GAS C	6/14/1962	39.6850113	-109.4900092	calc		
316	43047111200000	UINTAH OIL ASSOC 1	SINCLAIR OIL & GAS C	5/24/1962	39.7065907	-109.5972253	calc		
317	43047157640000	FLATROCK 2	PHILLIPS PETRLM CO	1/8/1963	39.5721461	-109.7175904	sp, gr, ohm		
318	43047161970000	FENCE CANYON UNIT 1	TEXACO INCORPORATED	4/19/1960	39.4678079	-109.3963089	gr, calc		x
319	43047161980000	FENCE CANYON UNIT 2	TEXACO INCORPORATED	9/28/1970	39.4809313	-109.4156085	sp, gr, ohm		x
320	43047300970000	FEDERAL 31-13	WEBB RESOURCES INC	1/6/1971	39.4640538	-109.2793972	gr, ohm		x

#	API	Well Label	Operator	Completion	Latitude	Longitude	.LAS	Other	#
321	43047301150000	TEXACO-CHORNEY B NCT-1	TEXACO INCORPORATED	6/2/1972	39.6740678	-109.42369	gr, ohm, dt, calc		x
322	43047301210000	SOUTHEAST FLANK-UINT 1-5	CHORNEY OIL CO	6/17/1972	39.5475793	-109.3587418	sp, gr, ohm, rho, nphi		x
323	43047301260000	SE FLANK UINTAH-FED 1-28	CHORNEY OIL CO	10/8/1972	39.4786416	-109.466269	sp, gr, ohm, rho, dphi, dt		x
324	43047301350000	SEEP RIDGE UNIT 2	TEXACO INCORPORATED	4/10/1973	39.6307242	-109.4335072	sp, gr, ohm		x
325	43047301430000	TEXACO-SKYLINE ETAL 1	TEXACO INCORPORATED	10/23/1974	39.6538858	-109.554684	sp, gr, ohm, rho	dst	x
326	43047301680000	TEXACO-SKYLINE ETAL 4	TEXACO INCORPORATED	2/5/1975	39.6738825	-109.4050738	gr, ohm		
327	43047301700000	TEXACO-SKYLINE ETAL 1	TEXACO INCORPORATED	4/6/1975	39.6775105	-109.5973819	sp, gr, ohm, rho		x
328	43047302260000	GRAYKNOLLS-FEDERAL 1	GULF OIL CORP	4/29/1977	39.7600853	-109.5504516	gr, ohm		x
329	43047302470000	BLACK HORSE CANYON 1	GREAT BASINS PET CO	6/17/1977	39.5070211	-109.2461106	sp, gr, ohm, rho		x
330	43047302710000	CROOKED CANYON UNIT 1	EXXON CO USA	1/12/1978	39.5909569	-109.3634696	sp, gr, ohm, rho		x
331	43047302760000	SEEP RIDGE UNIT 5	TEXACO INCORPORATED	8/25/1977	39.6586851	-109.4234767			
332	43047302840000	PINE SPRINGS UNIT 1	EXXON CO USA	1/21/1978	39.598263	-109.4428448	sp, gr, ohm, rho		x
333	43047303550000	WOLF POINT UNIT 1	EXXON CO USA	7/30/1978	39.5379146	-109.5283618	sp, gr, ohm, rho		x
334	43047303860000	CROOKED CANYON UNIT 2	EXXON CORPORATION	11/17/1981	39.6487126	-109.3242145	sp, gr, ohm, rho		x
335	43047303940000	MAIN CANYON UNIT 14-16	COSEKA RES (USA) LTD	9/23/1978	39.5184984	-109.3493436	sp, gr, ohm, rho		x
336	43047304480000	BLACK HORSE CANYON 6-9-15-24	COSEKA RES (USA) LTD	7/19/1983	39.5241026	-109.2382102	sp, gr, ohm, rho		x
337	43047305160000	FEDERAL 44-3	PACIFIC TRNSMSN SPLY	12/7/1978	39.6229473	-109.6574468	sp, gr, ohm, rho		x

#	API	Well Label	Operator	Completion	Latitude	Longitude	.LAS	Other	#
338	43047305710000	MAIN CANYON UNIT 6-15S-2-3E	COSEKA RES (USA) LTD	9/8/1979	39.508161	-109.3493341	sp, gr, ohm, rho		x
339	43047305820000	TRAP SPRINGS UNIT 4-25-14-23	COSEKA RES (USA) LTD	10/3/1979	39.565648	-109.2977614	sp, gr, ohm, rho		x
340	43047306160000	FEDERAL 11-9-15-23	COSEKA RES (USA) LTD	1/8/1980	39.5299117	-109.3499288	sp, gr, ohm, rho	dst	x
341	43047306180000	MAIN CANYON FEDERAL 13-15	ARCH OIL & GAS CO	4/3/1989	39.5186297	-109.3355216	sp, gr, ohm, rho		
342	43047306190000	23 CROOKED CANYON 13-17-14	COSEKA RES (USA) LTD	8/5/1980	39.6058125	-109.3728111	sp, gr, ohm, rho		
343	43047306210000	22 PINE SPRINGS 2X-16-14	COSEKA RES (USA) LTD	12/14/1979	39.5946393	-109.4566799	gr, ohm, rho		
344	43047306220000	WOLF UNIT-FEDERAL 3-11-15-21	COSEKA RES (USA) LTD	7/18/1980	39.5230082	-109.5363106	sp, gr, ohm, rho		x
345	43047306390000	MAIN CANYON FED 11-10-15-23	PIONEER NAT RES USA	12/9/1988	39.5285071	-109.3319874	sp, gr, ohm, rho		
346	43047307650000	BLACK HORSE CANYON 31-1	ARCO OIL & GAS CORP	11/13/1981	39.4672404	-109.2799574	sp, gr, ohm		
347	43047307940000	DUCK CREEK 30-9GR	BELCO DEV CORP		40.0480334	-109.6641319			
348	43047309600000	22 PINE SPRINGS 15-16-14	COSEKA RES (USA) LTD	7/2/1981	39.6048702	-109.461487	gr, ohm, rho		x
349	43047309630000	DUNCAN-FEDERAL 1	TEXAS O&G CORP	8/6/1981	39.4875945	-109.369005	sp, gr, ohm, rho		x
350	43047309770000	MAIN CANYON FED 8-7-15-23	PIONEER NAT RES USA	1/15/2006	39.5252832	-109.3774551	sp, gr, ohm, rho, dt		x
351	43047309780000	TRAP SPRING 3-25-14-23	COSEKA RES (USA) LTD	8/5/1981	39.5764252	-109.2975269	gr, ohm		
352	43047310030000	TRAP SPRINGS 3-26-14-23	COSEKA RES (USA) LTD	7/17/1981	39.5666831	-109.3132913	sp, gr, ohm, rho		
353	43047310050000	SQUIER 1	TEXAS O&G CORP	11/11/1981	39.4725686	-109.3854328			
354	43047310420000	PINE SPRINGS 7-21-14-22	COSEKA RES (USA) LTD	10/4/1981	39.5843945	-109.4584017	gr, ohm		x

#	API	Well Label	Operator	Completion	Latitude	Longitude	.LAS	Other	#
355	43047310630000	PINE SPRINGS UNIT 8-20-14-22	COSEKA RES (USA) LTD	3/4/1982	39.5839592	-109.4710045	gr, ohm, rho		x
356	43047310640000	BLACK HORSE CANYON-F 14-2-15-23	COSEKA RES (USA) LTD	1/21/1982	39.5469382	-109.3113781	sp, gr, ohm, rho		
357	43047310700000	MAIN CANYON UNIT 9-3-15-23	COSEKA RES (USA) LTD	11/4/1981	39.5438226	-109.3210949	sp, gr, ohm, rho		x
358	43047310710000	FEDERAL 7-15-15-21	COSEKA RES (USA) LTD	9/19/1981	39.5108165	-109.54895	sp, gr, ohm, rho		x
359	43047310730000	MAIN CANYON 6-8-15-23	COSEKA RES (USA) LTD	11/17/1981	39.525717	-109.3681747	sp, gr, ohm, rho		
360	43047310940000	MEADOW CREEK 1	TXO PROD CORP	1/8/1982	39.4750712	-109.4941897	sp, gr, ohm, rho		
361	43047310960000	PINE SPRINGS 9-12-14-21	COSEKA RES (USA) LTD	2/21/1982	39.6163826	-109.508234	sp, gr, ohm, rho		
362	43047311370000	FEDERAL 5-13-15-21	COSEKA RES (USA) LTD	11/25/1981	39.5112214	-109.5221374	sp, gr, ohm		
363	43047312430000	23 STATE 11-32-15	COSEKA RES (USA) LTD	7/13/1982	39.4721226	-109.3684455	sp, gr, ohm, rho		x
364	43047312470000	FEDERAL 7-30-15-23	COSEKA RES (USA) LTD	10/13/1982	39.4826055	-109.3829666	sp, gr, ohm, rho		
365	43047315110000	FEDERAL 36-5D	BEARTOOTH O&G CO	12/17/1984	39.4699979	-109.4108028	sp, gr, ohm, rho, ▫phi		
366	43047333340000	DEL-RIO/ORION 32-3A	DEL-RIO RESOURCES	5/12/2000	39.5572748	-109.7083015	sp, gr, ohm		
367	43047333350000	DEL-RIO/ORION 32-4A	DEL-RIO RESOURCES	4/20/2000	39.5580008	-109.7036664	sp, gr, ohm, rho		
368	43047333370000	UTE TRIBAL 32-6A	MILLER DYER & CO LLC	9/8/2005	39.5577	-109.6989869	sp, gr, ohm, rho		x
369	43047334470000	DEL-RIO/ORION CR 32-13	DEL RIO RES INC	8/22/2001	39.6382578	-109.5965497	sp, gr, ohm, rho		x
370	43047334480000	DEL-RIO/ORION CR 32-14	DEL RIO RES INC	10/6/2001	39.6373621	-109.5925996	sp, gr, ohm, rho		x
371	43047335570000	UTE TRIBAL 32-8A	MILLER DYER & CO LLC	3/1/2001	39.5610474	-109.6941288	sp, gr, ohm, rho		x

#	API	Well Label	Operator	Completion	Latitude	Longitude	.LAS	Other	#
372	43047335580000	UTE TRIBAL 32-12A	MILLER DYER & CO LLC	3/29/2001	39.5540045	-109.7089394			
373	43047335950000	DEL-RIO/ORION 28-1A	DEL-RIO RESOURCES	10/19/2001	39.5685799	-109.689544			
374	43047335960000	DEL-RIO/ORION 30-6A	DEL-RIO RESOURCES	11/7/2001	39.5654646	-109.7122646			
375	43047336160000	DEL-RIO/ORION 29-4A	DEL-RIO RESOURCES	10/19/2001	39.5650927	-109.6992308			
376	43047336170000	DEL-RIO/ORION 29-5A	DEL-RIO RESOURCES	10/18/2001	39.5649511	-109.6942335			
377	43047336180000	UTE TRIBAL 32-7A	WHITING OIL & GAS	12/27/2009	39.5612856	-109.6984882	sp, gr, ohm, rho		
378	43047336190000	DEL-RIO/ORION 32-9A	DEL-RIO RESOURCES	7/6/2001	39.5578846	-109.6944983	sp, gr, ohm, rho		
379	43047336200000	UTE TRIBAL 32-10A	MILLER DYER & CO LLC	1/20/2001	39.5540225	-109.6990328	sp, gr, ohm, rho		
380	43047336210000	UTE TRIBAL 32-11A	WHITING OIL & GAS	1/31/2001	39.5540155	-109.7036979	sp, gr, ohm, rho		x
381	43047340980000	DEL-RIO/ORION 32-16A	DEL-RIO RESOURCES	3/14/2002	39.5504058	-109.6943972			
382	43047341020000	DEL-RIO/ORION 29-6A	DEL-RIO RESOURCES	1/9/2002	39.568523	-109.7041057	sp, gr, ohm, rho		x
383	43047341030000	DEL-RIO/ORION 29-7A	DEL-RIO RESOURCES	3/18/2002	39.5721457	-109.7082257	gr, ohm, rho		x
384	43047341830000	FENCE CANYON FEDERAL 2	DOMINION OK TX E&P	5/16/2006	39.4676203	-109.3830526			
385	43047345520000	HILL CREEK NORTH 4-10-15-20	WIND RIVER RES CORP	8/14/2002	39.5324139	-109.6713035	gr, ohm, rho		
386	43047356850000	HORSE POINT STATE 43-32	NATIONAL FUEL CORP	10/18/2004	39.4668153	-109.3581342	gr, ohm, rho, nphi, dt		x
387	43047358800000	FR UTE TRIBAL 9P-36-14-19	QEP UINTA BASIN INC	2/14/2005	39.5539447	-109.7285561			
388	43047363690000	MUSTANG 1320-12A	SLATE RIVER RES LLC	2/8/2007	39.7059229	-109.6208549			
389	43047363720000	UINTAH OIL ASSOC 1321-7A	SLATE RIVER RES LLC	11/9/2005	39.7073549	-109.6030223			

#	API	Well Label	Operator	Completion	Latitude	Longitude	.LAS	Other	#
390	43047363750000	UTAH OIL SHALES 1321-9P	SLATE RIVER RES LLC	10/26/2005	39.6953551	-109.5657485			
391	43047363760000	UTAH OIL SHALES 1321-9L	SLATE RIVER RES LLC	11/2/2005	39.6998168	-109.5792248			
392	43047372890000	MUSTANG 1320-13D	SLATE RIVER RES LLC	8/9/2006	39.6923054	-109.6340268			
393	43047372910000	MUSTANG 1320-10I	SLATE RIVER RES LLC	6/23/2006	39.69995	-109.6574931	sp, gr, rho, nphi		x
394	43047372950000	MUSTANG 1320-11H	SLATE RIVER RES LLC	5/2/2006	39.7038935	-109.6388456			
395	43047372980000	MUSTANG 1320-24E	SLATE RIVER RES LLC	6/12/2006	39.6738623	-109.6344707			
396	43019162060000	UNIT 1-X	TIDEWATER OIL CO	12/11/1961	39.4211255	-109.3440863	sp, ohm		
397	43019162060001	HORSE POINT UNIT 1-X	TIDEWATER OIL CO	7/3/1962	39.4211255	-109.3440863			
398	43047303230000	SEEP RIDGE 8	TEXACO INCORPORATED	5/17/1978	39.6857165	-109.419813	sp, gr, ohm		x
399	43047307910000	WOLF UNIT 6-35-14-23	COSEKA RES (USA) LTD	1/7/1981	39.5533801	-109.3098056	sp, gr, ohm, rho		
400	43019307620000	HARNEY-FEDERAL 1-X	TEXAS O&G CORP	3/27/1980	39.4409834	-109.178781			
401	43019309550000	FEDERAL 24-1	FORTUNE OIL COMPANY	10/23/1982	39.406587	-109.2155636			
402	43047332810000	OURAY 5-67	COASTAL O&G CORP	7/28/1999	40.0632721	-109.582083	sp, gr, rho, dt		x
403	43047332910000	OURAY 34-79	COASTAL O&G CORP	11/16/1999	40.078214	-109.5415431	sp, gr, rho, dt		x
404	43047345070000	TRIBAL 36-148	WESTPORT O&G CO LP	2/17/2004	40.0738294	-109.4982611	sp, gr, rho		x
405	43047345070001	TRIBAL 36-148	WESTPORT O&G CO LP	2/4/2005	40.0738294	-109.4982611			
406	43047345400000	BAYLESS STATE 2-1	EL PASO PROD O&G CO	9/30/2002	40.0587569	-109.6309449	sp, gr, rho		x
407	43047345400001	BAYLESS STATE 2-1	WESTPORT O&G CO LP	5/10/2003	40.0587569	-109.6309449			

#	API	Well Label	Operator	Completion	Latitude	Longitude	.LAS	Other	#
408	43007300270000	COAL CREEK 1	PEASE WILLARD O&G CO	1/25/1975	39.6664305	-110.6858711	sp, ohm		
409	43015103740000	ARNOLD 25-1	FOREST OIL CORPORATN	10/19/1959	39.395924	-110.316198	sp, gr, ohm		
410	43019308350000	BUTLER CANYON UNIT 33-12	TENNECO OIL CO	11/15/1982	39.123795	-110.0214049	gr, ohm		x
411	43007202860000	STONE CABIN UNIT 1	CHEVRON U S A INC	7/12/1968	39.7506365	-110.2595364	gr, dt	palyn.	x
412	43007311580000	PETERS POINT UNIT FE 2-12D-13-16	BARRETT BILL CORP	3/26/2007	39.7181168	-110.0605969	gr, ohm, rho		x
413	43007311580001	PETERS POINT UNIT FE 2-12D-13-16	BARRETT BILL CORP	12/2/2010	39.7181168	-110.0605969			
414	43019153170000	LARSEN-STATE 1	CARTER OIL COMPANY	2/17/1955	39.1018967	-109.2313184	gr, nphi	palyn.	x
415	43019153170001	LARSEN-STATE 1	LARSEN RESOURCES	7/15/1958	39.1018967	-109.2313184			
416	43019307080000	BAILEY-FEDERAL 1	TEXAS O&G CORP	12/20/1980	39.3372951	-109.3751263	gr, ohm		
417	43019307700000	DIAMOND CANYON II 15-15	TENNECO OIL CO	9/7/1981	39.2348977	-109.4670572	sp, gr, ohm	palyn.	x
418	43047109160000	WATSON 2	JOHNSON ROY M	3/2/1956	39.9979287	-109.0947156	gr, nphi	palyn.	x
419	43047109160001	WATSON B 1	PHILLIPS OIL CO	3/2/1956	39.9979287	-109.0947156			
420	43047301110000	CONOCO-FEDERAL 22-1	CONTINENTAL OIL CO	8/16/1972	40.0157937	-109.6592635	gr, ohm		x
421	43047301110001	CONOCO-FEDERAL 22-1	DOLTON L LEX	5/2/1984	40.0157937	-109.6592635			
422	43047303570000	BUCK CAMP 1	AMOCO PROD CO	6/15/1978	39.7646168	-109.4348422	gr, ohm		x
423	43047392110000	FEDERAL 15-24-9-18	NEWFIELD EXPL CO	11/14/2008	40.011561	-109.8390445			
424	43049300120000	INDIANOLA UNIT 1	SOHIO PETROLEUM CO	9/26/1982	39.8303235	-111.3488089	gr, ohm		x
425	43007107910000	NORTH SPRINGS FED-1	SHELL OIL CO	7/27/1958	39.4858489	-110.901831	sp, ohm		
426	43007107910001	NORTH-SPRINGS-FED 1	PACIFIC NATURAL GAS	9/30/1964	39.4858489	-110.901831			

#	API	Well Label	Operator	Completion	Latitude	Longitude	.LAS	Other	#
427	43015300220000	NELSON UNIT 1	CHEVRON U S A INC	10/6/1975	39.4649006	-110.2363	sp, gr, ohm		x
428	43019102300000	BLAZE CANYON 1	CONTINENTAL OIL CO	3/17/1962	39.005876	-109.8540338	sp, ohm		
429	43047372780000	CWD 16D 32-8-24	QUESTAR EXPLOR &PROD	6/10/2008	40.0731828	-109.2305569			
430	43007100260000	ABBOTT 1	AMERADA HESS CORP	1/7/1963	39.5841688	-110.9349694	gr, ohm		x
431	43019302880000	WESTWATER M-11	PEASE WILLARD O&G CO	2/1/1977	39.3116195	-109.3079847	gr, ohm		
432	43019307040000	CALVINCO 31-12	TENNECO OIL CO	1/15/1981	39.3702698	-109.2060935	gr, ohm		
433	43019307340001	LOCKRIDGE 14-4	LOCKRIDGE JOHN P	10/21/1983	39.1609985	-109.6864608	sp, gr, ohm, rho, nphi		x
434	43019307660000	BARNHILL 1	TEXAS O&G CORP	3/10/1981	39.3168374	-109.259837	gr, ohm		
435	43019307720000	SULPHUR CANYON 1-15	TENNECO OIL CO	4/17/1981	39.2639658	-109.3177315	gr, ohm		
436	43019308040000	RATTLESNAKE CANYON 16-4	TENNECO OIL CO	9/23/1981	39.1573356	-109.8357207	sp, gr, ohm, rho, nphi, dt		x
437	43019308090000	RATTLESNAKE CANYON 2-12	TENNECO OIL CO	12/10/1981	39.1784765	-109.7953802	sp, gr, ohm, rho, nphi, dt		x
438	43019309620000	BEARTOOTH FED 33-16	BEARTOOTH O&G CO	10/12/1982	39.3680973	-109.1542685	gr, ohm		
439	43019310090000	VALENTINE FED 3	TXO PROD CORP	12/12/1982	39.3671748	-109.1267828	gr, ohm		
440	43019310200000	NICOR FEDERAL 2	TXO PROD CORP	2/12/1983	39.3774916	-109.1576475	gr, ohm		
441	43019312240000	QUINOCO 32-3	LONE MOUNTN PROD CO	6/14/1986	39.3775403	-109.0703465	gr, ohm		
442	43019312460000	SAMEDAN 1-13	CREDO PETROLEUM CORP	11/18/1987	39.3334161	-109.2052451	gr, ohm		
443	43019110130000	TUSCHER CREEK 1	SHAMROCK O&G CORP	8/15/1961	39.1213596	-109.8728063	sp, gr, ohm		
444	43019154100000	BOOK CLIFFS 1	GREAT YELLOWSTONE CO	6/13/1961	39.1922802	-109.5009104	sp, ohm		
445	43019111650000	SUNRAY 3	SUNRAY MID CONT OIL	12/31/1960	39.2961741	-109.4311764	gr, ohm, nphi, dt		x

#	API	Well Label	Operator	Completion	Latitude	Longitude	.LAS	Other	#
446	43019314480000	CEDAR CAMP 3-5-16-23	BARRETT BILL CORP	4/24/2005	39.4499009	-109.4049785	gr, ohm, rho, nphi, dt		
447	43047369310000	UTE 1-20-1319	FIML NATURAL RES LLC	4/4/2007	39.6779884	-109.8051423	sp, gr, ohm, rho, nphi, dt		x
448	43047389680000	V CANYON 20-1	ROYALE ENERGY	11/20/2007	39.5044044	-109.5914652	gr, ohm, dt, calc		x
449	43047109600000	RAYMOND GOVT 1	RAYMOND C F OIL CO	1/20/1963	39.6922692	-109.1485175	gr, ohm		x
450	43047156750000	EVACUATION CREEK 23-2-1	PACIFIC NATURAL GAS	10/7/1964	39.8026794	-109.0885109	gr, ohm		x
451	43047309760000	SWEETWATER CYN 42-23	NAT GAS CORP OF CALI	11/15/1984	39.5873291	-109.1906805	gr, ohm		x
452	43007312780000	PETERS PT 14-27D-12-16	BARRETT BILL CORP		39.7389985	-110.1125102	gr, rho, nphi	FMI log	x
453	43007313560000	BBC STATE 10-36-14-13	BARRETT BILL CORP		39.5621273	-110.407722	gr, ohm, rho, calc		
454	43007500380000	PETERS PT 15-36D-12-16	BARRETT BILL CORP	5/19/2011	39.725394	-110.073226	gr, ohm, rho, nphi	FMI log	x
455	43047335300000	FENCE CYN 30-2	DOMINION OK TX E&P	8/29/2002	39.4786813	-109.3866482	gr, ohm, rho,nphi		
456	43047369390000	PACK MTN 03-27H	XTO ENERGY INC	10/17/2008	39.8351725	-109.665089	gr, ohm, rho, nphi, calc		x
457	43049500020000	43049500020000	EOG Resources		39.860819	-111.104192	sp, gr, ohm, rho, nphi, pe		x
458	43013300150000	4301330015	Gulf Oil Corp.		40.50024	-110.27034			x

APPENDIX B

REVISED LOWER MANCOS STRATIGRAPHY

This study has identified a number of chronostratigraphic stratal relationships which have not been recognized in the previous literature. The Ferron Sandstone, which represents the most significant sandstone-rich, progradational, delta front deposit of the Turonian and Coniacian, has been correlated with relatively low gamma ray facies of the distal Lower Blue Gate (Figures 19 and 21). These low gamma ray strata correspond with sandstone rich, siltstone heterolith (facies 9 of Horton, 2012) likely sourced from a strong sediment source along the western margin of the seaway like the Ferron delta. It is unlikely that a package of sandstone and siltstone this thick (> 500 ft (150 m)) could be sourced from another feature of the seaway. Underlying these low gamma ray strata are a number of high gamma ray mudstone units, each about 100 ft (30 m) thick separated by relatively low gamma ray, coarser-grained facies (Figures 19 and 21). These high gamma ray mudstone beds are regionally extensive over the eastern 100 mi of the basin before pinching out to the east (Figure 19). These mudstone beds correspond to four sequences, which each step dominantly shoreward (retrogradational), and stack to form a transgressive and a highstand sequence set. The high gamma ray shale interval of this lower TSS correspond with the Juana Lopez of Molenaar and Cobban (1991). This same interval appears to be chronostratigraphically equivalent with the Frontier Formation of

the northern Uinta Basin (Figures 20 and 21). The high gamma ray interval identified by Molenaar and Cobban as the Juana Lopez is nearly morphologically identical to other high gamma ray shale beds of the lowermost Blue Gate.

In contrast to the stratigraphic relationships described above, previous correlations have identified the Juana Lopez member as synchronous (Molenaar and Cobban, 1991), and potentially overlying (Gardner, 1995b) portions of the Ferron Sandstone and Frontier Formation. These correlations are based largely on biostratigraphy (Fouch et al., 1983; Molenaar and Cobban, 1991). In addition, Molenaar and Cobban (1991) mapped cuesta forming outcrops of marine shale with thin, platy, very fine-grained interbedded sandstone previously identified as Ferron Sandstone, instead as Juana Lopez. However, the exact nature of the stratigraphic relationship between the Juana Lopez, Ferron Sandstone, and Frontier Formation, particularly the transition from the Juana Lopez to the east and the Ferron to the west, is not clearly defined by Molenaar and Cobban (1991).

A number of mitigating factors should be considered in order to reconcile new log-based correlations with previous stratigraphy. The Ferron delta system varies in age along the margin of the Western Interior Seaway, tending to young to the south (Gardner, 1995b), and consists of a number of members, which have been miscorrelated frequently by workers of different generations and research interests (Ryer, 2004), suggesting some biostratigraphy may have been miscorrelated (Schwans, 1988). While the Ferron Sandstone has been extensively subdivided by different workers, the Lower Bluegate and Juana Lopez shales have seen only limited research, which has been dominantly focused on the San Juan Basin in New Mexico (e.g., Rankin, 1944; Dane et al., 1966; Pasley et al., 1993). Given the poor quality and limited thickness of section of marine shale

outcrops and the dearth of marker layers in subsurface data from the Mancos Shale, the miscorrelation of limited section does not seem unreasonable. The similar gamma signature of multiple shale layers in the subsurface suggests there may be multiple stratigraphic intervals of highly organic, heterolithic shale matching the lithofacies of the Juana Lopez Member, which may have been mapped instead as a single unit in the past.

The Juana Lopez has been identified as the muddiest portion of the Western Interior Seaway. It seems unlikely this would be time correlative to a river-dominated, lowstand delta like the Ferron, given the tendency for basin floor sand deposition to correspond with lowstands (Posamentier and Allen, 1993) and shelf edge deltas (Dixon et al., 2012). Instead the relationship between these two intervals has likely been obscured by the poor quality of exposures of mud-rich offshore depositional systems. Significant shifts of shoreline along a shallow ramp and local delta lobe shifting likely create a complicated and frequently discontinuous stratigraphic record in the Turonian of eastern Utah.

REFERENCES

Abouelresh, M.O., and R.M. Slatt, 2012, Lithofacies and sequence stratigraphy of the Barnett Shale in east-central Forth Worth Basin, Texas: AAPG Bulletin, v. 96, p. 1–22, doi: 10.1306/04261110116.

Algeo, T.J., L. Schwark, and J.C. Hower, 2004, High-resolution geochemistry and sequence stratigraphy of the Hushpuckney Shale (Swope Formation, eastern Kansas): implications for climate-environmental dynamics of the Late Pennsylvanian Midcontinent Seaway: Chemical Geology, v. 206, p. 259–288, doi: 10.1016/j.chemgeo.2003.12.028

Allen, J.L. and C.L. Johnson, 2010, Sedimentary facies, paleoenvironments, and relative sea level changes in the John Henry Member, Cretaceous Straight Cliffs Formation, Southern Utah, USA, *in* S.M. Carney, D.E. Tabet, and C.L. Johnson, eds., Geology of south central Utah: Utah Geological Association Publication 39, p. 225–247.

Allen, J.L. and C.L. Johnson, 2011, Architecture and formation of transgressive regressive cycles in marginal marine strata of the John Henry Member, Straight Cliffs Formation,Upper Cretaceous of Southern Utah, USA: Sedimentology, v. 58, p. 1486–1513, doi: 10.1111/j.1365-3091.2010.01223.x

Anderson, D.S., and N.B. Harris, 2006, Integrated sequence stratigraphic and geochemical resource characterization of the Lower Mancos Shale, Uinta Basin, Utah: Utah Geological Survey, Open-File Report 483, 129 p.

Anderson, P.B., and T.A. Ryer, 2004, Regional stratigraphy of the Ferron Sandstone, *in* T.C. Chidsey, R.D. Adams, and T.H. Morris, eds., Analog for fluvial-deltaic reservoir modeling: Ferron Sandstone of Utah: AAPG Studies in Geology, v. 50, p. 211–224.

Anderson, T., 2012, Eagle Ford Ternary Diagram, In tri-plot_Mineral_types.xls (Ed.), *Excel,* EGI Internal Report: EGI.

Angulo, S., and L.A. Buatois, 2012, Integrating depositional models, ichnology, and sequence stratigraphy in reservoir characterization: the middle member of the Devonian Carboniferous Bakken Formation of subsurface Saskatchewan revisited: AAPG Bulletin, v. 96, p. 1017–1043, doi: 10.1306/11021111045.

Anna, L.O., 2012, West-east lithostratigraphic cross section of Cretaceous rocks from central Utah to western Kansas: U.S. Geological Survey Open-File Report 2012–1074, 2 sheets.

Aplin, A.C., and J.H.S. MacQuaker, 2011, Mudstone diversity: origins and implications for source, seal, and reservoir properties in petroleum systems: AAPG Bulletin, v. 95, p. 2031–2059, doi: 10.1306/03281110162.

Arthur, M.A., W.A. Dean, and S.O. Schlanger, 1985, Variations in the global carbon cycle in the Cretaceous related to climate, volcanism, and changes in atmospheric CO_2: Geophysical Monograph, v. 32, p. 504–529.

Arthur, M.A. and S.O. Schlanger, 1979, Cretaceous "ocean anoxic events" as causal factors in development of reef-reservoired giant oil fields: AAPG Bulletin, v. 63, p. 870–885.

Bann, K.L., and C.R. Fielding, 2004, An integrated ichnological and sedimentological comparison of non-deltaic shoreface and subaqueous delta deposits in Permian reservoir units of Australia, *in* D. McIlroy, ed., The application of ichnology to palaeoenvironmental and stratigraphic analysis: The Geological Society, London, SpecialPublications, v. 228, p. 273–310.

Bhattacharya, J.P., and J.A. MacEachern, 2009, Hyperpycnal rivers and prodeltaic shelves in the Cretaceous Seaway of North America: Journal of Sedimentary Research, v. 79, p. 184–209, doi: 10.2110/jsr.2009.026.

Bhuyan, K., and Q.R. Passey, 1994, Clay estimation from GR and neutron-density porosity logs: Transactions of the SPWLA, 35th Annual Logging Symposium, June 19-22, p. 1–15.

Blakey, R., 2013, http://cpgeosystems.com/images/NAM_key-85Ma_LateK-sm.jpg, accessed 7/17/2013.

Bohacs, K.M., 1998, contrasting expressions of depositional sequences in mudrocks from marine to non marine environs, *in* J. Schieber, Zimmerle, and P. Sethi, eds., Shales and Mudstones I, p. 33–78.

Bohacs, K.M., G.J., Grabowski Jr., A.R. Carroll, P.J. Mankiewicz, K.J. Miskell-Gerhardt, J.R. Schwalbach, M.B. Wegner, and J.A. Simo, 2005, Production, destruction, and dilution –the many paths to source rock development, The Deposition of Organic Carbon Rich Sediments: Models, Mechanisms, and Consequences: SEPM Special Publication no. 82, p. 61–101.

Boyce, M. L., and T.R. Carr, 2009, Lithostratigraphy andPetrophysics of the Devonian Marcellus Interval in West Virginia and Southwestern Pennsylvania, 29th Annual

GCSSEPM Foundation Bob F. Perkins Research Conference, Houston, TX, http://search.proquest.com/docview/916837583?accountid=14677.

Brett, C.E., and G.C. Baird, 1996, Middle Devonian sedimentary cycles and sequences in the northern Appalachian Basin, *in* B.J. Witzke, G.A. Ludvigson, and J. Day, eds., Paleozoic Sequence Stratigraphy: View from the North American Craton: GSA Special Paper 306, p. 213–241.

Bruner, K. R., and R. Smosna, 2011, A Comparative Study of the Mississippian Barnett Shale, Fort Worth Basin, and Devonian Marcellus Shale, Appalachian Basin *in* D. J. Soeder, Ed., National Energy Technology Laboratory: U.S. Department of Energy.

Catuneanu, O. and M. Zecchin, 2013, High-resolution sequence stratigraphy of clastic shelvesII: controls on sequence development: Marine and Petroleum Geology, v. 39, p. 26–38.

Catuneanu, O., V. Abreu, J.P. Bhattacharya, M.D. Blum, R.W. Dalrymple, P.G. Eriksson, C.R. Fielding, W.L. Fisher, W.E. Galloway, M.R. GIbling, K.A. Giles, J.M. Holbrook, R. Jordan, C.G.St.C. Kendall, B. Macurda, O.J. Martinsen, A.D. Miall, J.E. Neal, D.Nummedal, L. Pomar, H.W. Posamentier, B.R. Pratt, J.F. Sarg, K.W. Shanley, R.J.Steel, A. Strasser, M.E. Tucker, and C. Winker, 2009, Towards the standardization of sequence stratigraphy: Earth-Science Reviews, v. 92, p. 1–33.

Chalmers, G.R., R.M. Bustin, and I.M. Power, 2012, Characterization of gas shale pore systems by porosimetry, pycnometry, surface area, and field emission scanning electron microscopy/transmission electron microscopy image analyses: examples from the Barnett, Woodford, Haynesville, Marcellus, and Doig units: AAPG Bulletin, v. 96, p. 1099–1119, doi: 10.1306/10171111052.

Chan, M.A., S.L. Newman, and F.E. May, 1991, Deltaic and shelf deposits in the Cretaceous Blackhawk Formation and Mancos Shale, Grand County, Utah: Utah Geological Survey, Miscellaneous Publication 91-6, 83 p.

Cole, R.D., R.G. Young, and G.C. Willis, 1997, The Praire Canyon Member, a new unit of the Upper Cretaceous Mancos Shale, west-central Colorado and east-central Utah: Utah Geological Survey Miscellaneous Publication 97-4, 26 p.

Conrad, C.P., and L. Husson, 2009, Influence of dynamic topography on sea level and its rate of change: Lithosphere, v. 1, p. 110–120, doi: 10.1130/L32.1.

Cooper, M.R., 1977, Eustasy during the Cretaceous: its implications and importance: Paleogeography, Paleoclimatology, Paleoecology, v. 22, p. 1–60.

Creaney, S. and Q.R. Passey, 1993, Recurring patterns of total organic carbon and source rock quality within a sequence stratigraphic framework: AAPG Bulletin, v. 77, p. 386–401.

Cross, W. and C.W. Purington, 1899, Description of the Telluride Quadrangle, Colorado.

Curtice, R., 2013, Review of the deep Mancos shale gas wells in Utah, unpublished report, 33 p.

Dane, C.H., W.A. Cobban, and E.G. Kauffman, 1966, Stratigraphy and regional relationships of a reference section for the Juana Lopez Member, Mancos Shale, in the San Juan Basin, New Mexico: U.S. Geological Survey Bulletin 1224-H, 15 p.

DeCelles, P.G., 1994, Late Cretaceous – Paleocene synorogenic sedimentation and kinematic history of the Sevier thrust belt, northeast Utah and southwest Wyoming: GSA Bulletin, v. 106, p. 32–56.

Decelles, P.G., and J.C. Coogan, 2006, Regional structure and kinematic history of the Sevier fold-and-thrust belt, central Utah: GSA Bulletin, v. 118, p. 841–864, doi: 10.1130/B25759.1.

DeCelles, P.G., and K.A. Giles, 1996, Foreland basin systems: Basin Research, v. 8, p. 105–123.

Demaison, G.J., and G.T. Moore, 1980, Anoxic environments and oil source bed genesis: AAPG Bulletin, v. 64, p. 1179–1209.

Dickinson, W.R., M.A. Klute, M.J. Hayes, S.U. Janecke, E.R. Lundin, M.A. McKittrick, and M.A. Olivares, 1988, Paleogeographic and paleotectonic setting of Laramide sedimentary basins in the central Rocky Mountain region: GSA Bulletin, v. 100, p. 1023–1039.

Diecchio, R.J., and B.T. Brodersen, 1994, Recognition of regional (eustatic?) and local (tectonic?) relative sea level events in outcrop and gamma ray logs, Ordovician, West Virginia: Tectonic and Eustatic Controls on Sedimentary Cycles, SEPM Concepts in Sedimentology and Paleontology #4, p. 171–180.

Dixon, J.F., R.J. Steel, and C. Olariu, 2012, Shelf-edge delta regime as a predictor of deep water deposition: Journal of Sedimentary Research, v. 82, p. 681–687, doi: 10.2110/jsr.2012.59.

DOGM, <http://oilgas.ogm.utah.gov>

Dooling, P.R., 2012, Tidal facies, stratigraphic architecture, and along-strike variability of a high energy, transgressive shoreline, Late Cretaceous, Kaiparowits Plateau, Southern Utah, Master of Science, University of Utah, Salt Lake City, Utah.

Durham, L.S., 2012, Mancos-Niobrara play full of surprises: AAPG Explorer, <https://www.aapg.org/explorer/2012/08aug/mancos0812.cfm>, accessed 8/9/2013.

Edwards, C.M., J.A. Howell, and S.S. Flint, 2005, Depositional and stratigraphic architecture of the Santonian Emery Sandstone of the Mancos Shale: Implications for Late Cretaceous evolution of the Western Interior Foreland Basin of central Utah, U.S.A: Journal of Sedimentary Research, v. 75, p. 280–299, doi: 10.2110/jsr.2005.021.

Embry, A.F., 1990, Depositional sequences – theoretical considerations, boundary recognition, and relationships to other genetic units *in* A. Mørk, ed., Sequence Stratigraphy Field Workshop, Svalbard: Continental Shelf Institute (IKU), Trondheim, p. 1–26.

Embry, A.F., 2002, Transgressive-regressive (T-R) sequence stratigraphy, *in* J. Armentrout, and N. Rosen, eds., Gulf Coast SEPM Conference Proceedings, Houston, Texas, p. 151–172.

Embry, A.F. and E. Johannesen, 1992, T-R sequence stratigraphy, facies analysis, and reservoir distribution in the uppermost Triassic – Lower Jurassic succession, western Sverdrup Basin, Arctic Canada *in* T.O. Vorren, E. Bergsager, Ø.A. Dahl Stamnes, E. Holter, B. Johansen, E. Lie, and T.B. Lund, eds., Arctic Geology and Petroleum Potential: Norwegian Petroleum Society Special Publication 2, p. 121–146.

Fertl, W.H., and G.V. Chillingar, 1988, Total organic carbon content determined from well logs: SPE Formation Evaluation, SPE 15612, p. 407–419.

Fielding, C.R., 2010, Planform and facies variability in asymmetric deltas: facies analysis and depositional architecture of the Turonian Ferron Sandstone in the western Henry Mountains, south-central Utah, U.S.A: Journal of Sedimentary Research, v. 80, p. 455–479, doi: 10.2110/jsr.2010.047.

Flemings, P.B., and T.E. Jordan, 1989, A synthetic stratigraphic model of foreland basin development, Journal of Geophysical Research, v. 94 (B4), p. 3851-3866.

Fouch, T.D., T.F. Lawton, D.J. Nichols, W.B. Cashion, and W.A. Cobban, 1983, Patterns and timing of synorogenic sedimentation in Upper Cretaceous rocks of central and northeast Utah, *in* M.W. Reynolds, and E.D. Dolly, eds., Mesozoic Paleogeography of West Central United States: Rocky Mountain Section SEPM, Denver, Colorado, p. 305–336.

Franczyk, K.J., T.D. Fouch, R.C. Johnson, C.M. Molenaar, and W.A. Cobban, 1992, Cretaceous and Tertiary paleogeographic reconstructions for the Uinta-Piceance basin study area, Colorado and Utah: U.S. Geological Survey Bulletin 1787-Q, 48 p.

Galloway, W.E., 1989, Genetic stratigraphic sequences in basin analysis I: architecture and genesis of flooding-surface bounded depositional units: AAPG Bulletin, v. 73, p. 125–142.

Gardner, M.H., 1995a, The stratigraphic hierarchy and tectonic history of the mid Cretaceous foreland basin of central Utah: Stratigraphic Evolution of Foreland Basins, SEPM special Publication No. 52, p. 283–303.

Gardner, M.H., 1995b, Tectonic and eustatic controls on the stratal architecture of mid Cretaceous stratigraphic sequences, central Western Interior Foreland Basin of North America: Stratigraphic Evolution of Foreland Basins, SEPM Special Publication No. 52, p. 243–281.

Gardner, M.H., T.A. Cross, and M. Levorsen, 2004, Stacking patterns, sediment volume partitioning, and facies differentiation in shallow-marine and coastal-plain strata of the Cretaceous Ferron Sandstone, Utah, *in* T.C. Chidsey, R.D. Adams, and T.H. Morris, eds., Analogue for Fluvial-Deltaic Reservoir Modeling: Ferron Sandstone of Utah: AAPG Studies in Geology 50, p. 93–124.

Gradstein, F.M., J.G. Ogg, M.D. Schmitz, and G.M. Ogg, 2012, The Geologic Timescale 2012: Boston, USA, Elsevier, doi: 10.1016/B978-0-444-59425-9.00004-4.

Hammes, U., H.S. Hamlin, and T.E. Ewing, 2011, Geologic analysis of the Upper Jurassic Haynesville Shale in east Texas and west Louisiana: AAPG Bulletin, v. 95, p. 1643–1666, doi: 10.1306/02141110128.

Hampson, G.J., 2000, Discontinuity surfaces, clinoforms, and facies architecture in a wave dominated, shoreface – shelf parasequence: Journal of Sedimentary Research, v. 70, p. 325–340.

Hampson, G.J., P.M. Burgess, and J.A. Howell, 2001, Shoreface tongue geometry constrains history of relative sea level fall: examples from Late Cretaceous strata in the Book Cliffs area, Utah: Terra Nova, v. 13, p. 188–196.

Hampson, G.J., M.R. Gani, K.E. Sharman, N. Irfan, and B. Bracken, 2011, Along-strike and down-dip variations in shallow marine sequence stratigraphic architecture: Upper Cretaceous Star Point Sandstone, Wasatch Plateau, central Utah, USA: Journal of Sedimentary Research, v. 81, p. 159–184, doi: 10.2110/jsr.2011.15.

Hampson, G.J., J.A. Howell, and S.S. Flint, 1999, A sedimentological and sequence stratigraphic re-interpretation of the Upper Cretaceous Prairie Canyon Member

("Mancos B") and associated strata, Book Cliffs Area, Utah, U.S.A: Journal of Sedimentary Research, v. 69, p. 414–433.

Hancock, J.M., 1993, Transatlantic correlations in the Campanian-Maastrichtian stages by eustatic changes of sea-level, *in* E.A. Hailwood, and R.B. Kidd, eds., High Resolution Stratigraphy: Geological Society, London, Special Publication 70, p. 241–256.

Haq, B.U., J. Hardenbol, and P.R. Vail, 1987, Chronology of fluctuating sea levels since the Triassic: Science, v. 235, p. 1156–1167.

Haq, B.U., and S.R. Schutter, 2008, A chronology of Paleozoic sea-level changes: Science, v. 322, p. 64–68.

Hardenbol, J., J. Thierry, M.B. Farley, T. Jacquin, P.-C. De Graciansky, and P.R. Vail, 1998, Mesozoic and Cenozoic sequence chronostratigraphic framework of European Basins: Mesozoic and Cenozoic Sequence Stratigraphy of European Basins, SEPM SpecialPublications, v. 60, p. 3–13.

Hettinger, R.D., and M.A. Kirschbaum, 2003, Stratigraphy of the Upper Cretaceous Mancos Shale (upper part) and Mesaverde Group in the southern part of the Uinta and Piceance Basins, Utah and Colorado: Petroleum Systems and Geological Assessment of Oil and Gas in the Uinta-Piceance Province, Utah and Colorado: U.S. Geological Survey Digital Data Series DDS-69-B (1.0 ed., pp. 25). Denver, CO 80225: U.S. Geological Survey, Information Services.

Hillier, R., L. Stright, and R. Ressetar, 2013, Estimating total organic carbon content in the Cretaceous Mancos Shale: AAPG Rocky Mountain Section Meeting, Salt Lake City, September 22–24.

Horton, B., 2012, Variability of the Mancos Shale: Developing Preliminary Depositional Sequence Stratigraphic Models of a Developing Shale Gas Play. Master of Science, University of Utah, Salt Lake City, Utah.

Howell, J.A., and S.S. Flint, 2003, Siliciclastics case study: the Book Cliffs, *in* A. Coe, ed., The Sedimentary Record of Sea Level Change: Cambridge, U.K., Open University and Cambridge University Press, p. 135–208.

Jenkyns, H.C., 1980, Cretaceous anoxic events: from continents to oceans: Journal of the Geologic Society, London, v. 137, p. 171–188.

Johnson, J.G., G. Klapper, and C.A. Sandberg, 1985, Devonian eustatic fluctuations in Euramerica: GSA Bulletin, v. 96, p. 567–587.

Johnson, R.C., 2003a, Northwest to southeast cross section of Cretaceous and Lower Tertiary rocks across the eastern part of the Uinta Basin, UT: Petroleum Systems

and Geological Assessment of Oil and Gas in the Uinta-Piceance Province, Utah and Colorado: U.S. Geological Survey Digital Data Series DDS-69-B (1.0 ed., pp. 9). Denver, CO 80225: U.S. Geological Survey, Information Services.

Johnson, R.C., 2003b, Depositional framework of the Upper Cretaceous Mancos Shale and thelower part of the Upper Cretaceous Mesaverde group, Western Colorado and Eastern Utah: Petroleum Systems and Geological Assessment of Oil and Gas in the Uinta Piceance Province, Utah and Colorado: U.S. Geological Survey Digital Data Series DDS-69-B (1.0 ed., pp. 28). Denver, CO 80225: U.S. Geological Survey, Information Services.

Johnson, S.Y., 1992, Phanerozoic evolution of sedimentary basins in the Uinta-Piceance Basin region, northwestern Colorado and northeastern Utah: U.S. Geological Survey, Bulletin 1787, 48 p.

Jordan, T.E., 1981, Thrust loads and foreland basin evolution, Cretaceous, Western United States: AAPG Bulletin, v. 65, p. 2506–2520.

Kamola, D.L., and J.C. Van Wagoner, 1995, Stratigraphy and facies architecture of parasequences with examples from the Spring Canyon Member, Blackhawk Formation, Utah, *in* J.C. Van Wagoner, and G.T. Bertram, eds., Sequence Stratigraphy of Foreland Basin Deposits: Outcrop and Subsurface Examples from the Cretaceous of North America: AAPG Memoir, vol. 64, p. 27–54.

Karner, G.D., 1986, Effects of lithospheric in-plane stress on sedimentary basin stratigraphy: Tectonics, v. 5, p. 573–588.

Kauffman, E.G., 1969, Cretaceous marine cycles of the western interior: The Mountain Geologist, v. 6, p. 227–245.

Kauffman, E.G., 1977, Geological and biological overview: Western Interior Cretaceous Basin: The Mountain Geologist, v. 14, p. 75–99.

Kauffman, E.G., B.B. Sageman, J.I. Kirkland, W.P. Elder, P.J. Harries, and T. Villamil, 1993, Molluscan biostratigraphy of the Cretaceous Western Interior Basin, North America, *in* W.G.E. Caldwell, and E.G. Kauffman, eds., Evolution of the Western Interior Basin: Geological Association of Canada, Special Paper 39, p. 397–434.

Kennedy, A.D., 2011, Geological Predictors of the Hydrocarbon Extraction Potential of the Mancos Shale, Master of Science, University of Utah, Salt Lake City, Utah.

King, G.E., 2012, Hydraulic fracturing 101: what every representative, environmentalist, regulator, reporter, investor, university researcher, neighbor, and engineer should know about estimated frac risk and improving frac performance in unconventional gas and oil wells, SPE 152596, 80 p.

Kirschbaum, M.A., 2003, Geologic assessment of undiscovered oil and gas resources of the Mancos/Mowry total petroleum system, Uinta-Piceance Province, Utah and Colorado: Petroleum Systems and Geological Assessment of Oil and Gas in the Uinta-Piceance Province, Utah and Colorado: U.S. Geological Survey Digital Data Series DDS-69-B (1.0 ed., pp. 51). Denver, CO 80225: U.S. Geological Survey, Information Services.

Kirschbaum, M.A. and R.D. Hettinger, 2004. Facies analysis and sequence stratigraphic framework of Upper Campanian strata (Nelson and Mount Garfield Formations, Bluecastle Tongue of the Castlegate Sandstone, and Mancos Shale), eastern Book Cliffs, Colorado and Utah: U.S. Geological Survey Digital Data Series DDS-69 G, 46 p.

Kirschbaum, M.A. and T.J. Mercier, 2013, Controls on deposition and preservation of Cretaceous Mowry Shale and Frontier Formation equivalents, Rocky Mountain Region, Colorado, Utah, and Wyoming: AAPG Bulletin, vol. 97, p. 899–921, doi: 10.1306/10011212090.

Kominz, M.A., J.V. Browning, K.G. Miller, P.J. Sugarman, S. Mizintseva, and C.R. Scotese, 2008, Late Cretaceous to Miocene sea-level estimates from the New Jersey and Delaware coastal plain coreholes: an error analysis: Basin Research, v. 20, p. 211–226, doi: 10.1111/j.1365-2117.2008.00354.x.

Kosters, E.C., J.G. VanderZwaan, and F.J. Jorissen, 2000, Production, preservation, and prediction of source rock facies in deltaic settings: International Journal of Coal Geology, v. 43, p. 13–26.

Kuzniak, K., 2011, New Stratigraphic Interpretations, Geochemistry, and Petrophysics of the Lower Mancos Group, Douglas Creek Arch, Northwestern Colorado, U.S.A., Master of Science, Colorado School of Mines, Golden, Colorado.

Lash, G.G., and t. Engelder, 2011, Thickness trends and sequence stratigraphy of the Middle Devonian Marcellus Formation, Appalachian Basin: implications for Acadian foreland basin evolution, AAPG Bulletin, vol. 95, p. 61–103, doi: 10.1306/06301009150.

Lawton, T.F., 1986, Fluvial systems of the Upper Cretaceous Mesaverde group and Paleocene North Horn Formation, Central Utah: a record of transition from thin skinned to thick skinned deformation in the foreland region, *in* J.A. Peterson, ed., Paleotectonics and Sedimentation in the Rocky Mountain Region, United States: AAPG Memoir 41, p. 423–442.

Leythaeuser, D., 1973, Effects of weathering on organic matter in shales: Geochimica et Cosmochimica Acta, v. 37, p. 113–120.

Livaccari, R.F., 1991, Role of crustal thickening and extensional collapse in the tectonic evolution of the Sevier-Laramide orogeny, western United States: Geology, v. 19, p. 1104–1107.

Locklair, R.E., and B.B. Sageman, 2008, Cyclostratigraphy of the Upper Cretaceous Niobrara Formation, Western Interior, U.S.A.: a Coniacian-Santonian orbital timescale: Earth and Planetary Science Letters, v. 269, p. 540–553, doi: 10.1016/j.espl.2008.03.021.

Locklair, R.E., B.B. Sageman, and A. Lerman, 2011, Marine carbon burial flux and the carbon isotope record of Late Cretaceous (Coniacian – Santonian) Oceanic Anoxic Event III: Sedimentary Geology, v. 235, p. 38–49, doi: 10.1016/j.sedgeo.2010.06.026.

Longman, M.W., B.A. Luneau, and S.M. Landon, 1998, Nature and distribution of Niobrara lithologies in the Cretaceous Western Interior Seaway of the rocky mountain region: The Mountain Geologist, v. 35, p. 137–170.

Loucks, R.G., R.M. Reed, S.C. Ruppel, and U. Hammes, 2012, Spectrum of pore types and networks in mudrocks and a descriptive classification for matrix-related mudrock pores: AAPG Bulletin, v. 96, p. 1071–1098, doi: 10.1306/08171111061.

Loucks, R.G. and S.C. Ruppel, 2007, Mississippian Barnett Shale: lithofacies and depositional setting of a deep-water shale gas succession in the Fort Worth Basin, Texas: AAPG Bulletin, v. 91, p. 579–601, doi: 10.1306/11020606059.

Loucks, R.G., R.M. Reed, S.C. Ruppel, and D.M. Jarvie, 2009, Morphology, genesis, and distribution of nanometer-scale pores in siliceous mudstones of the Mississippian Barnett Shale: Journal of Sedimentary Research, v. 79, p. 848–861, doi: 10.2110/jsr.2009/092.

MacEachern, J.A., K.L. Bann, J.P. Bhattacharya, and C.D. Howell, 2005, Ichnology of deltas: organism responses to the dynamic interplay of rivers, waves, storms, and tides: River Deltas – Concepts, Models, and Examples, SEPM Special Publications No. 83, p. 49–85.

Macquaker, J.H.S., S.J. Bentley, and K.M. Bohacs, 2010, Wave-enhanced sediment gravity flows and mud dispersal across continental shelves: Reappraising sediment transport processes operating in ancient mudstone successions: Geology, v. 38, p. 947–950, doi: 10.1130/G31093.1.

Macquaker, J.H.S., K.G. Taylor, and R.L. Gawthorpe, 2007, High-resolution facies analysis of mudstones: implications for paleoenvironmental and sequence stratigraphic interpretations of offshore ancient mud-dominated successions: Journal of Sedimentary Research, v. 77, p. 324–339, doi: 10.2110/jsr.2007.029.

Meyers, S.R., S.E. Siewert, B.S. Singer, B.B. Sageman, D.J. Condon, J.D. Obradovich, B.R. Jicha, and D.A. Sawyer, 2012, Intercalibration of radioisotopic and astrochronologic time scales for the Cenomanian-Turonian boundary interval, Western Interior Basin, USA: Geology, v. 40, p. 7–10, doi: 10.1130/G32261.1.

Miall, A.D., 1992, The Exxon global cycle chart: an event for every occasion?: Geology, v. 20, p. 787–790.

Miall, A.D., 1994, Sequence stratigraphy and chronostratigraphy: problems of definition and precision in correlation, and their implications for global eustasy: Geoscience Canada, v. 21, p. 1–26.

Miall, A.D., and M. Arush, 2001, The Castlegate Sandstone of the Book Cliffs, Utah: sequence stratigraphy, paleogeography, and tectonic controls: Journal of Sedimentary Research, v. 71, p. 537–548.

Milici, R.C., and C.S. Swezey, 2006, Assessment of Appalachian Basin oil and gas resources: Devonian shale – middle and upper Paleozoic total petroleum system: U.S. Geological Survey, Open File Report Series 2006-1237, 70 p.

Miller, D.J. and K.A. Eriksson, 2000, Sequence stratigraphy of Upper Mississippian strata in the central Appalachians: a record of glacioeustasy and tectonoeustasy in a foreland basin setting: AAPG Bulletin, v. 84, p. 210–233.

Miller, K.G., M.A. Kominz, J.V. Browning, J.D. Wright, G.S. Mountain, M.E. Katz, P.J. Sugarman, B.S. Cramer, N. Christie-Blick, and S.F. Pekar, 2005, The Phanerozoic record of global sea-level change: Science, v. 310, p. 1293–1298.

Miller, K.G., P.J. Sugarman, J.V. Browning, M.A. Kominz, J.C. Hernández, R.K. Olsson, J.D. Wright, M.D. Feigenson, and W. Van Sickel, 2003, Late Cretaceous chronology of large, rapid sea level changes: glacioeustasy during the greenhouse world: Geology, v. 31, p. 585–588.

Milton, N. J. and D. Emery, 1996, Outcrop and Well Data, in Sequence Stratigraphy, D. Emery and K. Myers, eds., Blackwell Publishing Ltd., Oxford, UK, p. 61–79. doi: 10.1002/9781444313710.ch4.

Modica, C.J. and S.G. Lapierre, 2012, Estimation of kerogen porosity in source rocks as a function of thermal transformation: examples from the Mowry Shale in the Powder River Basin of Wyoming: AAPG Bulletin, v. 96, p. 87–108, doi: 10.1306/04111110201.

Molenaar, C.M. and W.A. Cobban, 1991, Middle Cretaceous stratigraphy on the South and East sides of the Uinta Basin, northeastern Utah and northwestern Colorado: U.S. Geological Survey Bulletin 1787: Evolution of Sedimentary Basins – Uinta and Piceance Basins, ch. P, 34 p.

Molenaar, C.M. and B.W. Wilson, 1990, The Frontier Formation and associated rocks of Northeastern Utah and Northwestern Colorado: U.S. Geological Survey Bulletin 1787: Evolution of Sedimentary Basins – Uinta and Piceance Basins, ch. M, 21 p.

Moucha, R., A.M. Forte, J.X. Mitrovica, D.B. Rowley, S. Quéré, N.A. Simmons, and S.P. Grand, 2008, Dynamic topography and long-term sea-level variations: there is no such thing as a stable continental platform: Earth and Planetary Science Letters, v. 271, p. 101–108.

Mullen, M., R. Roundtree, and B. Baree, 2007, A composite determination of mechanical rock properties for stimulation design (what to do when you don't have a sonic log), SPE 108139, 13 p.

Müller, R.D., M. Sdrolias, C. Gaina, B. Steinberger, and C. Heine, 2008, Long-term sea level fluctuations driven by ocean basin dynamics: Science, v. 319, p. 1357–1362, doi: 10.1126/science.1151540.

Nuccio, V.F. and L.N.R. Roberts, 2003, Thermal maturity and oil and gas generation history of petroleum systems in the Uinta-Piceance Province, Utah and Colorado: Petroleum Systems and Geological Assessment of Oil and Gas in the Uinta Piceance Province, Utah and Colorado: U.S. Geological Survey Digital Data Series DDS-69-B (1.0 ed., pp. 39). Denver, CO 80225: U.S. Geological Survey, Information Services.

O'Byrne, C.J. and S. Flint, 1995, Sequence, parasequence, and intraparasequence architecture of the Grassy Member, Blackhawk Formation, Book Cliffs, Utah, USA, *in* J.C. Van Wagoner, and G.T. Bertram, eds., Sequence Stratigraphy of Foreland Basin Deposits: Outcrop and Subsurface Examples from the Cretaceous of North America: AAPG Memoir, v. 64, p. 225–255.

Pang, M. and D. Nummedal, 1995, Flexural subsidence and basement tectonics of the Cretaceous Western Interior basin, United States: Geology, v. 23, p. 173–176.

Pasley, M.A., W.A. Gregory, and G.F. Hart, 1991, Organic matter variations in transgressive and regressive shales: Organic Geochemistry, v. 17, p. 483–509.

Pasley, M.A., G.W. Riley, and D. Nummedal, 1993, Sequence stratigraphic significance of organic matter variations: example from the Upper Cretaceous Mancos Shale of the San Juan Basin, New Mexico *in* B.J. Katz, and R.M. Pratt, eds., Source Rocks in a Sequence Stratigraphic Framework: AAPG Studies in Geology, v. 37, p. 221–241.

Passey, Q.R., K.M. Bohacs, W.L. Esch, R. Klimentidis, and S. Sinha, 2010, From oil prone source rock to gas-producing shale reservoir – geologic and petrophysical characterization of unconventional shale-gas reservoirs: SPE 131350, 29 p.

Passey, Q.R., S. Creaney, J.B. Kulla, F.J. Moretti, and J.D. Stroud, 1990, A practical method for organic richness from porosity and resistivity logs: AAPG Bulletin, v. 74, p. 1777–1794.

Pattison, A.J., 2005, Storm influenced prodelta turbidite complex in the lower Kenilworth member at Hatch Mesa, Book Cliffs, Utah, U.S.A.: implications for shallow marine facies models: Journal of Sedimentary Research, v. 75, p. 420–439.

Pattison, A.J., R.B. Ainsworth, and T.R. Hoffman, 2007, Evidence of across shelf transport of fine-grained sediments: turbidite-filled shelf channels in the Campanian Aberdeen Member, Book Cliffs, Utah, USA: Sedimentology, v. 54, p. 1033–1063, doi: 10.1111/j.13653091.2007.00871.x.

Pattison, S.A.J., K.G. Taylor, and J.H.S. Macquaker, 2009, A shore-to-basin transect through the Mancos Shale mud belt: sedimentological controls on lithofacies variability in unconventional hydrocarbon plays, Book Cliffs, Utah: Field Trip No. 18 Guidebook, Society for Sedimentary Geology (SEPM), AAPG Annual Convention and Exhibition, 7-10 June, Colorado Convention Center, Denver, Colorado, 168 p.

Plint, A.G., J.H.S. Macquaker, and B.L. Varban, 2012, Bedload transport of mud across a wide, storm influenced ramp: Cenomanian-Turonian Kaskapau Formation, western Canada foreland basin: Journal of Sedimentary Research, v. 82, p. 801–822. doi: 10.2110/jsr.2012.64

Posamentier, H.W., and G.P. Allen, 1993, Siliclastic sequence stratigraphic patterns in foreland ramp-type basins: Geology, v. 21, p. 455–458.

Posamentier, H.W., and W.R. Morris, 2000, Aspects of stratal architecture of forced regressive deposits *in* D. Hunt, and R.L. Gawthorpe, eds., Sedimentary Responses to Forced Regressions: Geological Society, London, Special Publications, v. 172, p. 19–46.

Posamentier, H.W. and P.R. Vail, 1988, Eustatic controls on clastic deposition II sequence and systems tract models. Sea Level Changes – An Integrated Approach, SEPM Special Publication no. 42, p. 125–154.

Quick, J.C. and R. Ressetar, 2012, Thermal maturity of the Mancos Shale within the Uinta Basin, Utah and Colorado: AAPG Search and Discovery Article # 50616.

Rankin, C.H., 1944, Stratigraphy of the Colorado group, Upper Cretaceous, in northern New Mexico: Colorado School of Mines Bulletin, v. 20, 27 p.

Ridgely, J.L., S.M. Condon, and J.R. Hatch, 2013, Geology and oil and gas assessment of the Mancos-Menefee composite total petroleum system. Ch. 4 of Petroleum Systems and Geological Assessment of Undiscovered Oil and Gas Resources in

the San Juan Basin Province, Exclusive of Paleozoic Rocks, New Mexico and Colorado: U.S. Geological Survey Digital Data Series DDS-69-F, p. 1–97.

Riemersma, P.E. and M.A. Chan, 1991, Facies of the Lower Ferron Sandstone and Blue Gate Shale members of the Mancos Shale: lowstand and early transgressive facies architecture: Special Publications of the International Association of Sedimentologists, v. 14, p. 489–510.

Rose, K.K., A.S.B. Douds, J.A. Pancake, H.R. Pratt III, and R. Boswell, 2004, Assessing sub economic natural gas resources in the Anadarko and Uinta Basins: AAPG Search and Discovery Article #10069.

Ryer, T.A., 2004, Previous studies of the Ferron Sandstone, *in* T.C. Chidsey, R.D. Adams, and T.H. Morris, eds., Analogue for Fluvial-Deltaic Reservoir Modeling: Ferron Sandstone of Utah: AAPG Studies in Geology 50, p. 3–38.

Sageman, B.B., A.E. Murphy, J.P. Werne, C.A. Ver Straeten, D.J. Hollander, and T.W. Lyons, 2003, A tale of shales: the relative roles of production, decomposition, and dilution in the accumulation of organic rich strata, Middle-Upper Devonian, Appalachian Basin: Chemical Geology, v. 195, p. 229–273.

Sageman, B.B., J. Rich, M.A. Arthur, G.E. Birchfield, and W.E. Dean, 1997, Evidence for Milankovitch periodicities in Cenomanian-Turonian lithologic and geochemical cycles, Western Interior U.S.A: Journal of Sedimentary Research, v. 67, p. 286–302.

Sahagian, D., O. Pinous, A. Olferiev, and V. Zakharov, 1996, Eustatic curve for the middle Jurassic – Cretaceous based on Russian platform and Siberian stratigraphy: zonal resolution: AAPG Bulletin, v. 80, p. 1433–1458.

Schamel, S., 2006, Shale gas resources of Utah: assessment of previously undiscovered gas discoveries: Utah Geological Survey, Open-File Report 499, 84 p.

Schieber, J., 1999, Distribution and deposition of mudstone facies in the Upper Devonian SonyeaGroup of New York: Journal of Sedimentary Research, v. 69, p. 909-925.

Schieber, J., J. Southard, and K. Thaisen, 2007, Accretion of mudstone beds from migrating floccule ripples: Science, v. 318, p. 1760–1763.

Schwans, P., 1988, Stratal Packages at the Subsiding Margin of the Cretaceous Foreland Basin, Utah. (Volumes I + II): PhD Dissertation, The Ohio State University, Columbus, Ohio.

Schwans, P., 1995, Controls on sequence stacking and fluvial to shallow-marine architecture in a foreland basin, *in* J.C. Van Wagoner, and G.T. Bertram, eds., Sequence Stratigraphy of Foreland Basin Deposits: Outcrop and Subsurface

Examples from the Cretaceous of North America. AAPG Memoir, v. 64, p. 103–136.

Seymour, D.L. and C.R. Fielding, 2013, High resolution correlation of the Upper Cretaceous stratigraphy between the Book Cliffs and the western Henry Mountains syncline, Utah, USA: Journal of Sedimentary Research, v. 83, p. 475–494. doi: http://dx.doi.org/10.2110/jsr.2013.37

Shanley, K.W. and P.J. McCable, 1995, Sequence stratigraphy of Turonian – Santonian strata, Kaiparowits Plateau, southern Utah, U.S.A.: implications for regional correlation and foreland basin evolution, *in* J.C. Van Wagoner, and G.T. Bertram, eds., Sequence Stratigraphy of Foreland Basin Deposits: Outcrop and Subsurface Examples from the Cretaceous of North America: AAPG Memoir, v. 64, p. 55 102.

Singh, P., R. Slatt, and W. Coffey, 2008, Barnett Shale – unfolded: sedimentology, sequence stratigraphy, and regional mapping: Gulf Coast Association of Geological Societies Transactions, v. 58, p. 777–795.

Slatt, R.M. and N.R. O'Brien, 2011, Pore types in the Barnett and Woodford gas shales: contribution to understanding gas storage and migration pathways in fine grained rocks: AAPG Bulletin, v. 95, p. 2017–2030, doi: 10.1306/03301110145.

Slatt, R.M. and N.D. Rodriguez, 2012, Comparative sequence stratigraphy and organic geochemistry of gas shales: commonality or coincidence?: Journal of Natural Gas Science and Engineering, v. 8, p. 68–84. doi: 10.1016/j.jngse.2012.01.008.

Slothower, C., 2012, Encana Corp. releases first Mancos Shale results: Farmington Daily Times, June 22, <http://www.daily-times.com/ci_20917335/encana-corp-releases first mancos-shale-results>, accessed 6/13/13.

Sonnenberg, S.A., 2011, The Niobrara petroleum system: a new resource play in the Rocky Mountain region, *in* J.E. Estes-Jackson, and D.S. Anderson, eds., Revisiting and Revitalizing the Niobrara in the Central Rockies: Rocky Mountain Association of Geologists, Denver, Colorado, p. 13–32.

Swift, D.J.P., P.M. Hudelson, R.L. Brenner, and P. Thompson, 1987, Shelf construction in a foreland basin: storm beds, shelf sandbodies, and shelf-slope depositional sequences in the Upper Cretaceous Mesaverde Group, Book Cliffs, Utah: Sedimentology, v. 34, p. 423–457.

Tibert, N.E., J.-P. Colin, and R.M. Leckie, 2009, Taxonomy, biostratigraphy and paleoecology of Cenomanian and Turonian ostracodes from the Western Interior Basin, Southwest Utah, USA: Revue de micropaleontology, v. 52, p. 85–105. doi: 10.1016/j.revmic.2007.02.006.

U.S. Energy Information Administration, 2013, Annual Energy Outlook, Early Release, 16 p.

Waanders, G., 2006, Palynology and thermal maturation report, Chevron USA Stone Cabin No.1 well, unpublished report.

Waanders, G., 2006, Palynology and thermal maturation report, Phillips Petroleum Watson 1B well, unpublished report.

Waanders, G., 2006, Palynology and thermal maturation report, Tenneco Oil Diamond Canyon II 15-15 well, unpublished report.

Van Wagoner, J.C., 1995, Sequence stratigraphy and marine to nonmarine facies architecture of foreland basin strata, Book Cliffs, Utah, USA, *in* J.C. Van Wagoner, and G.T. Bertram, eds., Sequence Stratigraphy of Foreland Basin Deposits: Outcrop and Subsurface Examples from the Cretaceous of North America: AAPG Memoir, v. 64, p. 137–223.

Van Wagoner, J.C. and G.T. Bertram, eds., 1996, Sequence Stratigraphy of Foreland Basin Deposits. Outcrop and Subsurface Examples from the Cretaceous of North America: AAPG Memoir, v. 64, xxi + 487 p.

Varban, B.L. and A.G. Plint, 2008, Paleoenvironments, paleogeography, and physiography of a large, muddy, shallow ramp: Late Cenomanian – Turonian Kaskapau Formation, Western Canada foreland basin: Sedimentology, v. 55, p. 201–233. doi: 10.1111/j.13653091.2007.00902.x

Vernik, L., and J. Milovak, 2011, Rock physics of organic shales: The Leading Edge, March, p. 318–323.

White, T., K. Furlong, and M. Arthur, 2002, Forebulge migration in the Cretaceous Western Interior basin of the Central United States: Basin Research, v. 14, p. 43–54.

Wolfe, J.A., and G.R. Upchurch Jr., 1987, North American nonmarine climates and vegetation during the Late Cretaceous: Palaeogeography, Palaeoclimatology, Palaeoecology, v. 61, p. 33–77.

Wright, S., 2012, An unconventional bonanza: The Economist, v. 404, 18 p.

Yoshida, S., 2000, Sequence and facies architecture of the upper Blackhawk Formation and the lower Castlegate Sandstone (Upper Cretaceous), Book Cliffs, Utah, USA: Sedimentary Geology, v. 136, p. 239–276.

Young, R.G., 1955, Sedimentary facies and intertonguing in the Upper Cretaceous of the Book Cliffs, Utah-Colorado: GSA Bulletin, v. 66, p. 177–202.